BioMed Research International

Advances in Neurovascular Treatments

Guest Editors: Robert M. Starke, Aaron S. Dumont, Stephen J. Monteith, Ricky Medel, and Webster Crowley

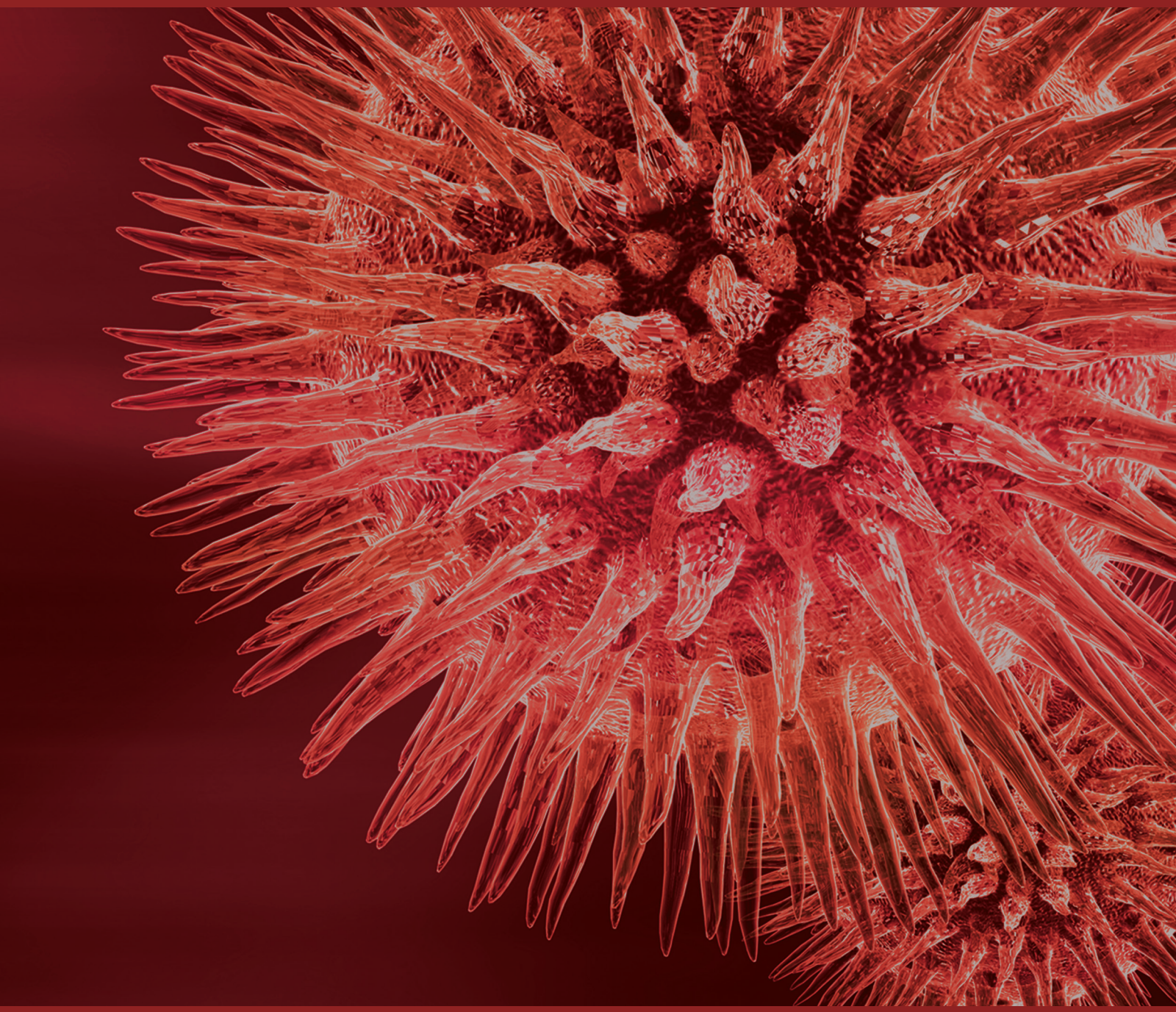

Advances in Neurovascular Treatments

BioMed Research International

Advances in Neurovascular Treatments

Guest Editors: Robert M. Starke, Aaron S. Dumont, Stephen J. Monteith, Ricky Medel, and Webster Crowley

Contents

Hindawi Publishing Corporation
BioMed Research International
Volume 2014, Article ID 641539, 2 pages
http://dx.doi.org/10.1155/2014/641539

Editorial

Advances in Neurovascular Treatments

Robert M. Starke,[1] Stephen J. Monteith,[2] Nohra Chalouhi,[3] Dale Ding,[1] Ricky Medel,[4] David Hasan,[5] and Aaron S. Dumont[4]

[1] *Department of Neurological Surgery, University of Virginia, P.O. Box 800212, Charlottesville, VA 22908, USA*
[2] *Department of Neurosurgery, Swedish Neuroscience Institute, Seattle, WA 98122, USA*
[3] *Department of Neurological Surgery, Thomas Jefferson University, Philadelphia, PA 19107, USA*
[4] *Department of Neurological Surgery, Tulane University, New Orleans, LA 70012, USA*
[5] *Department of Neurological Surgery, University of Iowa, Iowa City, IA 52242, USA*

Correspondence should be addressed to Robert M. Starke; bobby.starke@gmail.com

Received 27 April 2014; Accepted 27 April 2014; Published 5 June 2014

Neurovascular diseases compromise a heterogeneous group of disorders with a broad spectrum of phenotypes. Recent advances include greater understanding of both the genetic links and the basic mechanisms underlying the pathophysiology of cerebrovascular diseases. Improvements in neurovascular disease therapies have risen both from cell cultures and animal models of disease. Additionally, developments in technology have resulted in improvements in diagnosis, including a variety of advances in vascular imaging, medical therapies, and surgical and endovascular therapies. Recent randomized clinical trials have also helped to refine patient selection and optimal treatment modalities.

Stroke is a leading cause of morbidity and mortality. Three recent trials have challenged the use of endovascular therapy in acute cerebrovascular occlusion [1]. Limitations of these studies included lack of large vessel occlusions in many patients and the use of older thrombectomy devices. In the recent edition, S. Hann et al. demonstrate the benefits of next generation thrombectomy devices in clot removal. For patients with significant intracranial disease, recent trials have demonstrated that best medical therapy results in improved outcomes over intracranial stenting [2]. For patients who have failed best medical therapy, the optimal treatment options remain unclear. D. Ding et al. review potential options in the current edition, including balloon-mounted stents that may offer an effective alternative to self-expanding stents with lower rates of in-stent stenosis [3].

Cerebral arteriovenous malformations (AVMs) consist of an abnormal tangle of blood vessels that shunt blood directly from arteries to veins without an intervening capillary bed. The molecular mechanisms behind their development, progression, and hemorrhage remain incompletely defined, and further critical work is indicated for both risk stratification and the potential development of an alternative medical therapy. Recent studies have highlighted the altered role of Notch signaling pathway in AVMs [4], and the *in vivo* study by J. Tu and N. F. Jufri adds to the literature by demonstrating that wall shear stress likely contributes to AVM angiogenesis through activation of Notch. Further studies are necessary to determine how altered gene expression in critical vascular genes likely contributes to AVM instability and hemorrhage. Recent trials have challenged aggressive treatment of AVM patients at low risk for hemorrhage [5]. For patients with high risk features, intervention may be necessary. R. Dalyai et al. review clinical outcomes following radiosurgery with embolization in large AVMs.

Similarly, the molecular mechanisms underlying cerebral aneurysm formation and rupture remain unclear [6]. It has been known for some time that female gender is a significant risk factor for both aneurysm formation and subarachnoid hemorrhage. J. Tu et al. reviewed the role of estrogen receptors in signaling mechanisms in human cerebral vascular endothelial cells which may help to provide a preventative therapy for aneurysm progression. A number

of trials have recently addressed the role of endovascular therapy in cerebral aneurysms [7]. For mycotic aneurysms, the optimal therapy is incompletely defined, and this area is eloquently reviewed by M. Zanaty et al. Following aneurysm rupture, vasospasm is a significant cause of morbidity and mortality. A number of preventative and treatment measures may be beneficial, including alterations in cerebral blood flow dynamics as assessed by D. K. Kung et al. and the efficacy of intra-arterial nimodipine as tested by S. Ott et al.

Neurovascular diseases are often associated with devastating outcomes. Progression from *in vitro*, *in vivo*, translational, and clinical studies has led to many new developments. Additionally, developments in technology have improved treatment outcomes. Although there have been numerous advances in treatment for neurovascular diseases, there remain many areas of uncertainty. Through this collection of papers, we hope to highlight areas of uncertainty, recent advances, and future clinical necessity.

Robert M. Starke
Stephen J. Monteith
Nohra Chalouhi
Dale Ding
Ricky Medel
David Hasan
Aaron S. Dumont

References

[1] R. M. Starke, R. J. Komotar, and E. S. Connolly, "Endovascular therapy in acute ischemic stroke," *Neurosurgery*, vol. 72, no. 6, pp. N20–N23, 2013.

[2] C. P. Derdeyn, M. I. Chimowitz, M. J. Lynn et al., "Aggressive medical treatment with or without stenting in high-risk patients with intracranial artery stenosis (SAMMPRIS): the final results of a randomised trial," *The Lancet*, vol. 383, no. 9914, pp. 333–341, 2013.

[3] C. R. Durst, S. R. Geraghty, A. M. Southerland et al., "Stenting of symptomatic intracranial stenosis using balloon mounted coronary stents: a single center experience," *Journal of NeuroInterventional Surgery*, 2014.

[4] R. J. Komotar, R. M. Starke, and E. S. Connolly, "The role of notch in development and regression of vascular fistulas," *Neurosurgery*, vol. 71, no. 2, pp. N18–N19, 2012.

[5] R. M. Starke, R. J. Komotar, and E. S. Connolly, "A randomized trial of unruptured brain arteriovenous malformations," *Neurosurgery*, vol. 73, no. 4, pp. N13–N15, 2013.

[6] R. M. Starke, N. Chalouhi, M. S. Ali et al., "The role of oxidative stress in cerebral aneurysm formation and rupture," *Current Neurovascular Research*, vol. 10, no. 3, pp. 247–255, 2013.

[7] R. J. Komotar, R. M. Starke, and E. S. Connolly, "The natural course of unruptured cerebral aneurysms," *Neurosurgery*, vol. 71, no. 4, pp. N7–N9, 2012.

Hindawi Publishing Corporation
BioMed Research International
Volume 2014, Article ID 306518, 8 pages
http://dx.doi.org/10.1155/2014/306518

Clinical Study

Stereotactic Radiosurgery with Neoadjuvant Embolization of Larger Arteriovenous Malformations: An Institutional Experience

Richard Dalyai,[1] Thana Theofanis,[1] Robert M. Starke,[2] Nohra Chalouhi,[1] George Ghobrial,[1] Pascal Jabbour,[1] Aaron S. Dumont,[1] L. Fernando Gonzalez,[1] David S. Gordon,[1] Robert H. Rosenwasser,[1] and Stavropoula I. Tjoumakaris[1]

[1] *Department of Neurosurgery, Thomas Jefferson University and Jefferson Hospital for Neuroscience, 901 Walnut Street, 3rd Floor, Philadelphia, PA 19107, USA*
[2] *Department of Neurosurgery, University of Virginia, Charlottesville, VA, USA*

Correspondence should be addressed to Stavropoula I. Tjoumakaris; stavropoula.tjoumakaris@jefferson.edu

Received 13 September 2013; Accepted 28 November 2013; Published 22 January 2014

Academic Editor: Steven J. Monteith

Objective. This study investigates the safety and efficacy of a multimodality approach combining staged endovascular embolizations with subsequent SRS for the management of larger AVMs. *Methods.* Ninety-five patients with larger AVMs were treated with staged endovascular embolization followed by SRS between 1996 and 2011. *Results.* The median volume of AVM in this series was 28 cm^3 and 47 patients (48%) were Spetzler-Martin grade IV or V. Twenty-seven patients initially presented with hemorrhage. Sixty-one patients underwent multiple embolizations while a single SRS session was performed in 64 patients. The median follow-up after SRS session was 32 months (range 9–136 months). Overall procedural complications occurred in 14 patients. There were 13 minor neurologic complications and 1 major complication (due to embolization) while four patients had posttreatment hemorrhage. Thirty-eight patients (40%) were cured radiographically. The postradiosurgery actuarial rate of obliteration was 45% at 5 years, 56% at 7 years, and 63% at 10 years. In multivariate analysis, larger AVM size, deep venous drainage, and the increasing number of embolization/SRS sessions were negative predictors of obliteration. The number of embolizations correlated positively with the number of stereotactic radiosurgeries ($P < 0.005$). *Conclusions.* Multimodality endovascular and radiosurgical approach is an efficacious treatment strategy for large AVM.

1. Introduction

Cerebral arteriovenous malformations (AVM) are rare but potentially devastating vascular lesions that often affect young adults. Intracranial hemorrhage occurs at an average annual rate of 2 to 4% [1]. Surgical excision is the mainstay of treatment for Spetzler-Martin (SM) grade I and II AVM. Because of high procedural morbidity rates, surgery is avoided in larger and higher grade AVM, and alternative therapies are often considered for these lesions.

Radiosurgery, initially conceived by Leksell [2] in 1968, is a well-established treatment alternative to surgical resection for intracranial AVM. However, stand-alone stereotactic radiosurgery (SRS) may have limited utility for larger AVM [3]. For these larger lesions, we have explored a multimodality therapy of initial endovascular embolization for AVM volume reduction followed by SRS to treat the remaining nidus. By reducing the size of the nidus targeted by SRS, endovascular embolization is thought to improve AVM obliteration rates while also minimizing SRS-related complications. Previous series have reported conflicting results regarding the efficacy of preradiosurgical AVM embolization [4]. We report our 15-year experience in managing these challenging lesions with a combined embolization and SRS approach.

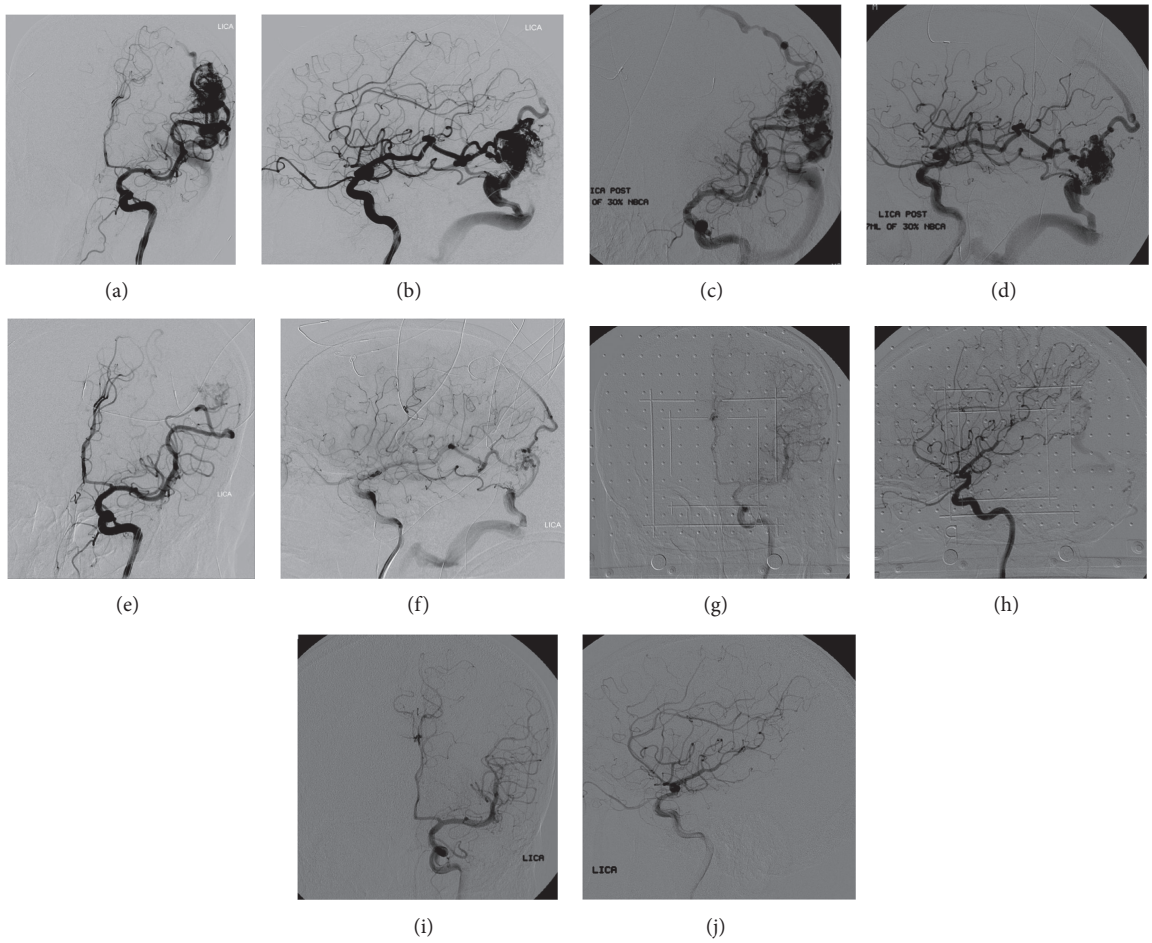

Figure 1: 57 yo M presenting with incapacitating migraines found in frontal and lateral views of digital subtraction angiogram, left carotid injection, to have Spetzler-Martin grade III left parietal AVM (a-b). Frontal and lateral views of digital subtraction angiogram showing reduction of AVM nidus after 1st endovascular embolization with NBCA (c-d). Frontal and lateral views of digital subtraction angiogram following third NBCA embolization session with remaining small nidus and fistula (e-f). Frontal and lateral views of digital subtraction angiogram showing small remaining nidus and fistula prior to Gamma Knife SRS planning (g-h). Frontal and lateral views of digital subtraction angiogram showing complete obliteration of AVM 2 years after SRS session (i-j).

2. Methods

2.1. Patient Selection. An Institutional Review Board approval was obtained prior to data collection. From 1996 to 2011, a total of 775 patients were treated for cerebral AVM in our institution. Of these, 95 patients were selected based on their clinical presentation, SM grade, and angioarchitecture to undergo staged embolization and SRS as seen in Figure 1. We were more likely to aggressively utilize radiosurgery with adjuvant embolization than any treatment at all in those patients with hemorrhagic presentation, SM grade II–IV, and those with arterial pedicles amenable to embolization. All patients had larger AVMs with a maximal diameter greater than 3 cm.

Medical charts, operative reports, SRS records, and pre- and posttreatment imaging results including MR and digital subtraction angiography (DSA) were carefully reviewed to determine patient demographics, AVM characteristics, procedural complications, posttreatment cerebral hemorrhage, radiological AVM obliteration, and neurological outcome.

2.2. Embolization Protocol. Embolization was performed with liquid embolic agents NBCA (Codman & Shurtleff, Inc., Raynham, Massachusetts, USA) and, later, Onyx 18 or 34 (eV3, Irvine, CA). Embolization sessions were performed at 6-week intervals, as necessary, until the AVM nidus had been reduced by a goal of 33% (usually to a volume of less than 10 cc). Target selection for AVMs was dependent on two issues, the size of feeding arterial pedicles and the location of arterial feeders on the AVM nidus. Targets were often selected that would treat and obliterate deeper portions of the nidus and those with large volume. Our strategy with embolization was to achieve volume reduction and not flow reduction and ideally to target fixed portions of a nidus that would allow for a discrete nidus when targeting with SRS. Postembolization AVM size was calculated during SRS planning.

2.3. Stereotactic Radiosurgery Protocol. A stereotactic head frame was placed for all patients using local anesthesia supplemented by intravenous sedation. Next, biplane digital subtraction stereotactic angiography was performed followed by MR imaging (Figures 1(g) and 1(h)). Volumetric 3D dose planning was performed using Leksell GammaPlan software. For patients with larger lesions and prospectively volume-staged SRS plans, the lesion was divided into approximately equal volumes using anatomic landmarks. SRS treatment plans consisted of the margin SRS dose including the entire AVM nidus volume. SRS was performed with Leksell Gamma Knife units (Elekta AB).

The median initial AVM volume was 28 cm^3 (largest being 112 cm^3). The mean Flickinger Pollock grade was 3.65 (range 1.1 to 11.8).

The postembolization mean maximal diameter was 2.2 cm (range 0.3–6 cm). The median total target volume was 4.24 cm^3 (range 0.26–9.1 cc^3) on the first SRS treatment and 5.09 cm^3 on successive SRS treatments. The median margin dose was 21 Gy.

2.4. Follow-Up Evaluation. Radiological success was defined as complete AVM obliteration on DSA (total disappearance of the nidus and early draining veins) or, alternatively, on MR angiography (total disappearance of the nidus and flow-voids) for patients with poor overall medical condition or for those refusing follow-up DSA. The median follow-up after SRS session was 32 months (range 9–136 months).

2.5. Statistical Analysis. Data are presented as median and range for continuous variables and as frequency for categorical variables. The Flickinger Pollock scale was tested as a continuous variable and as an ordinal variable by quartile. The Radiosurgery AVM Score was tested as previously described [5]. Kaplan Meier analysis was carried out to determine actuarial rate of obliteration. Univariate survival analysis was carried out using the logrank test to test covariates predictive of treatment obliteration. Factors predictive in univariate analysis ($P < 0.20$) were entered into a multivariate Cox proportional hazards model. Interaction and confounding was assessed through stratification and relevant expansion covariates. P values of ≤ 0.05 were considered statistically significant. Statistical analysis was carried out with Stata 10.0 (College Station, TX).

3. Results

Ninety-five patients with large and complex AVM underwent preoperative embolization followed by SRS. Patient characteristics are summarized in Table 1. Of the 95 patients, 41 (43%) were women and 54 (57%) were men. The median age was 39 years (range 9–73 years). Thirty-six percent of patients were active smokers and 23% were on oral antihypertensive medication at the time of diagnosis.

AVMs were predominantly located in the left hemisphere (57%). The parietal lobe was the most common location of AVM (27%). The median maximum diameter of AVMs was 4.3 cm. Sixteen (17%) AVM had a maximum diameter

Table 1

	N	%
Gender		
M	41	42%
F	54	58%
Age		
Median in yrs	38.54	
0–21	18	18.90%
22–40 yrs	32	33.70%
40–50 yrs	22	23.20%
50+	23	24.20%
AVM side		
L	54	57%
R	41	43%
Initial hemorrhage		
N	68	71%
Y	27	29%
Initial seizure		
N	58	61.10%
Y	37	38.90%
Initial neurological exam		
Intact	74	78.00%
Mild/moderate deficit	18	18.90%
Severe deficit (i.e., unresponsive)	3	3.10%
Location	*N*	%
Frontal	19	20.00%
Temporal	24	25.30%
Parietal	26	27.40%
Occipital	9	9.40%
Cerebellum	8	8.40%
Thalamus, brainstem	9	9.40%
Size		
Medium (3–6 cm)	80	84.20%
Large (>6 cm)	15	15.80%
Eloquence		
Noneloquent tissue	24	25.20%
Eloquent tissue	71	74.80%
Venous drainage		
Superficial	44	46.30%
Deep	51	53.70%
SM grade		
3	48	50.50%
4	38	40.00%
5	9	9.50%
Pollock-Flickinger score		
0–2.25	23	24.2%
2.25–3.5	24	25.3%
3.5–4.75	24	25.3%
>4.75	24	25.3%
Radiosurgery AVM scale		
1	12	12.6%

Table 1: Continued.

	N	%
2	46	46.3%
3	28	29.4%
4	11	11.6%

greater than 6 cm. The median pretreatment volume was 28 cm^3. Mean SM grade was 3.6 and almost 50% (47/95) of all lesions were SM grade IV or V. Seventy-one (75%) AVMs were located in eloquent areas and 51 had deep venous drainage (54%). Twenty (29%) patients initially presented with cerebral hemorrhage, and 37 (39%) presented with seizures. The remaining patients were initially diagnosed incidentally or as part of the imaging workup for headaches. In our patient population there were 5 patients with intranidal aneurysms (5%), 1 patient with a high flow fistula (1%), and 9 patients with proximal flow-related aneurysms treated (10%). The mean Flickinger Pollock scale was 3.65 (standard deviation 1.95). The mean Radiosurgery AVM Score was 2.4.

Thirty-four (36%) patients underwent a single embolization, 25 (26%) patients underwent 2 embolizations, 15 patients (16%) underwent 3 embolizations, and 21 patients (22%) underwent ≥4 embolizations (Tables 2 and 3). A single SRS session was performed in 64 (67%) patients, two SRS sessions in 17 patients (18%), and three to five SRS sessions in 14 (15%) patients. The median duration from last SRS session to follow-up was 32 months.

Overall procedural complications occurred in 14 (14.7%) patients. Thirteen (14%) patients experienced only minor or transient neurological complications that left no permanent morbidity. The remaining patient suffered a major neurological complication following embolization that left him severely disabled. Four (4%) patients suffered a hemorrhage during the follow-up period. One expired shortly thereafter. Thirty-eight (40%) patients had a radiographically confirmed obliteration. AVM obliteration was confirmed on DSA in 31 patients (32%) and MRA in 7 patients (8%).

Statistical analysis is detailed in Tables 4 and 5. In multivariate logistic regression analysis, larger AVM size, deep venous drainage, and increasing number of embolization or SRS sessions were negative predictors of complete obliteration. The number of embolizations correlated positively with the number of stereotactic radiosurgeries ($P < 0.005$). We analyzed patients who had a favorable outcome (complete obliteration and no neurologic deficits). Those with less than 4 embolization treatments (OR = 0.26, $P = 0.036$) and without deep venous drainage (OR = 0.22, $P = 0.001$) were significantly more likely to have favorable outcome. The postradiosurgery actuarial rate of obliteration was 36% at 3 years, 45% at 5 years, 56% at 7 years, and 63% at 10 years (Figure 2).

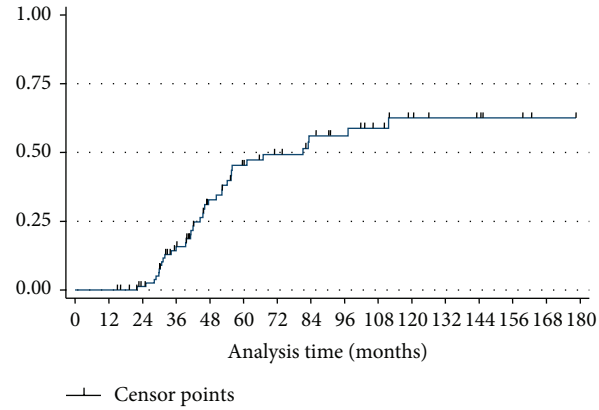

Figure 2: Plot showing AVM obliteration rate versus time after treatment.

Table 2

Total number of embolizations	N (mean 2.44)	%
1	34	35.80%
2	25	26.30%
3	15	15.80%
4+	21	22.10%
Time to complete multiple embolizations	Avg months (mean 7.7)	N
2 embolizations	1.9	28
3 embolizations	7.8	17
4 embolizations	11.3	15
5+ embolizations	30.8	11
Type of embolization	N	%
NBCA	230	83%
Onyx	46	17%
Total number of radiation treatments	N	%
1	64	67.30%
2	17	17.90%
3+	14	14.70%

Table 3

SRS Tx	Total embo Tx						
	1	2	3	4	5	6	7
1	28	17	10	7	1	1	0
2	5	4	2	5	1	0	0
3	1	3	2	0	2	0	1
4	0	1	0	1	0	1	1
5	0	0	1	0	0	0	0

Spearman's rho 0.403, $P < 5.982e - 6$.

4. Discussion

In AVMs deemed inappropriate for surgical resection, SRS is a well-established treatment alternative. Large series have reported excellent results with occlusion rates as high as 84% at 2-year angiographic follow-up [6]. Pollock et al. [7] reported a 73% rate of complete obliteration and a 14% rate of major complications. In their study, the rate of hemorrhage after treatment was 8% over a 2–5 year

Table 4

	Total (%)	No. w/residual AVM (%)		No. w/100% obliteration (%)		*P* value
Sex, *n* (%)						0.396
M	41	21	51.20%	20	48.80%	
F	54	36	66.70%	18	33.30%	
Age, *n* (%)						0.795
0–21	18	10	55.60%	8	44.40%	
22–40 yrs	32	21	65.60%	11	34.40%	
40–50 yrs	22	14	63.60%	8	36.40%	
50+	23	12	52.20%	11	47.80%	
Location						0.252
Frontal	19	14	73.70%	5	26.30%	
Temporal	24	13	54.20%	11	45.80%	
Parietal	26	12	46.20%	14	53.80%	
Occipital	9	7	87.80%	2	22.20%	
Cerebellum	8	4	50%	4	50%	
Thalamus, brainstem	9	7	87.80%	2	22.20%	
Size, *n* (%)						0.022
Medium (3–6 cm)	80	44	55%	36	45%	
Large (>6 cm)	15	13	86.70%	2	13.30%	
Venous drainage, *n* (%)						<0.001
Superficial	44	18	40.90%	26	59.10%	
Deep	51	39	76.50%	12	23.50%	
Smoker? *n* (%)						0.664
Y	35	20	57.10%	15	42.90%	
N	60	37	61.70%	23	38.30%	
Hypertension? *n* (%)						0.669
Y	18	11	61.10%	7	38.90%	
N	77	46	59.70%	31	40.30%	

Table 5

	Total (*n*)	No w/residual AVM	%	No. w/100% obliteration	%	*P* value
Initial hemorrhage						0.926
Y	27	16	59%	11	41%	
N	68	40	59%	28	41%	
Initial seizure						0.731
Y	37	25	68%	12	32%	
N	58	31	53%	27	47%	
Initial neurological exam						0.25
Intact	74	45	61%	29	39%	
Mild/moderate deficit	18	8	44%	10	56%	
Severe deficit	3	3	100%	0	0%	
Total number of embolizations						0.017
1	34	18	53%	16	47%	
2	25	13	52%	12	48%	
3	15	8	53%	7	47%	
4+	21	17	81%	4	19%	
Total number of radiation treatments						0.025
1	64	33	52%	31	48%	
2	17	12	72%	5	29%	
3+	14	12	79%	2	14%	

follow-up period. Along similar lines, Yashar et al. [8] reported a 4-year radiographic obliteration rate of 67% with a hemorrhage rate of approximately 8%. With increasing clinical experience, several predictors of outcome after SRS were identified including AVM nidus volume, geometry of nidus distribution, eloquence of surrounding brain, and the presenting symptom of hemorrhage [5].

Despite overall high obliteration rates and low complication rates, SRS efficacy remains severely limited in large and complex AVM. In fact, SRS treatment efficacy and safety profile diminish sharply with increasing AVM size [4]. In a series of 30 large AVMs, Miyawaki et al. [9] noted only a 23% obliteration rate when utilizing a LINAC dose of 16 Gy with 22% of these cases requiring surgical intervention due to symptomatic radiation necrosis. Using LINAC with a mean dose >10 Gy, Ellis et al. [10] reported an obliteration rate of 44% in AVMs larger than 10 cm^3. Results from single-session Gamma Knife Radiosurgery (GKR) have been similarly discouraging for large AVM. Pan et al. [11] reported only a 50% obliteration rate in 76 AVMs larger than 10 cm^3 (mean dose 17 Gy). Furthermore, the authors reported that 49% of their patients had developed moderate to severe radiation-related edema with 6.3% having treatment related symptomatic complications.

Given the poor efficacy of SRS in large and complex AVM, neurosurgeons have attempted to develop alternative treatment strategies. Our center and others have utilized endovascular embolization to reduce the volume of large AVM in an attempt to improve SRS efficacy. With a reduction in the size of these lesions by embolization, SRS may potentially prove as effective as in initially small AVM treated with appropriate SRS margin dosages. Mathis et al. [12] embolized 24 AVMs with a mean initial volume of 37 cm^3 prior to GKR and noted a 50% obliteration rate with only 4% morbidity. In their series, procedural morbidity was exclusively related to radiosurgery. In another series, Mizoi et al. [13] treated 14 patients with AVMs >3 cm (mean volume 17.9 cm^3) with particle embolization followed by GKR (19.2 Gy) and reported a 38% obliteration rate with an 11% permanent morbidity rate (related exclusively to the endovascular embolization). In these initial reports, particulate agents such as PVA were utilized. These agents have several drawbacks mainly related to treatment durability and technical complications. Since then, newer embolic agents with improved penetrance, selectivity, and safety profile have been developed. Gobin et al. [14] reported their experience with NBCA embolization followed by LINAC (25 Gy) in large AVM (mean initial volume 22 cm^3). The authors were able to achieve a cure in 60% of patients with a 12.6% morbidity rate due primarily to the endovascular procedure. More recently, Blackburn et al. [15] reported an impressive 84% obliteration rate in 19 patients with AVM (average size of 20.1 cm^3) treated with NBCA embolization (average of 2.1 sessions) followed by SRS (mean dose of 17.9 Gy at the 50% isodense line). The procedural morbidity rate was 19% in their series. Blackburn reported a 7% permanent morbidity rate per endovascular embolization and 5% permanent morbidity rate per SRS session.

Our experience with embolization prior to SRS has been positive, albeit with a more modest 40% obliteration rate. Our criteria for radiographic AVM cure included only patients in whom a frank obliteration was documented on DSA or, alternatively, on MRA in those unable or unwilling to undergo catheter angiography. We also attribute this lower angiographic cure rate to the higher proportion of patients with SM grade IV/V lesions and the larger median AVM size in our study. Median AVM volume was as high as 28 cm^3 and nearly 50% of all lesions were SM grade IV and V.

Our protocol had a safety profile with a rate of morbidity of 14%. Most importantly, although 29% of patients presented with a ruptured AVM, only 4 (4%) patients experienced a posttreatment hemorrhage. This low rate of hemorrhage should be interpreted in light of the poor natural history of the AVMs included in our study. As such, young patients, known to have a particularly high rupture risk as demonstrated by Laakso et al. [16], accounted for up to 50% of the study population. Many patients also had larger symptomatic lesions in or abutting eloquent locations with medically intractable epilepsy or continued neurologic decline. The risk of open surgery is prohibitively high in these patients, and without preradiosurgical embolization many would not have been treatable with SRS alone due to the risks of high dose SRS radiation necrosis.

Despite the positive results previously reported by centers undertaking embolization, the use of embolization as an adjunctive tool in the treatment of large AVMs remains controversial. Some investigators reported that embolization may decrease obliteration rates and increase treatment morbidity [17]. Andrade-Souza et al. [17] retrospectively matched 47 patients who underwent Embo/SRS with 47 patients treated with SRS alone. They found an obliteration rate of 47% with Embo/SRS compared to 70% with SRS alone. However, this study is severely limited by the difficulty in matching a complex group of patients retrospectively, which may have introduced significant bias into the analysis. The authors also theorized that the lower obliteration rate observed with preradiosurgical embolization was attributable to the recanalization of the embolized portion of the nidus as well as the difficulty with radiosurgical planning since embolization may convert a fairly uniform geometric target into a poorly defined target with multiple irregular components. However, newer liquid embolic agents, such as Onyx, offer significant improvements in these areas which may theoretically increase treatment success.

Other groups have utilized different radiosurgical strategies to manage large unresectable AVM. Karlsson et al. [18] presented their data with planned staged SRS beginning with a low initial dose for volume reduction followed several years later by a follow-up SRS treatment. They treated 19 AVMs with an average volume of 16 cm^3 and achieved an obliteration rate of 68%, with a 7% risk of morbidity and a 7% annual risk of posttreatment hemorrhage. Using the same strategy in a series of 41 patients with large AVM (average volume of 13.8 cm^3), Foote et al. [19] achieved an obliteration rate of 59%, with a 2% permanent SRS-related morbidity and a 1.5% annual risk of posttreatment hemorrhage. Purely

volume-staged SRS is a more recently reported approach with prospectively planned follow-up SRS sessions on separate portions of the AVM at six-month intervals. Richling et al. [20] reported their initial results of volume-staged SRS with 28 large AVMs (average volume of 24.9 cm^3) achieving a 33% obliteration rate with only a 4% complication rate. A fairly similar obliteration rate (35%) was reported by the same group in a follow-up report that included 48 patients with large AVM [21]. The authors cautioned against the use of preoperative embolization, though nearly half of their patients received some form of embolization. Of their prospectively planned stereotactic staged radiosurgery, the same authors reported a 36% actuarial obliteration rate at 5 years and a 56% obliteration rate at 10 years when including salvage treatments. Importantly, 10 hemorrhages with 5 deaths occurred during follow-up, highlighting the main limitation of this treatment strategy, namely, the slow and delayed response of high risk AVMs to therapy.

We believe that the use of endovascular embolization remains a valuable option as an adjunctive modality for large AVM. We achieved a fairly reasonable obliteration rate, which could potentially improve with further angiographic followup. Furthermore, at the time of embolization, we were able to treat high-risk fistulas and proximal flow-related aneurysms as reflected in our low posttreatment hemorrhage rate. Endovascular embolization may therefore reduce the risk of hemorrhage during the treatment latency period. Additionally, our treatment success came with a low complication rate that compares favorably to previous studies. The question of whether this complication rate is better than the natural history of these lesions left untreated cannot be definitively answered in the present study. For some patients included in this study, SRS without prior embolization or even surgical resection could have been potential alternatives. Future advances in endovascular techniques and liquid embolic agents will undoubtedly improve the safety and efficacy of AVM embolization. Accordingly, recent data may suggest that Onyx allows more permanent lesion obliteration, with better visualization on SRS planning, MR imaging, and less embolic complications; however, this remains controversial [22].

5. Conclusions

SRS preceded by adjuvant embolization is a controversial yet potentially efficacious treatment strategy in patients with large AVMs that are not amenable to surgical excision. We were able to achieve complete AVM obliteration in a significant number of patients. Larger prospective studies are needed to explore the long-term safety and efficacy of this approach.

Abbreviations

AVM: Arteriovenous malformations
SM: Spetzler-Martin
SRS: Stereotactic radiosurgery
GKR: Gamma Knife Radiosurgery.

Conflict of Interests

The authors declare that there is no conflict of interests regarding the publication of this paper.

References

[1] N. Chalouhi, A. S. Dumont, C. Randazzo et al., "Management of incidentally discovered intracranial vascular abnormalities," *Neurosurgical Focus*, vol. 31, no. 6, article E1, 2011.

[2] L. Leksell, "Stereotactic radiosurgery," *Journal of Neurology Neurosurgery and Psychiatry*, vol. 46, no. 9, pp. 797–803, 1983.

[3] W. A. Friedman and F. J. Bova, "Radiosurgery for arteriovenous malformations," *Neurological Research*, vol. 33, no. 8, pp. 803–819, 2011.

[4] S. Sirin, D. Kondziolka, A. Niranjan, J. C. Flickinger, A. H. Maitz, and L. D. Lunsford, "Prospective staged volume radiosurgery for large arteriovenous malformations: indications and outcomes in otherwise untreatable patients," *Neurosurgery*, vol. 58, no. 1, pp. 17–26, 2006.

[5] S. J. Raffa, Y.-Y. Chi, F. J. Bova, and W. A. Friedman, "Validation of the radiosurgery-based arteriovenous malformation score in a large linear accelerator radiosurgery experience," *Journal of Neurosurgery*, vol. 111, no. 4, pp. 832–839, 2009.

[6] J. C. Flickinger, B. E. Pollock, D. Kondziolka, and L. D. Lunsford, "A dose-response analysis of arteriovenous malformation obliteration after radiosurgery," *International Journal of Radiation Oncology Biology Physics*, vol. 36, no. 4, pp. 873–879, 1996.

[7] B. E. Pollock, D. A. Gorman, R. J. Coffey et al., "Patient outcomes after arteriovenous malformation radiosurgical management: results based on a 5- to 14-year follow-up study," *Neurosurgery*, vol. 52, no. 6, pp. 1291–1297, 2003.

[8] P. Yashar, A. P. Amar, S. L. Giannotta et al., "Cerebral arteriovenous malformations: issues of the interplay between stereotactic radiosurgery and endovascular surgical therapy," *World Neurosurgery*, vol. 75, no. 5-6, pp. 638–647, 2011.

[9] L. Miyawaki, C. Dowd, W. Wara et al., "Five year results of LINAC radiosurgery for arteriovenous malformations: outcome for large AVMS," *International Journal of Radiation Oncology Biology Physics*, vol. 44, no. 5, pp. 1089–1106, 1999.

[10] T. L. Ellis, W. A. Friedman, F. J. Bova, P. S. Kubilis, and J. M. Buatti, "Analysis of treatment failure after radiosurgery for arteriovenous malformations," *Journal of Neurosurgery*, vol. 89, no. 1, pp. 104–110, 1998.

[11] D. H.-C. Pan, W.-Y. Guo, W.-Y. Chung, C.-Y. Shiau, Y.-C. Chang, and L.-W. Wang, "Gamma knife radiosurgery as a single treatment modality for large cerebral arteriovenous malformations," *Journal of Neurosurgery*, vol. 93, no. 3, pp. 113–119, 2000.

[12] J. A. Mathis, J. D. Barr, J. A. Horton et al., "The efficacy of particulate embolization combined with stereotactic radiosurgery for treatment of large arteriovenous malformations of the brain," *American Journal of Neuroradiology*, vol. 16, no. 2, pp. 299–306, 1995.

[13] K. Mizoi, H. Jokura, T. Yoshimoto et al., "Multimodality treatment for large and critically located arteriovenous malformations," *Neurologia Medico-Chirurgica*, vol. 38, pp. 186–192, 1998.

[14] Y. P. Gobin, A. Laurent, L. Merienne et al., "Treatment of brain arteriovenous malformations by embolization and radiosurgery," *Journal of Neurosurgery*, vol. 85, no. 1, pp. 19–28, 1996.

[15] S. L. Blackburn, W. W. Ashley Jr., K. M. Rich et al., "Combined endovascular embolization and stereotactic radiosurgery in the treatment of large arteriovenous malformations: clinical article," *Journal of Neurosurgery*, vol. 114, no. 6, pp. 1758–1767, 2011.

[16] A. Laakso, R. Dashti, S. Juvela, P. Isarakul, M. Niemelä, and J. Hernesniemi, "Risk of hemorrhage in patients with untreated spetzler-martin grade IV and V arteriovenous malformations: a long-term follow-up study in 63 patients," *Neurosurgery*, vol. 68, no. 2, pp. 372–378, 2011.

[17] Y. M. Andrade-Souza, M. Ramani, D. Scora, M. N. Tsao, K. Ter-Brugge, and M. L. Schwartz, "Embolization before radiosurgery reduces the obliteration rate of arteriovenous malformations," *Neurosurgery*, vol. 60, no. 3, pp. 443–451, 2007.

[18] B. Karlsson, H. Jokura, M. Yamamoto, M. Söderman, and I. Lax, "Is repeated radiosurgery an alternative to staged radiosurgery for very large brain arteriovenous malformations?" *Journal of Neurosurgery*, vol. 107, no. 4, pp. 740–744, 2007.

[19] K. D. Foote, W. A. Friedman, T. L. Ellis, F. J. Bova, J. M. Buatti, and S. L. Meeks, "Salvage retreatment after failure of radiosurgery in patients with arteriovenous malformations," *Journal of Neurosurgery*, vol. 98, no. 2, pp. 337–341, 2003.

[20] B. Richling, M. Killer, A. R. Al-Schameri, L. Ritter, R. Agic, and M. Krenn, "Therapy of brain arteriovenous malformations: multimodality treatment from a balanced standpoint," *Neurosurgery*, vol. 59, no. 5, pp. S148–S157, 2006.

[21] H. Kano, D. Kondziolka, J. C. Flickinger et al., "Stereotactic radiosurgery for arteriovenous malformations—part 6: multistaged volumetric management of large arteriovenous malformations," *Journal of Neurosurgery*, vol. 116, no. 1, pp. 54–65, 2012.

[22] D. N. Loy, K. M. Rich, J. Simpson, I. Dorward, L. Santanam, and C. P. Derdeyn, "Time-of-flight magnetic resonance angiography imaging of a residual arteriovenous malformation nidus after Onyx embolization for stereotactic radiosurgery planning. Technical note," *Neurosurgical Focus*, vol. 26, no. 5, article E13, 2009.

Hindawi Publishing Corporation
BioMed Research International
Volume 2014, Article ID 368082, 13 pages
http://dx.doi.org/10.1155/2014/368082

Research Article

Notch1 and 4 Signaling Responds to an Increasing Vascular Wall Shear Stress in a Rat Model of Arteriovenous Malformations

Jian Tu,[1] Yang Li,[1] and Zhiqiang Hu[2]

[1] *Australian School of Advanced Medicine, Macquarie University, 2 Technology Place, North Ryde, Sydney, NSW 2109, Australia*
[2] *Department of Neurosurgery, The 9th Medical Clinical College of Beijing University, Beijing 100038, China*

Correspondence should be addressed to Jian Tu; james.tu@mq.edu.au

Received 27 September 2013; Accepted 11 December 2013; Published 20 January 2014

Academic Editor: Robert M. Starke

Notch signaling is suggested to promote the development and maintenance of cerebral arteriovenous malformations (AVMs), and an increasing wall shear stress (WSS) contributes to AVM rupture. Little is known about whether WSS impacts Notch signaling, which is important for understanding the angiogenesis of AVMs. WSS was measured in arteriovenous fistulas (AVF) surgically created in 96 rats at different time points over a period of 84 days. The expression of Notch receptors 1 and 4 and their ligands, Delta1 and 4, Jagged1, and Notch downstream gene target Hes1 was quantified in "nidus" vessels. The interaction events between Notch receptors and their ligands were quantified using proximity ligation assay. There was a positive correlation between WSS and time ($r = 0.97$; $P < 0.001$). The expression of Notch receptors and their ligands was upregulated following AVF formation. There was a positive correlation between time and the number of interactions between Notch receptors and their ligands aftre AVF formation ($r = 0.62$, $P < 0.05$) and a positive correlation between WSS and the number of interactions between Notch receptors and their ligands ($r = 0.87$, $P < 0.005$). In conclusion, an increasing WSS may contribute to the angiogenesis of AVMs by activation of Notch signaling.

1. Introduction

Cerebral arteriovenous malformations (AVMs) consist of an abnormal tangle of fistulas that shunt blood from the arterial system to the venous system without an intervening capillary bed [1]. As the direct communication of high pressure arterial blood into the thin-walled venous vessels, AVMs present an altered hemodynamic state [2]. The increased shear stress upon the vessel wall in combination with the structural immaturity of AVM vasculature presents an increased risk of rupture. Their effects on the blood flow of the surrounding parenchyma may be responsible for other clinical manifestations of AVMs. It has been suggested that high flow conditions and the increased diameter and variability of the vessels within the nidus predispose to the development of turbulent flow [3]. While the existence of turbulence has not been demonstrated by direct measurement *in vivo* [4], many of the physiological and histological hallmarks of turbulent flow are present within AVMs. The increased rate of endothelial cell turnover [5], focal dilatation of vessels [3], and platelet aggregation [6] are indicative of high wall shear stress (WSS) associated with turbulence. It is unclear whether these derangements represent a primary abnormality of the AVM blood vessels or whether they are a secondary response to the abnormal hemodynamic environment within the AVM. The altered expression of angiogenic factors may be important in the vascular remodeling and continued angiogenesis that occur in these dynamic lesions [7]. Until the precise mechanism of action of many of these angiogenic factors is clarified, it is difficult to draw conclusions on the relevance of these abnormalities to AVM pathogenesis.

Notch signaling pathway has been implicated as a regulator of vascular angiogenesis and in the development of the human AVMs [8, 9]. Activation of the Notch receptor1 or 4 in mice causes AVMs-like abnormalities [8, 10–12]. Recently, normalization of Notch4 has been suggested as a strategy to reduce blood vessel size in a mouse model of AVMs [13]. Notch1 is expressed in vascular endothelial cells and

smooth muscle cells while Notch4 is expressed primarily in endothelial cells [14]. Notch ligands, Delta1 and 4, and Jagged1 are expressed in vascular endothelial cells and smooth muscle cells [15, 16]. Both Notch receptors and their ligands are transmembrane proteins; therefore, signaling is restricted to neighboring cells. Although the intracellular transduction of the Notch signal is remarkably simple, with no secondary messengers, this pathway functions in an enormous diversity of developmental processes. The specific roles of individual Notch receptors and their ligands in human vascular homeostasis are little known. The majority of knowledge implicating the Notch signaling in vessel homeostasis and development has arisen through gain and loss of function studies in mice [17, 18]. Observations in mice suggest that Notch1 plays a role in angiogenesis [18] and AVM pathogenesis [8]. Notch4 is involved in the initiation and maintenance of arteriovenous communications [12]; though Notch4 is not critical to vascular development, it shares functional redundancy with Notch1 in vascular development [17]. Delta1 is suggested to be critical to vascular maturation and vessel integrity [19]. Delta4 plays a critical role in early vascular remodelling, arterial and venous specialization, and Notch1-mediated signaling in early vascular development [20, 21]. Jagged1 contributes to vascular maturation and plays a distinct role in Notch1 signaling [22, 23]. The direct targets of Notch signaling remain vague. Notch expression activates transcription of Hairy/Enhancer of Split (Hes) family genes and subsequently results in repression of Hes target genes [24], many of which are tissue-specific transcriptional activators [25]. Thus, Notch activation of Hes can modulate cellular differentiation. It has been reported that Notch signaling pathway responds to Notch1 activator by increased angiogenesis and Jagged1 inhibitor by reduced angiogenesis in adult rats [9]. However, the knowledge of how does Notch signaling pathway respond to an increasing WSS in AVM vessels remains absent from the literature. This study was undertaken to examine whether endothelial Notch signaling responds to an increasing WSS in the "nidus" vessels in a rat model of AVMs. If so, how does WSS regulate the function of Notch signaling pathways?

2. Materials and Methods

2.1. AVF Rat Model. Animal experimentation was approved (Animal Ethics Approval numbers 08/97a, 2009/047, 2009/048, and 2010/037) and performed in accordance with the guidelines of the institutional Experimental Animal Care and Ethics Committee, Guide for the Care and Use of Laboratory Animals (Institute for Laboratory Animal Research, National Research Council, Washington, DC: National Academy Press, 1996), and the Code of Practice for the Care and Use of Animals for Scientific Purposes [26]. AVF rat model was created in 96 Sprague-Dawley male rats (7 weeks old, 230 ± 9 g) by an anastomosis of the left common carotid artery to the left external jugular vein as shown in Figure 1 and as previously reported [27–31]. Rats were allowed to acclimatize to new surroundings before the experiment began. Surgical procedures were not performed in the presence of other rats. General anaesthesia was induced using a mixture of 4% isoflurane and oxygen (2 L/min) via a nose cone. The depth of anaesthesia was assessed using the respiratory rate and by checking the hind limb withdrawal to pain. No procedure was commenced until there was a consistent absence of response to pain. A heating blanket was used for the duration of the procedure.

The procedure was performed in a sterile field using aseptic technique. The left common carotid artery (CCA) was exposed, and blood flow was measured through the CCA using a 1 mm Doppler ultrasonic probe (Transonic Systems, Ithaca, NY, USA). The left external jugular vein (EJV) was then exposed and ligated with 10/0 nylon suture at its junction with the subclavian vein. An aneurysm clip was placed across the rostral EJV. Microclips were also applied proximally and distally on the CCA, and a small arteriotomy made on the lateral aspect. An end-to-side anastomosis of the EJV to the CCA was performed using a continuous 10/0 nylon suture. The clips were sequentially removed from the EJV, distal CCA, and proximal CCA. Blood flow was measured through the proximal CCA and the vein using 1 and 2 mm Doppler ultrasonic probes (Transonic Systems). The wound was closed, and isoflurane was turned off, allowing the animal to breathe oxygen until the time of awakening. Once awake, the animal was placed in an individual cage and housed singly for one week postoperatively. Observations were carried out daily for the first week and then weekly thereafter. Observations included weight, assessment of motor function, behavior, and wound health. Six weeks after surgery, angiography was performed in 6 AVF rats, and their dilated small vessels and capillaries formed a "nidus" (Figure 1). There was no evidence of significant morbidity and mortality associated with AVF formation. The sham-AVF controls were treated identically but did not receive AVF formation surgical procedures. The sham-AVF controls were subjected to the same analysis as AVF rats. Data obtained from sham-AVF controls were expressed as the pre-AVF formation at −1 day time point in comparison with AVF rats at different time points over a follow-up period of 84 days after AVF formation.

2.2. Vascular WSS in AVF Rat Model. Blood blow was measured in the carotid artery before and after fistula creation, and in the jugular vein after fistula creation, using a flow probe (1 or 2 RB, Transonic Systems) connected to a transit time perivascular flowmeter (T420, Transonic Systems) [27]. Blood flow rate was recorded through a data acquisition system (PowerLab/8sp System, ADInstruments, Castle Hill, NSW, Australia). Shear stress was estimated using the Poiseuille formula $\tau = 4\eta Q/(\pi R_i^3)$, where τ is wall shear stress, η is blood viscosity, Q is blood flow rate, and R_i is the internal radius. It has been demonstrated that Poiseuille's law can be applied to the flow within blood vessels of diameters greater than 0.1 mm [32]. Therefore, it is applicable to this arteriovenous fistula model.

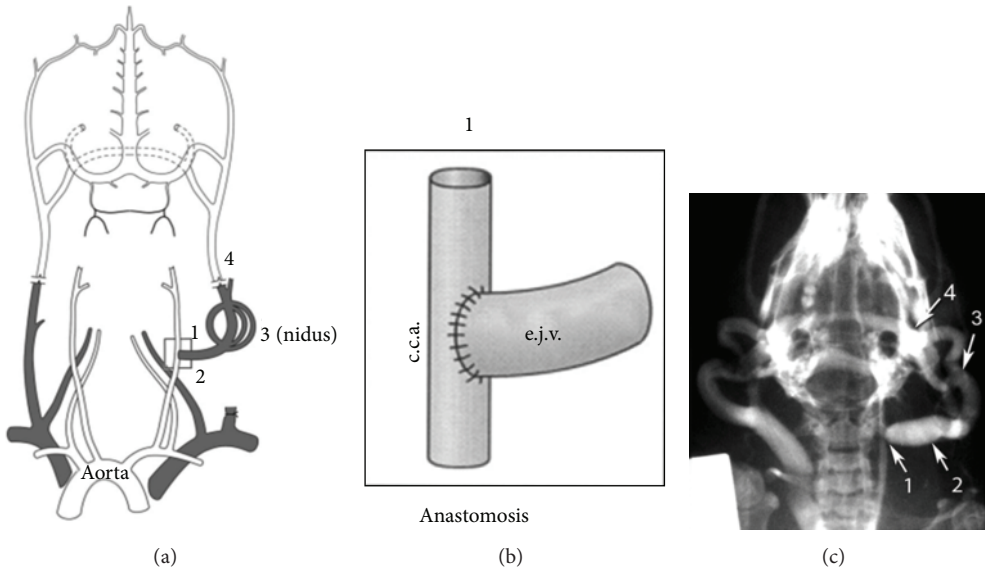

Figure 1: Arteriovenous fistula in a rat model of arteriovenous malformation. (a) Schematic representation shows an AVF in a rat model of AVM. The normal primary outflow for intracranial venous blood is the external jugular vein (e.j.v.) via the posterior facial vein and the vein from transverse sinus. The left external jugular vein is ligated at the confluence of subclavian vein, and (b) an end-to-side anastomosis was performed onto the left common carotid artery (c.c.a.). 1: carotid-jugular anastomosis; 2: arterialized feeding vein; 3: "nidus" consists of dilated small vessels and capillaries; 4: draining vein. (c) Representative angiogram obtained 42 days after creation of the rat AVF model. Portions of the rat AVF model are indicated: 1: proximal fistula; 2: arterialized jugular vein; 3: "nidus"; 4: draining vein.

2.3. Immunohistochemistry. Rats were anaesthetized and perfused with 4% paraformaldehyde. Specimens, including carotid-jugular anastomosis, arterialized feeding vein, the "nidus," and draining vein, were embedded in tissue freezing medium (ProSciTech, QLD, Australia) with liquid nitrogen for immunohistochemistry and proximity ligation assay. Immunohistochemistry was performed in specimens obtained from 32 AVF rats and 4 sham AVF controls as previously described [28–31, 33]. Briefly, sections were washed, and nonspecific binding was blocked by 10% horse serum. Anti-rat primary antibody (Table 1) was applied and incubated at 4°C overnight. Slides were washed, incubated with Alexa Fluor conjugated secondary antibody (Table 1) for 2 hours in dark, and examined using a confocal microscope (Leica SP5, Germany), and imaging data was analyzed using Leica LAS AF software. Each staining was triplicated and repeated 6 times. Fluorescence intensity units (FIU) were corrected using primary antibody controls. The FIU has been quantified as mean gray value. Slides were viewed by three observers blinded to the sample nature.

Table 1: Antibodies used in immunohistochemistry.

Antibodies	Dilution	Suppliers
Notch receptor1	1 : 50	R&D System, Minneapolis, MN, USA
Notch receptor4	1 : 50	Cell Signaling, Beverly, MA, USA
Delta-like1	1 : 500	Rockland, Gilbertsville, PA, USA
Delta-like4	1 : 500	Rockland, Gilbertsville, PA, USA
Jagged1	1 : 500	Rockland, Gilbertsville, PA, USA
Hes1	1 : 200	Abcam, Cambridge, UK
Caspase3	1 : 500	Abcam, Cambridge, UK
CD31	1 : 1,000	Abcam, Cambridge, UK
Alexa Fluor 488 goat anti-rabbit IgG	1 : 800	Molecular Probes, Eugene, OR, USA
Alexa Fluor 594 goat anti-mouse IgG	1 : 800	Molecular Probes, Eugene, OR, USA

2.4. Proximity Ligation Assay. Proximity ligation assay (PLA) was applied to examine the interaction between Notch receptor and its ligand in specimens obtained from 64 AVF rats and 8 sham AVF controls as previously described [34]. All reagents used for the PLA were purchased from Olink Bioscience (Uppsala, Sweden). The *in situ* PLA was performed according to the manufacturer's instructions. Briefly, tissue sections were permeabilized in 0.2% TX-100, 0.5% BSA in PBS, then blocked in 10% BSA in PBS, and incubated with anti-rat primary antibodies (Table 1). Duolink MINUS and PLUS conjugated secondary antibody incubation, ligation, and amplification steps for PLA were performed as suggested by Olink using 40 μL volume. Following amplification, slides were washed for 10 min in Olink Buffer B, pH 7.5, followed by a 10 min wash in 0.5% BSA. Fluorescent images were obtained using a confocal microscope (Leica TCS SP5X, Wetzlar, Germany). Z-Stacks were composed of 6 consecutive images with a total Z volume of 12 μm.

Images captured for PLA events were analyzed using Leica LAS AF software (Version 2.4.1; Leica Microsystems GmbH, Wetzlar, Germany). First, Z-stack images were converted into maximum representations. Three polygon regions of interest were drawn evenly along the vessel lumen 5 μm into the tunica intima as to envelope the vessel's endothelium. Three more circular regions of interest were evenly placed within the tunica media. The regions of interest were between 0.5 and 1.0 mm^2 in size. The positive PLA events were observed as fluorescent particles (size from 2 to 50 pixels in diameter). When PLA events merged to create particles larger than 50 pixels, the area was measured, and the number of events was assumed to be particle area divided by 10 since 10 pixels were the median size of most PLA events. The number of fluorescent spots obtained from PLA in regions of interest were automatically quantified and recorded. A threshold of 100 (gray values) was set for a positive signal prior to signal counting. To account for nonspecific signals, "background" signal/mm^2 values for each specimen's endothelial and medial regions of interest were generated from each specimen's negative control and then subtracted from each respective region of interest signal/mm^2 value. The number of PLA events was assessed by two observers blinded to the sample nature.

2.5. Data Analysis. Data were expressed as means ± SE (number of experiments). Statistical difference between groups was determined using the unpaired two-tailed t-test. When there were more than two groups, differences were analyzed using analysis of variance if the variances were equal, and the Mann-Whitney nonparametric test if variances were unequal [35]. Linear regressions were calculated using a statistical computer package, Number Cruncher Statistical Systems [35]. A value of $P < 0.05$ was considered statistically significant.

3. Results

3.1. Hemodynamic Changes in an AVF Rat Model. Before anastomosing the caudal end of the external jugular vein to the side of the common carotid artery, the blood flow through the left carotid artery was 5.2 ± 0.07 mL/min. Immediately after fistula creation, the common carotid flow (proximal to the fistula) increased by 140 ± 7% ($P < 0.05$). The blood flow changes over 84 days are depicted in Figure 2. Flow rate increased with time and peaked at 42 days (Figure 2(a)). There was a strong positive correlation between fistula blood flow and time up to 42 days after fistula formation ($r = 0.96$; $P < 0.001$). There was no statistical difference in the flow rate measured between day 42 and day 84. The maximum flow at day 42 was 11 times greater than the initial fistula flow.

Flow through the fistula was pulsatile. Turbulent blood flow was observed at the proximal fistula as red and blue colors in Figure 2(b) indicating two different blood flow directions. Laminar blood flow was observed at the through the arterialized jugular vein as blue color in Figure 2(b) indicates the same blood flow direction. There was a net positive mean shear stress that increased over time (Figure 2(c)). Shear amplitude in the fistula vein increased from 3.5 to 46 dynes/cm^2 from day 0 to day 42. There was a strong positive correlation between shear stress and time up to 42 days ($r = 0.97$; $P < 0.001$). There was no statistical difference in shear stress between day 42 and day 84. The maximum shear amplitude achieved at day 42 was 14 times the level at the time of fistula formation.

3.2. Increasing WSS Induces Apoptosis in an AVF Rat Model. Caspase3 was selected as a marker for apoptosis. The levels of caspase3 expression in "nidus" vessel wall in the AVF rats over a period of 84 days after AVF formation were shown in Figures 3(a) and 4(a). There was a significant upregulation of caspase3 expression in "nidus" vessels after AVF formation. The levels of caspase3 overexpression were 10% at 1 day after AVF formation and peaked at 35% at 42 days after AVF creation ($P < 0.05$).

3.3. Expression of Notch Receptors and Their Ligands in an AVF Rat Model. CD31 was selected as a marker for endothelium of the "nidus" vessel wall. Its expression was shown in Figures 3 and 4. The expression of Notch receptor1, Notch receptor4, Delta-like1, Delta-like4, Jagged1, and Hes1 was predominantly expressed in the endothelium of the "nidus" vessel wall (Figure 3).

3.4. Increasing WSS Activates Notch Receptors 1 and 4. The expression of Notch receptor1 was significantly upregulated in the "nidus" vessel wall since day 1 after AVF formation (Figure 4(b)). The level of Notch1 expression increased by 81% on day 3 ($P < 0.01$), which was sustainable over an 84-day follow-up period. Prior to AVF formation, the level of Notch receptor4 expression was greater than that of Notch1 expression ($P < 0.01$; Figure 4(b)). There was a 3-week delay in upregulated Notch4 expression comparing with that of Notch1 (Figure 4(b)). The expression of Notch4 was significantly upregulated by 45% on day 21 after AVF formation ($P < 0.01$; Figure 4(b)) and sustained for another 9 weeks of the follow-up period. There was a positive correlation between the levels of Notch4 expression and time over a period of 84 days after AVF formation ($r = 0.7252$, $P < 0.05$).

3.5. Increasing WSS Activates Notch Receptor Ligands and Hairy Enhancer of Split1. The expression of Notch receptor ligands, Delta1 and 4, was significantly upregulated in the "nidus" vessel wall 3 weeks after AVF formation ($P < 0.05$; Figure 4(c)) while Jagged1 was responsively upregulated 2 weeks earlier than that of Delta1 and 4 ($P < 0.04$; Figure 4(d)). The highest levels of Delta1 and 4 expression were observed on day 84 following AVF formation, which increased by 61% and 74%, respectively, compared to the pre-AVF formation ($P < 0.01$). The greatest level of Jagged1 expression was observed on day 42 after AVF formation, which elevated by 58% compared to the pre-AVF formation ($P < 0.01$). Increasing expression of Delta1 and 4 and Jagged1 was positively correlated with time following AVF formation

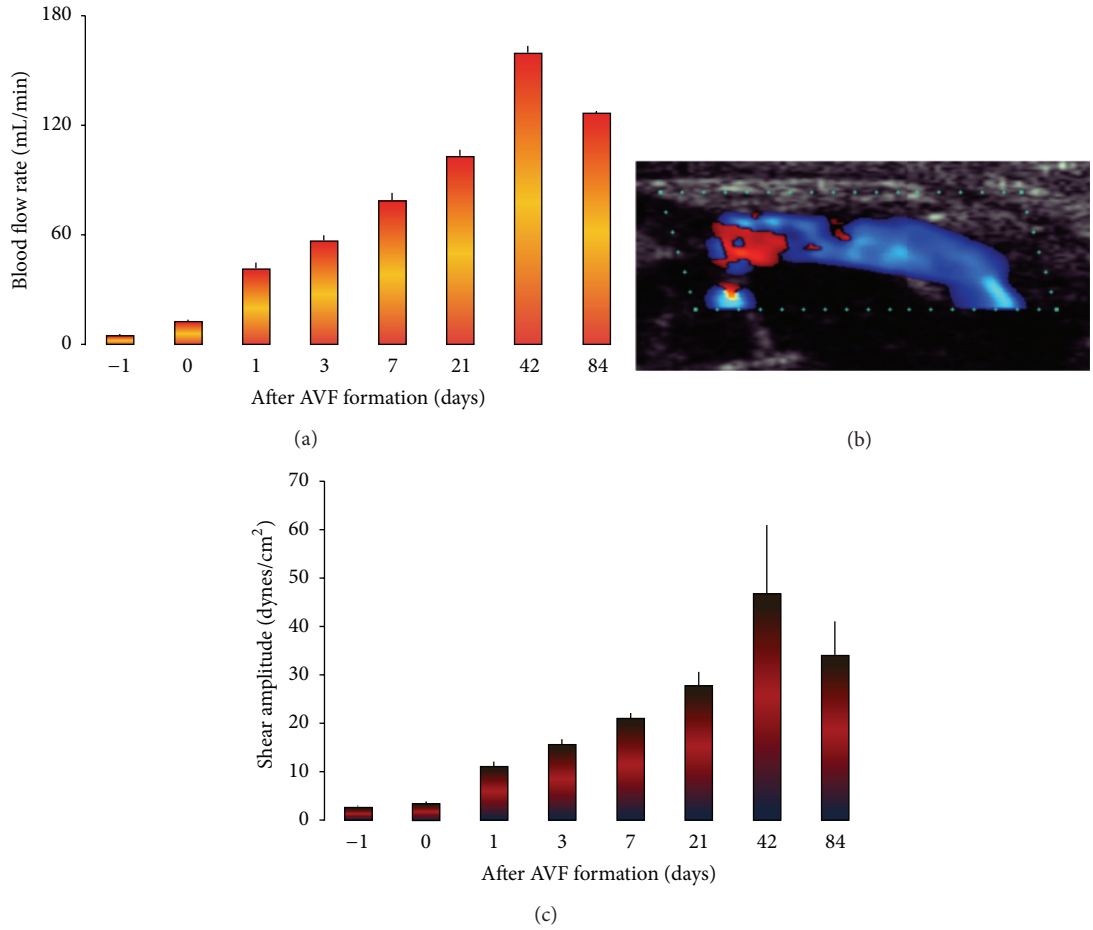

Figure 2: Pulsatile blood flow and shear stress in the arterialized jugular vein. (a) Fistula blood flow rate. (b) Representative Doppler ultrasound image of blood flow through the arterialized jugular vein. Red and blue colors indicate two different blood flow directions, suggesting turbulent blood flow at the proximal fistula. Blue color indicates the same blood flow direction, suggesting laminar blood flow at the through the arterialized jugular vein. (c) Fistula shear stress. Data were expressed as means ± SE ($n = 6$). Day −1: flow in the common carotid artery prior to fistula creation.

($r = 0.8489$, $P < 0.008$; $r = 0.8874$, $P < 0.004$; $r = 0.7734$, $P < 0.03$; resp.).

Hes1 represents the overall activity of Notch signaling. The level of Hes1 expression peaked in the "nidus" vessel wall 42 days after AVF formation, which was 64% greater than the pre-AVF formation ($P < 0.05$). There was a positive correlation between Hes1 expression and time following AVF formation ($r = 0.8185$, $P < 0.02$). This phenomenon was also observed in the expression time-course of Jagged1 (Figure 4).

3.6. Increasing WSS Activates Interaction between Notch Receptors and Their Ligands. Confirmation of interaction events between Notch receptor1 or 4 and Delta1, Delta4, or Jagged1 in the "nidus" vessel wall was performed using *in situ* proximity ligation assay (Figure 5). Proximity ligation revealed that the number of interaction events between Notch receptor1 and Delta1 in the "nidus" vessel wall was significantly upregulated 84 days after AVF formation, which was 23% more than the pre-AVF formation ($P < 0.05$; Figure 6(a)). The number of interaction events between Notch receptor1 and Delta1 was positively correlated with time following AVF formation ($r = 0.716$, $P < 0.05$). The number of interaction events between Notch1 and Delta4 or Notch1 and Jagged1 in the "nidus" vessel wall was significantly upregulated 42 and 84 days after AVF formation, which was 31% and 22% more than the pre-AVF formation, respectively ($P < 0.05$; Figures 6(b) and 6(c)). There was a positive correlation between the number of interaction events between Notch1 and Delta4 or Notch1 and Jagged1 and time following AVF formation ($r = 0.6289$, $P < 0.05$; $r = 0.635$, $P < 0.05$; resp.).

The number of interaction events between Notch4 and Delta1 in the "nidus" vessel wall was positively correlated with time after AVF formation ($r = 0.6727$, $P < 0.05$; Figure 6(d)). The number of interaction events between Notch4 and Delta4 in the "nidus" vessel wall was significantly upregulated 3 days after AVF formation, which ranged from 24% to 35% over a period of day−3 to −84 ($P < 0.05$; Figure 6(e)). The number of interaction events between Notch4 and Delta4 was positively correlated with time post-AVF formation ($r = 0.7285$, $P < 0.05$). The number of interaction events

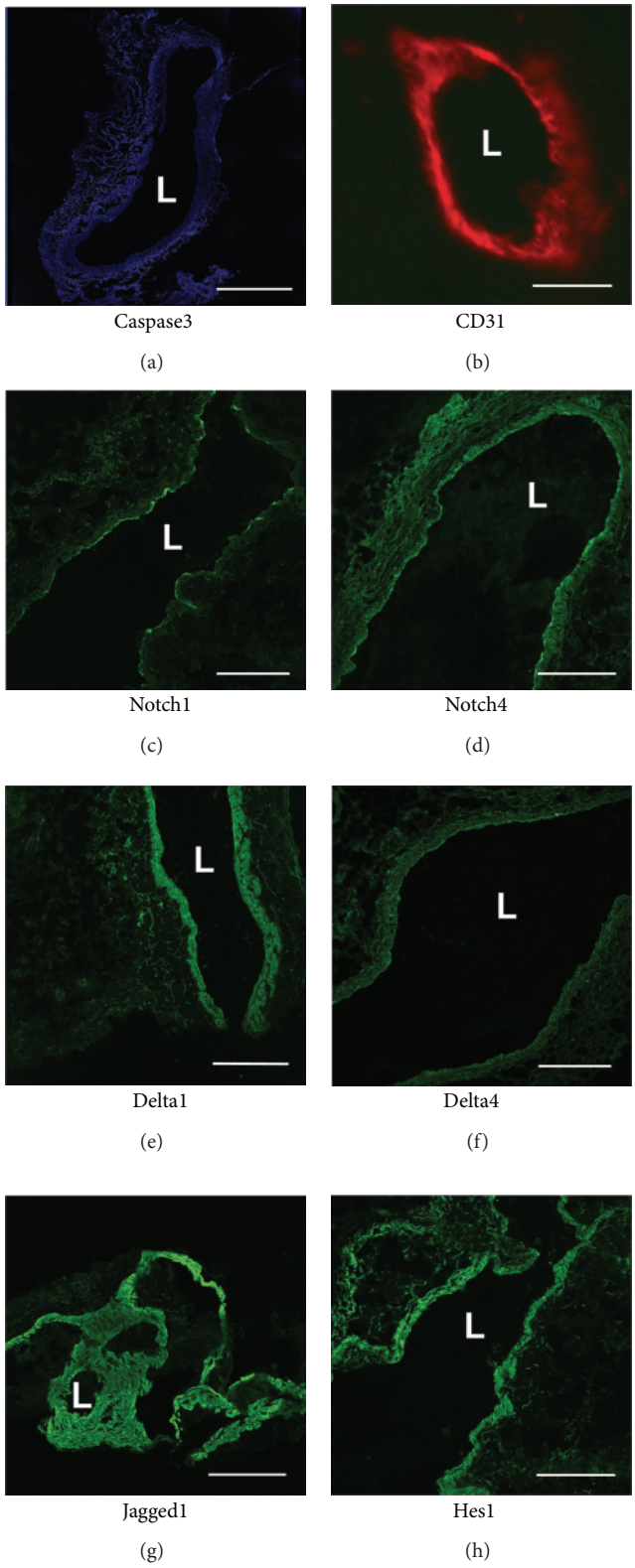

Figure 3: The positive immunofluorescence of caspase3 staining in blue in the "nidus" vessels. CD31 was stained positively in red. The positive immunofluorescence of Notch1 and 4 receptors, their ligands Jagged1, Delta1 and 4, and Notch downstream target Hes1 in green in the "nidus" vessels 42 days after AVF formation. L: lumen. Immunohistochemistry, bar = 300 μm.

between Notch4 and Jagged1 in the "nidus" vessel wall was significantly upregulated 3 days after AVF formation, which ranged from 21% to 35% over a period of day−3 to −84 ($P < 0.05$; Figure 6(f)). The number of interaction events between Notch4 and Jagged1 was positively correlated with time after AVF formation ($r = 0.6937$, $P < 0.05$).

3.7. A Positive Correlation between WSS and the Number of Interaction Events between Notch Receptors and Their Ligands. A positive correlation was observed between an increasing WSS and the interaction events between Notch receptor 1 or 4 and their ligands in the "nidus" vessel wall over a period of 84 days following AVF formation (Figure 7). An increasing WSS positively correlated to an increased interaction events between Notch1 and Delta1 ($r = 0.8943$, $P < 0.003$), Notch1 and Delta4 ($r = 0.8389$, $P < 0.01$), Notch1 and Jagged1 ($r = 0.8743$, $P < 0.005$), Notch4 and Delta1 ($r = 0.9209$, $P < 0.002$), Notch4 and Delta4 ($r = 0.9171$, $P < 0.002$), and Notch4 and Jagged1 ($r = 0.9238$, $P < 0.002$), respectively.

4. Discussion

The hemodynamic state in the human AVMs appears to be altered [2]. An increasing WSS increases the risk of hemorrhage and induces vascular remodeling in the AVM. However, the mechanism remains a mystery. In this study, we compared the changes of hemodynamic state and Notch signaling activation before and after an arteriovenous fistula creation in rats. We found that an increasing WSS enhances the interaction events between Notch receptors and their ligands, resulting in a significant activation of Notch signaling in "nidus" vessels in the rat AVF model. A mechanism of an increasing WSS associated to AVM formation could be through the activation of Notch signaling pathways in blood vessel endothelial cells.

4.1. An Increasing WSS in the AVF Model. The shear stress against the vascular wall of the arterialized vein increased 11-fold over the study period, and shear amplitude linearly correlated with time. In an AVM, the inflow of feeding arteries is pulsatile and blood flow in the nidus is nonuniform, whereas the outflow from draining vein is probably relatively uniform. Vascular walls are elastic, which results in a variable R_i. Poiseuille's equation is applied to transform flow rate into average shear stress. Since wall velocity is always zero, increasing flow rate results in a rise of velocity difference between the flow and the wall surface. The shear stress is directly correlated to the above velocity difference. As observed from our experiments, therefore, increasing flow rate is positively correlated to shear stress even if it is not an accurate quantification. Nevertheless, the level of shear stress shown in this study is a general estimation. It is likely that the molecular changes observed in the model are a response to the shear stress from increased blood flow following AVF formation.

A primary determinant of the hemodynamic nature of AVMs is an increasing WSS within the nidus. This is a function of the narrowest cross-sectional area of the fistula,

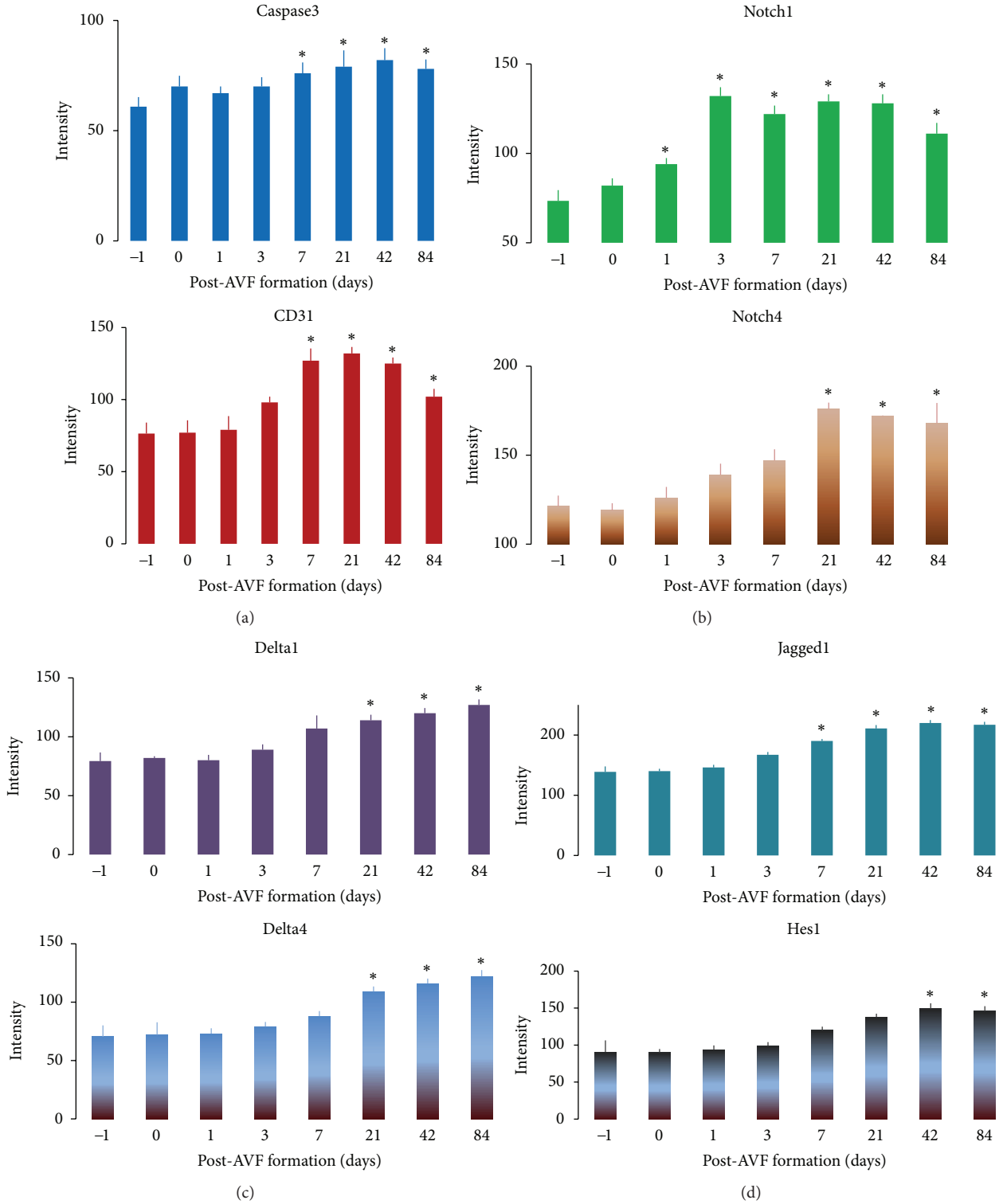

FIGURE 4: The intensity of immunofluorescence of caspase3, CD31 (a), Notch1 and 4 receptors (b), their ligands Delta1 and 4 (c), Jagged1 and Notch downstream target Hes1 (d) in the "nidus" vessels was quantified using a confocal microscope over a period of 84-day after AVF formation. Data were expressed as means ± SE of 4 rats at each time point. $^{*}P < 0.05$ paired comparison between pre- (−1 day) and post-AVF formation at different time points. There was a positive correlation between the intensity of immunofluorescence of caspase3 and time ($r = 0.8866$, $P < 0.005$), Notch4 and time ($r = 0.7252$, $P < 0.05$), Delta1 and time ($r = 0.8489$, $P < 0.008$), Delta4 and time ($r = 0.8874$, $P < 0.004$), and Hes1 and time ($r = 0.8185$, $P < 0.02$) over a period of 84 days after AVF formation.

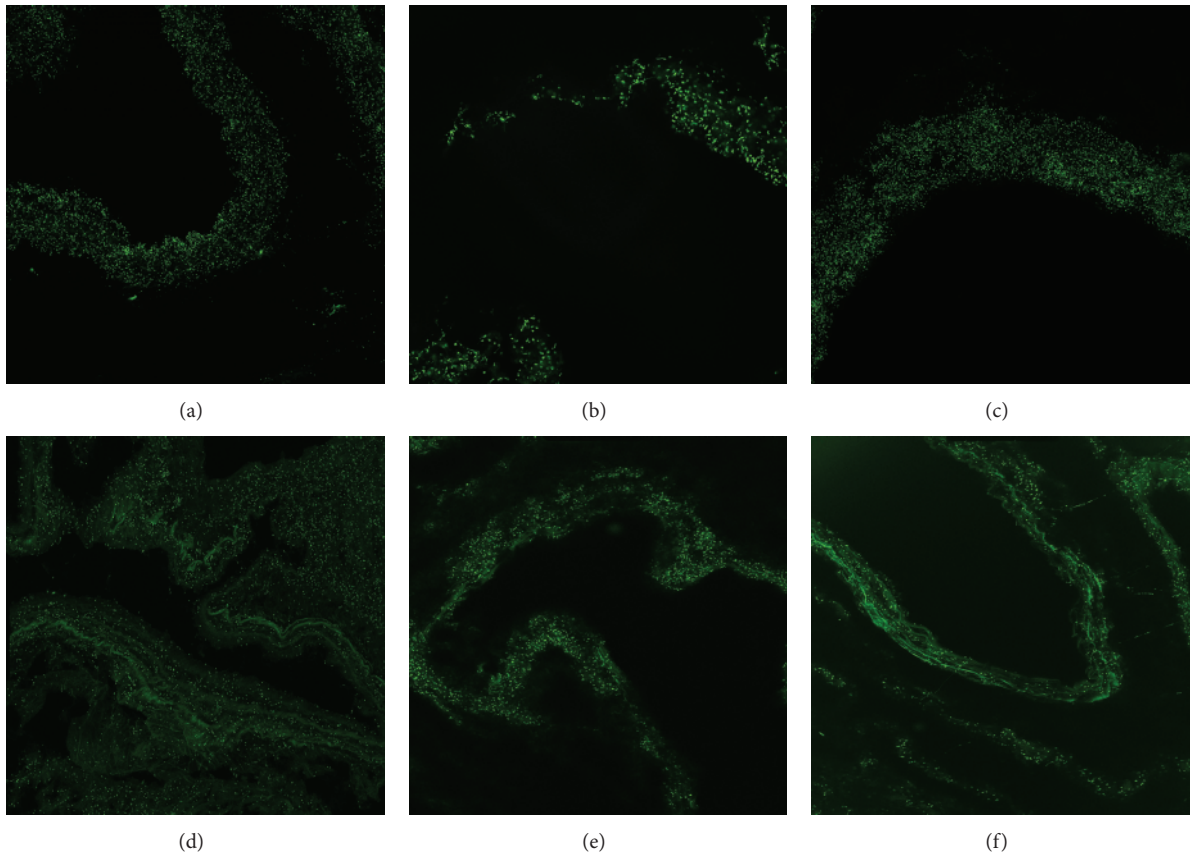

Figure 5: Blood flow shear stress induces the interaction events between Notch receptor1 or 4 and their ligands in the "nidus" vessel wall 42 days after AVF formation. Green dots indicate interaction events: the interaction events between Notch receptor1 and its ligand Delta1 (a), Notch1 and Delta4 (b), Notch1 and Jagged1 (c), Notch receptor4 and Delta1 (d), Notch4 and Delta4 (e), and Notch4 and Jagged1 (f), respectively. *In situ* proximity ligation assay, original magnification ×10 for (a), and ((c)–(f)); ×63 for (b).

with the most significant increases in resistance occurring in the smallest vessels. The majority of AVMs have as their narrowest point vessels that are greater in diameter than normal capillaries and therefore have a lower resistance than the normal cerebral vasculature [3, 4, 36]. Lower resistance and increased vessel diameter in the nidus lead to increased flow velocity. An important consequence of high flow through the fistula is hypotension in the dilated feeding arteries [3, 4]. This situation is predicted from Poiseuille's equation and has been confirmed in human AVMs by measurement of intra-arterial pressures by direct puncture or superselective catheterization [37]. Reported pressures vary from 45 to 71% of concurrently measured femoral or radial artery pressures [3]. This is significantly lower than normal distal pial arterial pressure, these being around 90% of systemic arterial pressure.

The draining veins appear to be relatively hypertensive compared with normal cerebral veins [4]. Hypertension has been confirmed by pressure measurements in the superficial draining veins at surgery. Deep veins are more difficult to access, although angiographic findings of slower transit of contrast in the deep system relative to the superficial system suggest higher pressures in the deep system [4]. The pathogenesis of spontaneous hemorrhage from AVMs is likely to be multifactorial, involving both anatomical and physiological components. High transmural pressures associated with vascular wall fragility would be expected to produce hemorrhage. It has been reported that the likelihood of presentation with hemorrhage from an AVM was positively correlated with feeding artery pressures [38]. This may explain why larger AVMs, having lower feeding artery pressures, appear to present less frequently with hemorrhage. Higher feeding artery pressures in small AVMs may lead to larger volume hemorrhages due to a higher driving arterial force [4]. An increase in venous resistance due to venous drainage occlusion or stenosis may increase the risk of hemorrhage [3, 4]. Platelet aggregation and thrombosis that occur secondary to turbulence in the nidus and draining veins may compromise the outflow of the lesion and cause hemorrhage.

4.2. An Increasing WSS Activates Notch Signaling in the Rat AVF Model. We found that an increasing WSS activates Notch receptors and their ligands in the rat AVF model. The pathogenesis of AVMs was related to the alteration of molecular signaling pathways that regulate vascular homeostasis [39, 40]. The Notch signaling pathway is hypothesized to contribute to AVM pathogenesis via abnormal regulation of vascular development and maintenance. Notch signaling

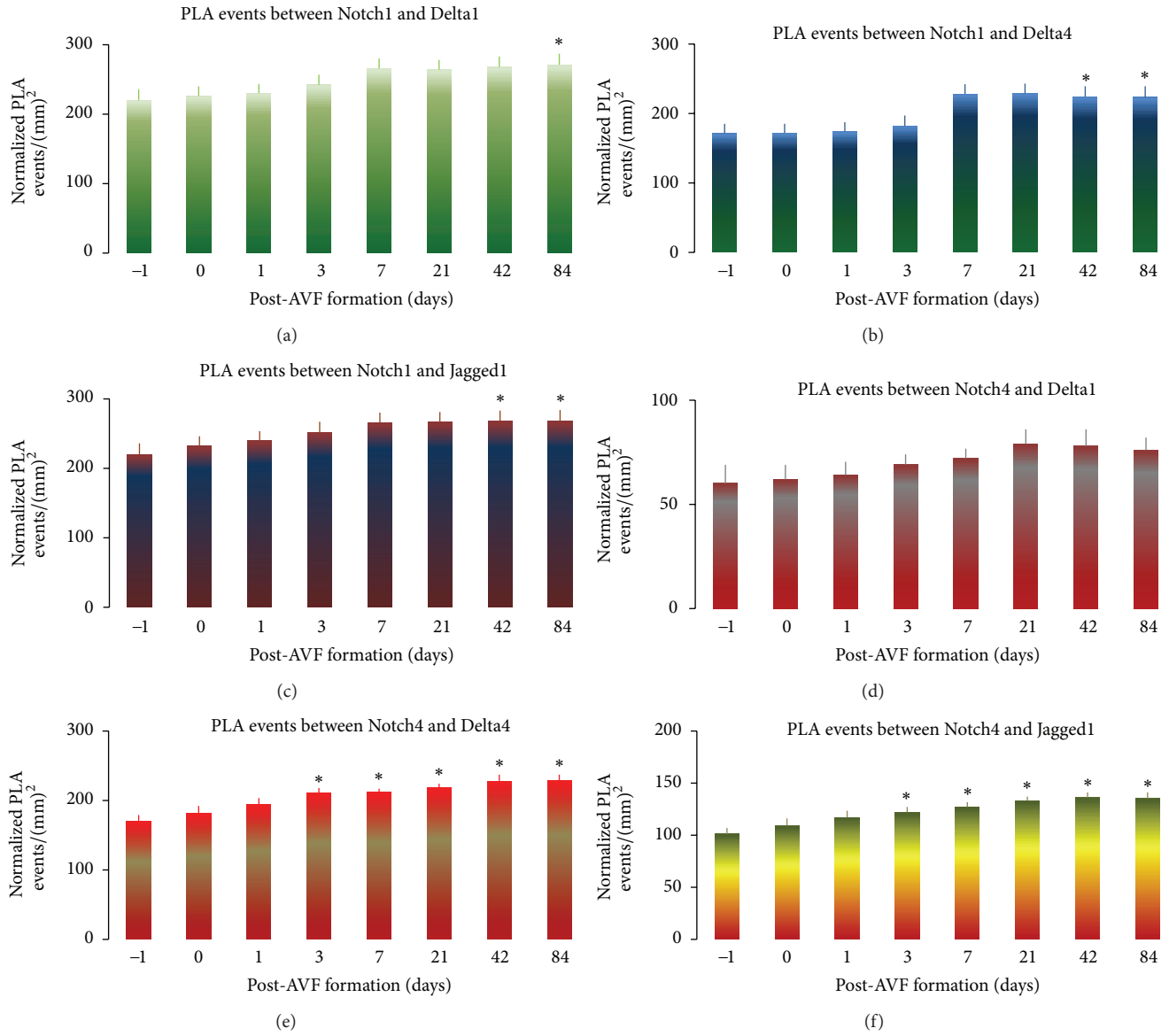

FIGURE 6: Blood flow shear stress increases interaction events between Notch receptor1 or 4 and their ligands in the "nidus" vessel wall with time over a period of 84 days after AVF formation. Time-course of interaction events between Notch receptor1 and its ligand Delta1 ((a); $r = 0.716$, $P < 0.05$), Notch1 and Delta4 ((b); $r = 0.6289$, $P < 0.05$), Notch1 and Jagged1 ((c); $r = 0.635$, $P < 0.05$), Notch receptor4 and Delta1 ((d); $r = 0.6727$, $P < 0.05$), Notch4 and Delta4 ((e); $r = 0.7258$, $P < 0.05$), and Notch4 and Jagged1 ((f); $r = 0.6937$, $P < 0.05$), respectively. Data were expressed as means ± SE of 4 rats at each time point. $^*P < 0.05$ paired comparison between pre- (−1 day) and post-AVF formation at different time points.

activation was ubiquitous in that activation was observed in both Notch1 and 4 via interaction with their ligands Delta1, Delta4 and Jagged1. The expression of Notch1 and 4, Delta1, Delta4 and Jagged1, and Notch downstream target Hes1 was observed in the endothelial cells of "nidus" vessels in the rat AVF model. The expression of multiple receptors and ligands indicates that activated Notch1 and Notch4 signaling pathways interact between each other. As Hes1 is a downstream target of both activated Notch1 and Notch4 signaling pathways [41], its expression in the endothelial cells of "nidus" vessels in the AVF rats indicates overall activation of Notch signaling in both pathways.

Notch1 and 4 signaling was activated through interaction with Delta1, Delta4, and Jagged1 in the endothelial cells of AVMs. Evidence obtained from loss of function studies supports a critical function of Notch1- and Notch4-mediated signaling in vascular maintenance; disruption of Notch1 results in vascular immaturity and hyperplasia, and even death due to vascular complications [18]. Activation of Notch1 signaling has been reported to result in vessel enlargement and the arteriovenous communication [9, 11]. Notch4 signaling was also activated through interaction with Delta1, Delta4, and Jagged1 in the endothelial cells in the rat AVF model. Previous studies have demonstrated that increasing Notch4 activation

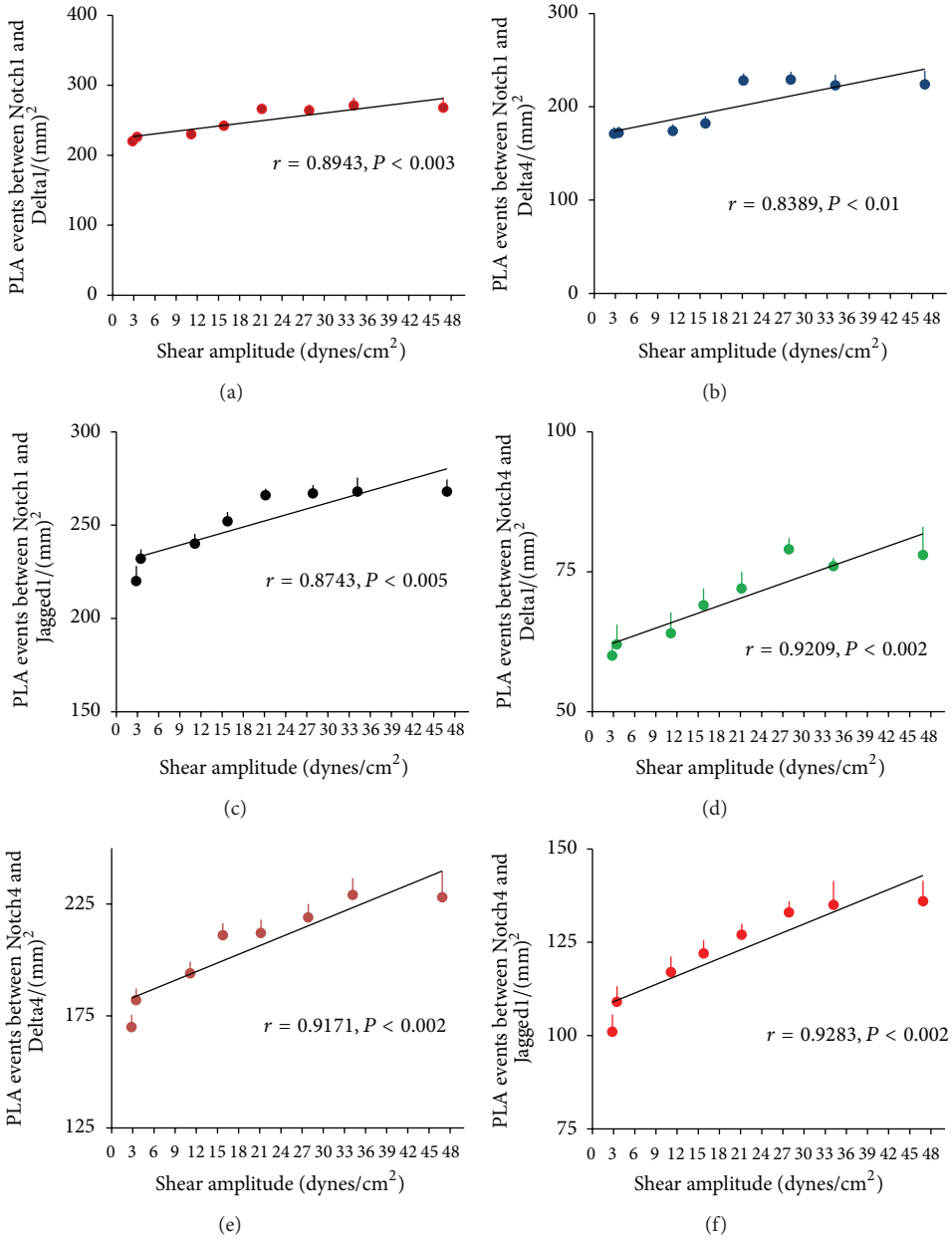

FIGURE 7: A positive correlation between WSS and the interaction events between Notch receptor1 or 4 and their ligands in the "nidus" vessel wall over a period of 84 days after AVF formation. A positive correlation between WSS and the interaction events between Notch1 and Delta1 (a), Notch1 and Delta4 (b), Notch1 and Jagged1 (c), Notch4 and Delta1 (d), Notch4 and Delta4 (e), and Notch4 and Jagged1 (f), respectively. Data were expressed as means ± SE of 4 rats at each time point. $^*P < 0.05$ paired comparison between pre- (−1 day) and post-AVF formation at different time points.

in the mouse vasculature produces dilated vessels, reduced smooth muscle cell populations, and arteriovenous communications within the cerebral circulation [10]. Studies also demonstrated the cessation of Notch4 activation stops the progression vascular abnormalities and promotes reversion to the normal vasculature [13]. The observed expression of Notch1 and 4 activation in the endothelial cells of "nidus" vessels in the rat AVF model suggests that an increasing WSS contributes to AVM formation.

The interaction between Notch receptors and their ligand in the vascular development and homeostasis has yet fully characterized. Notch ligands are known to display different binding affinities and suborgan patterns of expression [42]. It would appear that ligand-specific function is dictated by the geographical location of the receptor. Delta1 is expressed in the venous and arterial vasculature during angiogenesis [43]. Inactivation of Delta1 has been observed to impact the overall strength and integrity of the vascular wall [19].

It has been hypothesized that activation of Notch signaling through Delta1 might be associated with the abnormal vascular maturation and arteriovenous specification [25]. Delta4 is expressed throughout the development of both veins and arteries. Delta4 mimics the expression of Notch1 and has been suggested to be the primary activator of Notch1 during angiogenesis [43]. Inactivation of Delta4 has been shown to disrupt remodeling of the vascular plexus with complications in the organization of the vascular bed, vessel diameter, arterial branching, and arteriovenous communication and inhibition of vessel sprouting during angiogenesis [20, 21, 44]. Jagged1 is expressed throughout the development of vasculature [16, 42]. Inactivation of Jagged1 results in insufficient remodeling of the vascular plexus with the loss of vascular integrity and depleted smooth muscle cell population [22, 23]. Jagged1 is involved in insufficient homeostatic maintenance of the tunica media in AVM pathogenesis. Notch activation controls endothelial cell behavior via which receptor-ligand interaction is modified independent of transcriptional regulation, posttranslational modification, and cellular trafficking. Briefly, Notch ligands on the signal-sending cell trigger Notch1 or 4 on the adjacent signal-receiving cell, leading to sequential receptor cleavages within the transmembrane domain, resulting in the release of the Notch intracellular domain (NICD). NICD moves into the signal-receiving cell nucleus and binds to transcriptional factor j kappa-recombination signal-binding protein (RBP-j). Association of NICD and RBP-j replaces the core-pressors with a coactivating complex containing Mastermind-like protein and activates the transcription of target genes such as Hes. The activated Notch signaling downregulates vascular endothelial growth factor (VEGF) receptor2 and upregulates VEGF receptor1, leading to cell differentiation during angiogenesis [17, 45, 46]. In this study, the expression of Notch receptor1 and 4, Jagged1, Delta-like1 and Delta-like4, and Hes1 suggests that upregulation of Notch signaling in response to an increasing WSS is via a "universal" modulator that does not discriminate between ligand or receptor type.

It is generally considered that AVMs are congenital abnormalities that fail to regress [47]; however, by suppressing Notch4 transgene could result in reprograming arterial endothelial cells in the enlarged AVM vessels to a venous endothelial cell specification, leading to a decrease in AVM vessel size [13]. Observation of postnatal AVM formation [48] and the reoccurrence of de novo AVM growth in the adult vasculature after surgical resection [49, 50] support the notion that AVMs are dynamic and proliferative pathologies. This study suggests that WSS could activate reprograming of vascular endothelial cells of AVMs by activation of Notch receptors and their ligands.

A question that pertains to the implication of Notch signaling in the rat AVF model is whether Notch activation is due to angiogenesis or is a secondary effect of endothelium response to an altered state of hemodynamic stress following an AV-fistula formation. VEGF was upregulated in the "nidus" vessels of the rat AVF model over a period of 84 days after creation of an AV-fistula [29], suggesting that angiogenesis occurred. In the current study, examination of "nidus" vessels in the same AVF model revealed that Notch signaling was activated in the endothelial cells of AVM-like vessels. It is possible that an increased hemodynamic stress following an AV-fistula formation induces the activation of Notch signaling, contributing to the angiogenesis of AVM "nidus."

5. Conclusions

An increasing vascular wall shear stress induces apoptosis, and activates Notch1 and 4 signalling pathways in blood vessel endothelial cells, which may contribute to the angiogenesis of AVMs, suggesting a possible mechanism associated with AVM formation and/or reoccurrence of AVMs after surgical resection. This mechanism requires further validation in human.

Abbreviations

AVF: Arteriovenous fistula
AVMs: Arteriovenous malformations
CCA: Common carotid artery
EJV: External jugular vein
FIU: Fluorescence intensity units
PLA: Proximity ligation assay
WSS: Wall shear stress.

Conflict of Interests

The authors do not have any conflict of interests with the content of the paper.

Acknowledgments

This study was partially supported by an Australian Research Council Discovery Project Grant (DP0986183) to Jian Tu, a China-New South Wales Research Collaborative Program Grant to Jian Tu and Zhiqiang Hu; a postgraduate scholarship for overseas study from Shanghai Jiao Tong University, Shanghai, China, to Yang Li.

References

[1] R. M. Starke, C. Yen, D. Ding, and J. P. Sheehan, "A practical grading scale for predicting outcome after radiosurgery for arteriovenous malformations: analysis of 1012 treated patients," *Journal of Neurosurgery*, vol. 119, no. 4, pp. 981–987, 2013.

[2] S. Yamada, F. S. Brauer, A. R. T. Colohan et al., "Concept of arteriovenous malformation compartments and surgical management," *Neurological Research*, vol. 26, no. 3, pp. 288–300, 2004.

[3] M. Morgan and M. Winder, "Haemodynamics of arteriovenous malformations of the brain and consequences of resection: a review," *Journal of Clinical Neuroscience*, vol. 8, no. 3, pp. 216–224, 2001.

[4] W. L. Young, "Intracranial arteriovenous malformations. pathophysiology and hemodynamics," in *Vascular Malformations of the Central Nervous System*, J. J. Jafar, I. A. Awad, and R. H. Rosenwasser, Eds., pp. 95–126, Lippincott Williams & Wilkins, Philadelphia, Pa, USA, 1999.

[5] T. Hashimoto, R. Mesa-Tejada, C. M. Quick et al., "Evidence of increased endothelial cell turnover in brain arteriovenous malformations," *Neurosurgery*, vol. 49, no. 1, pp. 124–132, 2001.

[6] G. R. Sutherland, M. E. King, C. G. Drake, S. J. Peerless, and W. C. Vezina, "Platelet aggregation within cerebral arteriovenous malformations," *Journal of Neurosurgery*, vol. 68, no. 2, pp. 198–204, 1988.

[7] M. R. Harrigan, N. Ole-Schmidt, P. M. Black et al., "Angiogenic factors in the central nervous system," *Neurosurgery*, vol. 53, no. 3, pp. 639–661, 2003.

[8] P. A. Murphy, G. Lu, S. Shiah, A. W. Bollen, and R. A. Wang, "Endothelial Notch signaling is upregulated in human brain arteriovenous malformations and a mouse model of the disease," *Laboratory Investigation*, vol. 89, no. 9, pp. 971–982, 2009.

[9] Q. Zhuge, M. Zhong, W. Zheng et al., "Notch-1 signalling is activated in brain arteriovenous malformations in humans," *Brain*, vol. 132, no. 12, pp. 3231–3241, 2009.

[10] T. R. Carlson, Y. Yan, X. Wu et al., "Endothelial expression of constitutively active Notch4 elicits reversible arteriovenous malformations in adult mice," *Proceedings of the National Academy of Sciences of the United States of America*, vol. 102, no. 28, pp. 9884–9889, 2005.

[11] L. T. Krebs, C. Starling, A. V. Chervonsky, and T. Gridley, "Notch1 activation in mice causes arteriovenous malformations phenocopied by EphrinB2 and EphB4 mutants," *Genesis*, vol. 48, no. 3, pp. 146–150, 2010.

[12] P. A. Murphy, M. T. Y. Lam, X. Wu et al., "Endothelial Notch4 signaling induces hallmarks of brain arteriovenous malformations in mice," *Proceedings of the National Academy of Sciences of the United States of America*, vol. 105, no. 31, pp. 10901–10906, 2008.

[13] P. A. Murphy, T. N. Kim, G. Lu, A. W. Bollen, C. B. Schaffer, and R. A. Wang, "Notch4 normalization reduces blood vessel size in arteriovenous malformations," *Science Translational Medicine*, vol. 4, no. 117, p. 117ra8, 2012.

[14] S. S. Nijjar, H. A. Crosby, L. Wallace, S. G. Hubscher, and A. J. Strain, "Notch receptor expression in adult human liver: a possible role in bile duct formation and hepatic neovascularization," *Hepatology*, vol. 34, no. 6, pp. 1184–1192, 2001.

[15] V. Lindner, C. Booth, I. Prudovsky, D. Small, T. Maciag, and L. Liaw, "Members of the Jagged/Notch gene families are expressed in injured arteries and regulate cell phenotype via alterations in cell matrix and cell-cell interaction," *American Journal of Pathology*, vol. 159, no. 3, pp. 875–883, 2001.

[16] N. Villa, L. Walker, C. E. Lindsell, J. Gasson, M. L. Iruela-Arispe, and G. Weinmaster, "Vascular expression of Notch pathway receptors and ligands is restricted to arterial vessels," *Mechanisms of Development*, vol. 108, no. 1-2, pp. 161–164, 2001.

[17] S. P. Herbert and D. Y. R. Stainier, "Molecular control of endothelial cell behaviour during blood vessel morphogenesis," *Nature Reviews Molecular Cell Biology*, vol. 12, no. 9, pp. 551–564, 2011.

[18] Z. Liu, A. Turkoz, E. N. Jackson et al., "Notch1 loss of heterozygosity causes vascular tumors and lethal hemorrhage in mice," *Journal of Clinical Investigation*, vol. 121, no. 2, pp. 800–808, 2011.

[19] M. H. De Angelis, J. McIntyre II, and A. Gossler, "Maintenance of somite borders in mice requires the Delta homologue Dll1," *Nature*, vol. 386, no. 6626, pp. 717–721, 1997.

[20] A. Duarte, M. Hirashima, R. Benedito et al., "Dosage-sensitive requirement for mouse Dll4 in artery development," *Genes and Development*, vol. 18, no. 20, pp. 2474–2478, 2004.

[21] N. W. Gale, M. G. Dominguez, I. Noguera et al., "Haploinsufficiency of delta-like 4 ligand results in embryonic lethality due to major defects in arterial and vascular development," *Proceedings of the National Academy of Sciences of the United States of America*, vol. 101, no. 45, pp. 15949–15954, 2004.

[22] F. A. High, M. L. Min, W. S. Pear, K. M. Loomes, K. H. Kaestner, and J. A. Epstein, "Endothelial expression of the Notch ligand Jagged1 is required for vascular smooth muscle development," *Proceedings of the National Academy of Sciences of the United States of America*, vol. 105, no. 6, pp. 1955–1959, 2008.

[23] Y. Xue, X. Gao, C. E. Lindsell et al., "Embryonic lethality and vascular defects in mice lacking the Notch ligand Jagged1," *Human Molecular Genetics*, vol. 8, no. 5, pp. 723–730, 1999.

[24] I. N. King, I. S. Kathiriya, M. Murakami et al., "Hrt and Hes negatively regulate Notch signaling through interactions with RBP-Jκ," *Biochemical and Biophysical Research Communications*, vol. 345, no. 1, pp. 446–452, 2006.

[25] A. Limbourg, M. Ploom, D. Elligsen et al., "Notch ligand delta-like 1 is essential for postnatal arteriogenesis," *Circulation Research*, vol. 100, no. 3, pp. 363–371, 2007.

[26] National Health and Medical Research Council, "Australian code of practice for the care and use of animals for scientific purposes," 7th ed., 2004, http://www.nhmrc.gov.au/_files_nhmrc/publications/attachments/ea16.pdf.

[27] R. Yassari, T. Sayama, B. S. Jahromi et al., "Angiographic, hemodynamic and histological characterization of an arteriovenous fistula in rats," *Acta Neurochirurgica*, vol. 146, no. 5, pp. 495–504, 2004.

[28] K. P. Storer, J. Tu, M. A. Stoodley, and R. I. Smee, "Expression of endothelial adhesion molecules after radiosurgery in an animal model of arteriovenous malformation," *Neurosurgery*, vol. 67, no. 4, pp. 976–983, 2010.

[29] A. Karunanyaka, J. Tu, A. Watling, K. P. Storer, A. Windsor, and M. A. Stoodley, "Endothelial molecular changes in a rodent model of arteriovenous malformation: laboratory investigation," *Journal of Neurosurgery*, vol. 109, no. 6, pp. 1165–1172, 2008.

[30] J. Tu, Z. Hu, and Z. Chen, "Endothelial gene expression and molecular changes in response to radiosurgery in in vitro and in vivo models of cerebral arteriovenous malformations," *BioMed Research International*, vol. 2013, Article ID 408253, 10 pages, 2013.

[31] K. Storer, J. Tu, A. Karunanayaka et al., "Coadministration of low-dose lipopolysaccharide and soluble tissue factor induces thrombosis after radiosurgery in an animal arteriovenous malformation model," *Neurosurgery*, vol. 61, no. 3, pp. 604–610, 2007.

[32] W. L. Young, E. Gao, G. J. Hademenos, and T. F. Massoud, "Use of modeling for the study of cerebral arteriovenous malformations," in *Intracranial Arteriovenous Malformations*, P. E. Stieg, H. H. Batjer, and L. Samson, Eds., pp. 49–71, Informa Healthcare, New York, NY, USA, 2007.

[33] J. Tu, Z. Hu, and Z. Chen, "A combination of radiosurgery and soluble tissue factor enhances vascular targeting for experimental glioblastoma," *BioMed Research International*, vol. 2013, Article ID 390714, 11 pages, 2013.

[34] J. Tu and N. F. Jufri, "Estrogen signaling through estrogen receptor beta and G-protein-coupled estrogen receptor 1 in human cerebral vascular endothelial cells: implications for cerebral aneurysms," *BioMed Research International*, vol. 2013, Article ID 524324, 9 pages, 2013.

[35] J. L. Hintze, "Analysis of variance," in *Number Cruncher Statistical Systems (NCSS) 97-USer's Guide-I*, pp. 205–278, Kaysville, Utah, USA, 1997.

[36] G. J. Hademenos and T. F. Massoud, "The physics of intracranial arteriovenous malformations," in *The Physics of Cerebrovascular Diseases*, pp. 238–290, Springer, New York, NY, USA, 1998.

[37] P. Fogarty-Mack, J. Pile-Spellman, L. Hacein-Bey et al., "The effect of arteriovenous malformations on the distribution of intracerebral arterial pressures," *American Journal of Neuroradiology*, vol. 17, no. 8, pp. 1443–1449, 1996.

[38] D. H. Duong, W. L. Young, M. C. Vang et al., "Feeding artery pressure and venous drainage pattern are primary determinants of hemorrhage from cerebral arteriovenous malformations," *Stroke*, vol. 29, no. 6, pp. 1167–1176, 1998.

[39] B. Larrivée, C. Prahst, E. Gordon et al., "ALK1 signaling inhibits angiogenesis by cooperating with the notch pathway," *Developmental Cell*, vol. 22, no. 3, pp. 489–500, 2012.

[40] G. G. Leblanc, E. Golanov, I. A. Awad, and W. L. Young, "Biology of vascular malformations of the brain," *Stroke*, vol. 40, no. 12, pp. e694–e702, 2009.

[41] S. Jarriault, C. Brou, F. Logeat, E. H. Schroeter, R. Kopan, and A. Israel, "Signalling downstream of activated mammalian notch," *Nature*, vol. 377, no. 6547, pp. 355–358, 1995.

[42] J. J. Hofmann and M. L. Iruela-Arispe, "Notch signaling in blood vessels: who is talking to whom about what?" *Circulation Research*, vol. 100, no. 11, pp. 1556–1568, 2007.

[43] J. J. Hofmann and M. Luisa Iruela-Arispe, "Notch expression patterns in the retina: an eye on receptor-ligand distribution during angiogenesis," *Gene Expression Patterns*, vol. 7, no. 4, pp. 461–470, 2007.

[44] M. Hellström, L.-K. Phng, J. J. Hofmann et al., "Dll4 signalling through Notch1 regulates formation of tip cells during angiogenesis," *Nature*, vol. 445, no. 7129, pp. 776–780, 2007.

[45] G.-R. Dou, L. Wang, Y.-S. Wang, and H. Han, "Notch signaling in ocular vasculature development and diseases," *Molecular Medicine*, vol. 18, no. 1, pp. 47–55, 2012.

[46] D. Nichol and H. Stuhlmann, "EGFL7: a unique angiogenic signaling factor in vascular development and disease," *Blood*, vol. 119, no. 6, pp. 1345–1352, 2012.

[47] M. Vikkula, L. M. Boon, J. B. Mulliken, and B. R. Olsen, "Molecular basis of vascular anomalies," *Trends in Cardiovascular Medicine*, vol. 8, no. 7, pp. 281–292, 1998.

[48] R. L. Jeffree and M. A. Stoodley, "Postnatal development of arteriovenous malformations," *Pediatric Neurosurgery*, vol. 45, no. 4, pp. 296–304, 2009.

[49] K. R. Bulsara, M. J. Alexander, A. T. Villavicencio et al., "De novo cerebral arteriovenous malformation: case report," *Neurosurgery*, vol. 50, no. 5, pp. 1137–1141, 2002.

[50] O. A. Harris, S. D. Chang, B. T. Harris, and J. R. Adler, "Acquired cerebral arteriovenous malformation induced by an anaplastic astrocytoma: an interesting case," *Neurological Research*, vol. 22, no. 5, pp. 473–477, 2000.

Hindawi Publishing Corporation
BioMed Research International
Volume 2014, Article ID 970741, 11 pages
http://dx.doi.org/10.1155/2014/970741

Clinical Study

Continuous Selective Intra-Arterial Application of Nimodipine in Refractory Cerebral Vasospasm due to Aneurysmal Subarachnoid Hemorrhage

Stephanie Ott,[1] Sheila Jedlicka,[1] Stefan Wolf,[2] Mozes Peter,[3] Christine Pudenz,[1] Patrick Merker,[4] Ludwig Schürer,[1] and Christianto Benjamin Lumenta[1]

[1] *Department of Neurosurgery, Academic Teaching Hospital Munich-Bogenhausen, Technical University of Munich, Englschalkinger Straße 77, 81925 Munich, Germany*
[2] *Department of Neurosurgery, Charité University Hospital, Augustenburger Platz 1, 13353 Berlin, Germany*
[3] *Department of Radiology, Academic Teaching Hospital Munich-Bogenhausen, Technical University of Munich, Englschalkinger Straße 77, 81925 Munich, Germany*
[4] *Department of Neurosurgery, Academic Teaching Hospital Munich-Schwabing, Ludwig Maximilian University of Munich, Kölner Platz 1, 80804 Munich, Germany*

Correspondence should be addressed to Stephanie Ott; stephanie.ott@lrz.tu-muenchen.de

Received 13 September 2013; Revised 8 December 2013; Accepted 11 December 2013; Published 16 January 2014

Academic Editor: Robert M. Starke

Background. Cerebral vasospasm is one of the leading courses for disability in aneurysmal subarachnoid hemorrhage. Effective treatment of vasospasm is therefore one of the main priorities for these patients. We report about a case series of continuous intra-arterial infusion of the calcium channel antagonist nimodipine for 1–5 days on the intensive care unit. *Methods*. In thirty patients with aneurysmal subarachnoid hemorrhage and refractory vasospasm continuous infusion of nimodipine was started on the neurosurgical intensive care unit. The effect of nimodipine on brain perfusion, cerebral blood flow, brain tissue oxygenation, and blood flow velocity in cerebral arteries was monitored. *Results*. Based on Hunt & Hess grades on admission, 83% survived in a good clinical condition and 23% recovered without an apparent neurological deficit. Persistent ischemic areas were seen in 100% of patients with GOS 1–3 and in 69% of GOS 4-5 patients. Regional cerebral blood flow and computed tomography perfusion scanning showed adequate correlation with nimodipine application and angiographic vasospasm. Transcranial Doppler turned out to be unreliable with interexaminer variance and failure of detecting vasospasm or missing the improvement. *Conclusion*. Local continuous intra-arterial nimodipine treatment for refractory cerebral vasospasm after aSAH can be recommended as a low-risk treatment in addition to established endovascular therapies.

1. Introduction

The incidence of aneurysmal subarachnoid hemorrhage is located between 6 and 8 people out of every 100,000 each year [1, 2]. 46% [1] to over 50% [3] of patients die within the first two weeks of their aSAH. Medical care is not reached by about 10–15% [4]. Complications such as neurogenic pulmonary edema or neurogenic stunned myocardium kill 25% of the treated patients [5]. Vasospasm is one of the main causes for prolonged neurologic deficit in patients who reach either neurosurgical or endovascular treatment for the aneurysm. 7% die of vasospasm and another 7% develop severe neurologic deficit [6]. Treatment of vasospasm is therefore one of the main priorities for these patients.

Mechanical endovascular interventions such as balloon angioplasty or stenting are options for vasospasm of the great vessels; however, the distally located smaller vessels cannot be reached by the neuroradiologist and therefore need to be treated with pharmacologic agents [7]. Amrinone [8], l-arginine [9], colforsin daropate hydrochloride [10], papaverine [11], verapamil [12], nicardipine [13], and nimodipine

[14, 15] have been tested for their effect on vasospasm, but none have shown significant difference to the others.

The pharmacological effect on the vessels is in some cases limited to the period of infusion—either the procedure has to be repeated [16] or the agent has to be applied continuously for a few days until there is no more evidence of vasospasm in neuromonitoring and angiography.

At our hospital all patients with aSAH are treated with intravenous or oral nimodipine from the day of admission for at least 21 days. Patients with detected vasospasm on angiography receive intra-arterial nimodipine as a bolus application in the angiography unit. Side effects as rapid increase in ICP, thrombocytopenia, seizures, transient neurologic deficits (mydriasis and brainstem depression), monocular blindness, and paradoxical worsening of vasospasm as it is reported for intra-arterial papaverine [16–19] were not seen.

We want to report our experience with continuous selective intra-arterial infusion of nimodipine via a catheter in the internal carotid artery in refractory cerebral vasospasm.

2. Materials and Methods

2.1. Patient Population. From March 2006 until July 2013, 27 patients, who suffered aneurysmal subarachnoid hemorrhage and developed cerebral vasospasm refractory to standard hyperdynamic and endovascular therapy, were respectfully treated with locally infused nimodipine via catheter in the internal carotid artery for minimum of one day at the neurosurgical intensive care unit at the Academic Teaching Hospital of the Technical University of Munich, Klinikum Munich-Bogenhausen. Two patients with clipped incidental median cerebral artery (MCA)-aneurysms, who developed refractory vasospasm seven and five days after the operation, were included as well. One patient was treated at the interdisciplinary surgical intensive care unit at the academic teaching hospital of the Ludwig Maximilian University Munich, Klinikum Munich-Schwabing. Data from 2006 to September 2009 were analyzed retrospectively. During that period of time, nine patients were treated by continuous infusion of intra-arterial nimodipine. All patients, who were treated from October 2009 to July 2013, were included in the study prospectively. No patient was excluded. Randomization was not performed.

2.2. Management of Subarachnoid Hemorrhage. In 26 patients, the aneurysm, causing the hemorrhage, was clipped. There was one reclipping of a right-sided media aneurysm located at the bifurcation. Vasospasm occurred nine days after the second operation. In one case, there was only a distal median cerebral artery (segment 1 (M1)-) aneurysm, diagnosed in the computed tomography angiography, which was clipped. After rebleeding, a digital subtraction angiography was performed, showing a second aneurysm located at the supraclinoidal internal carotid artery (ICA), which wascoiled in the same session. The MCA aneurysm was shown to be completely obstructed by the clip. We therefore proposed that the ICA aneurysm had been ruptured initially. One patient with a communicating artery aneurysm died before treatment of the aneurysm. We recorded only two patients who were exclusively treated by coiling.

Detection of vasospasm depended on the initial Hunt & Hess grade. Patients grouped from H&H 0–2 usually developed either a focal neurologic deficit, for example, speech disturbance and hemiparesis, or loss of consciousness. Those who were classified as Hunt & Hess 3 or higher on admission were monitored with regional cerebral blood flow (rCBF) with the Bowman system (Hemedex Inc., Cambridge, MA, USA) and local tissue oxygenation with Licox probes (Integra Neuroscience, Andover, UK). External ventricular drainages were placed in the right lateral ventricle to measure intracranial pressure and drain cerebrospinal fluid (CSF) when necessary. If Hunt & Hess 0–2 patients lost consciousness due to vasospasm or other reason they were monitored equally to the Hunt & Hess 3+ patients. When angiography was performed prior to placing rCBF and ptiO2 probes, they were located in an area supplied by a vasospastic vessel. Depending on CSF circulation an external ventricular drainage or a parenchymal probe was placed.

Data were monitored by ICUpilot (CMA, Solna, Sweden) with sampling frequency of 1/min. Depth of anesthesia could be supervised with bispectral index (BIS) (Covidien Healthcare).

Transcranial Doppler measurements were taken daily or every second day.

2.3. Management of Vasospasm. After clipping or coiling of the aneurysm systolic blood pressure was elevated to 150 mmHg. When detecting vasospasm we started standard triple H therapy with hypertension, hypervolemia, and hemodilution.

In cases of neurologic or neuromonitoring parameter deterioration, a CAT scan in combination with perfusion CT was performed to rule out causes other than vasospasm and to detect areas of reduced or delayed cerebral perfusion and blood flow or manifested ischemic areas marked as infarctions already. The perfusion scan should represent all territories of the three main cerebral arteries, namely, the anterior, middle, and posterior cerebral artery, and is therefore located at the upper basal ganglia as an axial slice.

Digital subtraction angiography was performed in general anesthesia without exception. Every patient with vasospasm was treated with a thirty-minute lasting intra-arterial infusion of 10 mL (=2 mg) nimodipine via the catheter in the internal carotid artery. If postinfusion angiography showed complete recurrence of vasospasm the catheter was taken out. When vasospasm persisted after short-time local intraarterial nimodipine infusion, the catheter was left in place and continuous intra-arterial nimodipine infusion was started on the intensive care unit. During the period of intra-arterial nimodipine application, all patients who had lost consciousness before angiography were sedated and mechanically ventilated during the period of intra-arterial nimodipine application on the ICU. Patients, who suffered from specific focal neurologic deficit without impairment of consciousness, were awakened after initial angiography with

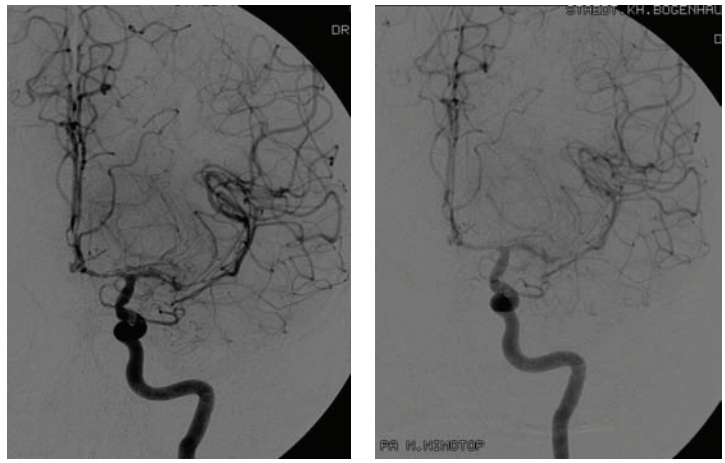

(a) (b)

Figure 1: DSA before and after nimodipine application at the angiography unit. Digital subtraction angiography of the left internal carotid artery before (a) and after (b) nimodipine application in the angiography unit. It shows slight improvement of vasospasm after nimodipine infusion. Intra-arterial infusion of the calcium channel antagonist was continued on the neurosurgical intensive care unit.

catheter placement in order to monitor either the paresis or speech deficit. In cases of elevated intracranial pressure (ICP), all standard conservative treatment options were exhausted before surgery was performed. Three of our thirty patients underwent decompressive hemicraniectomy. One had developed infarction of the right cerebellar hemisphere due to vasospasm of the posterior inferior cerebellar artery (PICA) and therefore had to be craniectomied suboccipitally.

For angiography, four or five French introducer sheaths with a microcatheter were used. Before administration of nimodipine, digital subtraction angiography was performed by contrast application into both internal carotid arteries. After identification of vasospastic vessels (see Figure 1), 0.2–0.4 mg nimodipine (1-2 mL nimodipine solution) was administered via the catheter in the right or left ICA, depending on the side of leading vasospasm, as a bolus. A 30-minute infusion containing 2 mg nimodipine (10 mL nimodipine solution) was then administered. To visualize the effect of nimodipine on the vessels, a further angiography was performed. Patients where no vasospasm could be noticed on the second angiography had their catheters removed. These patients included in our study showed slight improvement of vasospasm but not complete normalization of vessel diameter and configuration. The catheter was fixed with the tip in the extracranial internal carotid artery for further continuous nimodipine infusion at the ICU. In our retrospective analyzed patient data, four patients were treated with a 30-minute infusion of 10 mL (2 mg) nimodipine every 8 hours for 2–5 days. In five of our retrospective patient data and all of the prospective treated patients, the protocol was changed to an infusion rate of 5 mL/h (1 mg/h) applied continuously. Via a second line, which was connected to the catheter with the tip placed in the external iliac artery, 10.000 IU/24 h of heparin was given to prevent clotting of the introducer sheaths with the microcatheter and avoid thrombosis related to the nimodipine catheter tip in the internal carotid artery.

Depending on the neuromonitoring parameters or, in wake patients, their improvement of symptoms, intra-arterial nimodipine infusion was stopped after 1–5 days. In most cases before catheter removal, another angiographic control was performed to observe the therapeutic effect on the vessels in correlation with clinical improvement. On the other hand, to avoid missing persistent vasospasm, that requires further treatment. Nevertheless, we missed the final angiography in a few cases because of weekend or public holiday on the day of catheter removal.

3. Results

3.1. Baseline Characteristics. Patient data are listed in Table 1. Mean patient age was 49.77 ± 10.67 standard deviation (SD) years. The youngest was a 27-year-old woman and the oldest a 76-year-old man. Mean Hunt & Hess grade was 3.07 ± 1.41 with 27% of the patients being graded Hunt & Hess 2. Hunt & Hess 3 was documented in 23% and 20% were Hunt & Hess 4 and 5 each.

Mean onset of continuous intra-arterial nimodipine application was day 9.19 ± 3.31.

3.2. Treatment Results. Mean outcome of all patients was GOS 3.27 ± 1.46. From 19 patients with Hunt & Hess grade 3 and higher four patients died (GOS 1), three were in a persistent vegetative state (GOS 2), and six had severe disability with dependence on support (GOS 3). One case received GOS 4 with minor disability and five patients left the hospital without apparent deficits (GOS 5). Persistent ischemic areas were seen in 100% of patients with GOS 1–3 and in 69% of GOS 4-5 patients.

In four patients vasospasm was shown to be refractory to local nimodipine administration. They died from vasospastic induced major cerebral infarcts. Another patient died

Table 1: Clinical patient and treatment data.

Case no.	Age (years)	Sex	H & H grade	Fisher grade	Aneurysm localization	Treatm. ons. (day)	Treatm. dur. (days)	Outcome (GOS)	Coiling versus clipping
1	54	f	3	4	A com A	9	4	1	Clipping
2	42	f	5	4	MCA l	10	5	1	Clipping
3	43	f	5	4	MCA r	9	4	1	Clipping
4	42	m	3	3	MCA l + ICA l	5	2	5	Clipping
5	53	f	4	4	MCA r	8	4	5	Clipping
6	56	m	2	2	A com A	9	3	2	Clipping
7	43	f	3	4	MCA l	13	3	3	Clipping
8	29	m	5	3	P com A r	7	3	1	Clipping
9	48	f	2	2	A com A	5	3	4	Clipping
10	52	m	5	4	MCA r	14	2	2	Clipping + reclipping
11	48	f	3	4	MCA r + ICA r	6 + 10	3 + 3	5	Clipping + coiling
12	76	m	2	2	A com A	9	4	1	\
13	50	f	5	4	MCA l	6	3	2	Clipping
14	56	f	2	3	A com A	8	3	4	Clipping
15	27	f	2	2	MCA l + carotid T l	7	3	5	Clipping
16	40	m	4	4	A com A	8 + 12	3 + 3	4	Clipping
17	68	f	2	2	ICA l	10	3	3	Clipping
18	55	f	4	4	C1/C2 r	9	3	3	Clipping
19	62	f	2	3	A com A	6	2	5	Clipping
20	48	m	0	1	MCA r	7	3	3	Clipping
21	49	m	5	4	ICA r	11	3	3	Clipping
22	66	m	4	4	MCA r	12	2	3	Clipping
23	41	f	2	3	MCA l	10	5	4	Clipping
24	61	f	3	4	MCA r	1 + 10	3 + 3	3	Clipping
25	48	m	0	1	MCA l	5	2	5	Clipping
26	47	f	1	4	A com A	7	3	5	Coiling
27	42	f	3	3	MCA r	11	2	3	Clipping
28	38	m	3	4	P com A l	2 + 8 + 13	3 + 4 + 4	5	Coiling
29	53	f	4	4	A com A	12	3	2	Clipping
30	56	f	4	4	MCA r	20	1	5	Clipping

Case no.: case number; H & H grade: Hunt and Hess grade; treatm. ons. (day): first day of selective continuous intra-arterial nimodipine infusion; treatm. dur. (days): duration of selective continuous intra-arterial nimodipine infusion in days; outcome (GOS): clinical outcome on discharge in Glasgow outcome scale score; coiling versus clipping: interventional neuroradiologic aneurysm coiling versus microsurgical aneurysm clipping; f: female; m: male; r: right; l: left; A com A: anterior communicating artery; MCA: median cerebral artery; ICA: internal carotid artery; P com A: posterior communicating artery; carotid T: bifurcation of internal carotid artery; C1/C2: segments of the internal carotid artery; \: no coiling or clipping.

from other reason than vasospasm, which was angiographically cured. Overall results from continuous intra-arterial nimodipine infusion were promising. 26 patients improved from angiographically documented refractory vasospasm. Anyway from the 25 survivors only 4 (16%) did not have ischemic brain tissue areas at discharge. All of them reached GOS 5. 17 (68%) patients showed minor cerebral infarcts, which were in multiple locations in 6 (24%) cases. Depending on eloquence of the ischemic brain tissue, patients varied between GOS 3 and 5. Patients having major cerebral infarcts, which occurred in 4 of the 25, left the hospital in a persistent vegetative state (GOS 2).

After having finished the continuous intra-arterial nimodipine therapy with resolved vasospasm on angiography, four patients relapsed in having vasospasm and needed further intra-arterial nimodipine treatment. One patient even had to undergo three cycles before he recovered and ended up without any neurologic deficit on discharge. The 56-year-old female patient with a noted treatment onset on day 20 after bleeding had had two sessions of intra-arterial nimodipine bolus applications at the angiography unit of Klinikum Schwabing.

11 patients were graded Hunt & Hess equal or better than 2. One of those patients died of refractory cerebral vasospasm

Table 2: rCBF before, at 2 and 6 hours, and 1–5 days after starting continuous selective intra-arterial nimodipine infusion, rCBF (mL/100 g/min).

Case no.	rCBF before	rCBF at 2 hours	rCBF at 6 hours	rCBF day 1	rCBF day 2	rCBF day 3	rCBF day 4	rCBF day 5
1	14	22	24	23.3	17.6	9.5	6.3	0
2	17	61	66	44.7	34.8	24.3	7.3	4.2
3	17	46	48	47.3	45.8	36.3	37.5	0
4	16	61	63	50.1	44.4	0	0	0
5	19	58	54	45.6	38.3	33.7	35.1	0
6	12	38	34	33.1	28.4	19.0	0	0
7	13	46	46	43.8	36.2	33.4	0	0
8	12	49	44	23.0	19.3	12.5	0	0
9	17	47	50	48.7	43.9	38.3	0	0
10	16	23	25	22.3	14.5	0	0	0
11	16	73	68	53.8	49.7	45.7	0	0
12	14	24	20	23.7	22.6	12.2	9.3	0
13	12	40	33	30.4	24.0	22.2	0	0
16	15	53	54	45.3	39.3	37.2	0	0
18	8	57	50	38.4	30.6	20.4	0	0
21	12	46	44	29.6	22.9	17.5	0	0
22	7	40	39	35.2	33.8	0	0	0
23	15	55	51	44.8	41.6	37.9	33.9	35.6
24	16	60	54	46.2	42.9	26.7	0	0
27	14	43	44	36.2	22.3	0	0	0
28	12	45	43	36.7	36.8	39.4	0	0
29	9	24	34	23.0	15.7	13.5	0	0

rCBF: regional cerebral blood flow; 0: no continuous selective intra-arterial nimodipine application.

even before treatment of the aneurysm. Two had severe disabilities and one is in a persistent vegetative state. Of the five patients, who died during hospital stay, four developed limiting infarctions due to refractory cerebral vasospasm and one died of sepsis three days after ICA-catheter removal. Microbiological tests found the catheter tip to be sterile. Since the catheter is at least 50 cm in length and only the tip was sent away for tests, the result cannot be representative of the whole catheter.

On CT angiography, we saw thrombotic vessel wall adhesions within the extracranial common or internal carotid artery in three patients. As all of these patients had cerebral infarctions, an additional embolic insult cannot be excluded. The ischemic areas anyway were all limited to territories of vasospastic vessels.

Thirteen patients survived in a good clinical condition (Glasgow outcome scale (GOS 4 and 5)). Five patients classified as Hunt & Hess 3 and 4 on admission left the hospital without apparent deficits (GOS 5).

Addressing the neuromonitoring modalities, we noticed the greatest effects of intra-arterial nimodipine infusion to rCBF parameters; see Table 2. ptiO2 values showed prompt but lower alterations; see Table 3. Changes of intracranial pressure were no indicator for vasospasm. Perfusion CT scans showed vasospasm related changes in 90% of our cases and showed improvement correlating with angiographic results and clinical symptoms; see Figure 2. Data from transcranial Doppler were shown not to be reliable for exclusion or detection of vasospasm; see Table 4. For patient 1 improvement of vasospasm is not shown and in patients 4 and 9 vasospasm is not detected at all. Worsening of vasospasm is missed in patients 25 and 30; only patient 10 showed adequate changes in blood flow velocity.

We could not detect correlation between patient age and duration of selective intra-arterial nimodipine application (Spearman $r = -0.2290$ (corrected for ties), 95% confidence interval: −0.5522 to 0.1541, two-tailed P value is 0.2236) or outcome (Spearman $r = -0.1642$ (corrected for ties), 95% confidence interval: −0.5036 to 0.2192, two-tailed P value is 0.3860, considered not significant). Results were the same for correlation of sex and other parameters (Fisher's exact test and Spearman correlation test). Hunt & Hess did not predict the duration of therapy (Spearman $r = 0.07569$ (corrected for ties), 95% confidence interval: −0.3028 to 0.4336, two-tailed P value is 0.6910), but the Spearman rank correlation test showed significant difference in outcome (Spearman $r = -0.4353$ (corrected for ties), 95% confidence interval: −0.6936

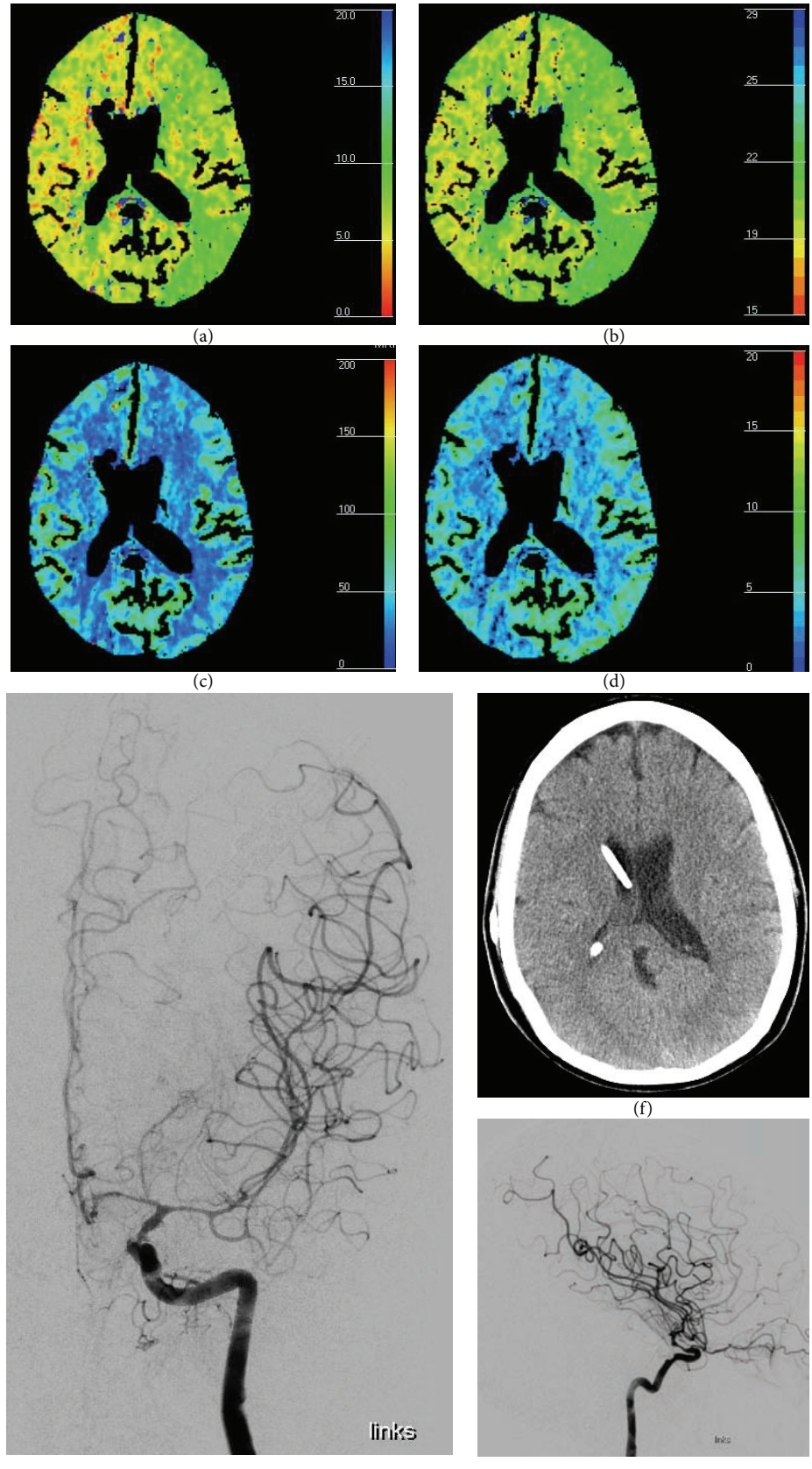

Figure 2: Perfusion CT correlating with DSA. CT perfusion with MTT (sec) (a), TTP (sec) (b), CBF (mL/100 g/min) (c), and CBV (mL/100 g) (d) showing circumscribed perfusion deficit on the territory of the left MCA. No evidence of infarction as shown on native CT scan (f). Digital subtraction angiography (e, g) of the left ICA from the same patient on the same day showing vasospasm of the left ICA above the ophthalmic artery of the median and anterior cerebral artery.

Table 3: ptiO2 before, 2 and 6 hours, and 1–5 days after starting continuous selective intra-arterial nimodipine infusion, ptiO2 (mmHg).

Case no.	ptiO2 before	ptiO2 at 2 hours	ptiO2 at 6 hours	ptiO2 day 1	ptiO2 day 2	ptiO2 day 3	ptiO2 day 4	ptiO2 day 5
1	9	21	20	15.4	10.9	4.3	3.7	0
2	4	20	19	19.2	19.4	14.3	4.8	2.9
3	14	22	23	19.3	21.5	22.3	22.4	0
4	14	27	26	23.4	23.5	0	0	0
5	15	29	26	26.3	26.8	24.2	27.9	0
6	9	18	17	17.5	18.3	12.2	0	0
7	11	14	16	16.3	17.2	17.5	0	0
8	6	15	16	14.2	9.3	4.2	0	0
9	12	19	22	22.3	24.8	24.7	0	0
10	10	18	17	17.9	18.0	0	0	0
11	14	22	25	23.4	22.9	22.6	0	0
12	5	16	17	14.3	14.9	7.9	6.6	0
13	8	20	22	23.6	22.8	22.0	0	0
16	13	21	24	22.4	21.8	22.9	0	0
18	5	18	19	21.1	18.3	18.6	0	0
21	11	20	19	19.3	20.4	18.3	0	0
22	8	18	18	19.5	17.3	0	0	0
23	10	23	22	24.7	24.4	28.7	30.5	29.3
24	14	20	22	20.3	12.3	9.8	0	0
27	14	21	21	22.3	19.5	0	0	0
28	14	25	24	24.3	24.0	25.6	0	0
29	7	17	16	16.9	18.3	16.2	0	0

ptiO2: partial tissue oxygenation; 0: no continuous selective intra-arterial nimodipine application.

Table 4: Transcranial Doppler mean flow values (cm/s) of the right- and left-sided median cerebral artery in six patients before and during continuous intra-arterial nimodipine therapy.

Case no.	Before i.a. nimodipine		Day 1		Day 2		Day 3		Day 4	
	Right	Left	Right	Left	Right	Left	Right	Left	Right	Left
1	184	156	190	183	174	199	168	186	193	205
4	115	94	110	114	89	74				
9	83	87	75	73	70	81	92	80		
10	204	220	164	156	128	140				
25	98	110	95	112	92	98				
30	90	86	73	71						

to −0.07778, two-tailed P value is 0.0162); see Figure 3. The onset of continuous intra-arterial nimodipine treatment significantly correlates with the outcome (GOS) (Spearman $r = -0.4070$ (corrected for ties), 95% confidence interval: −0.675 to −0.04351, two-tailed P value is 0.0256); see Figure 4.

Linear correlation of rCBF and ptiO2 before intra-arterial nimodipine treatment was not significant (correlation coefficient (r) = −0.4147, 95% confidence interval: −0.7119 to 0.008456, Coefficient of determination (r squared) = 0.1720, two-tailed P value is 0.0550). Correlating rCBF and ptiO2 during intra-arterial nimodipine infusion, we get high significance from 2 hours until day 4 with too little data on day 5 to get valuable statistic information. We have picked out "day one" to show correlation (correlation coefficient (r) = −0.7348, 95% confidence interval: −0.8829 to −0.4538, coefficient of determination (r squared) = 0.5400, two-tailed P value is <0.0001); see Figure 5.

Spearman rank test shows significant correlation for ptiO2 before treatment (Spearman $r = 0.6667$ (corrected for ties), 95% confidence interval: 0.3290 to 0.8532, two-tailed P value is 0.0007) and during continuous intra-arterial nimodipine therapy (Spearman $r = 0.8008$ (corrected for ties), 95% confidence interval: 0.5633 to 0.9160, two-tailed P value is <0.0001) with GOS on discharge.

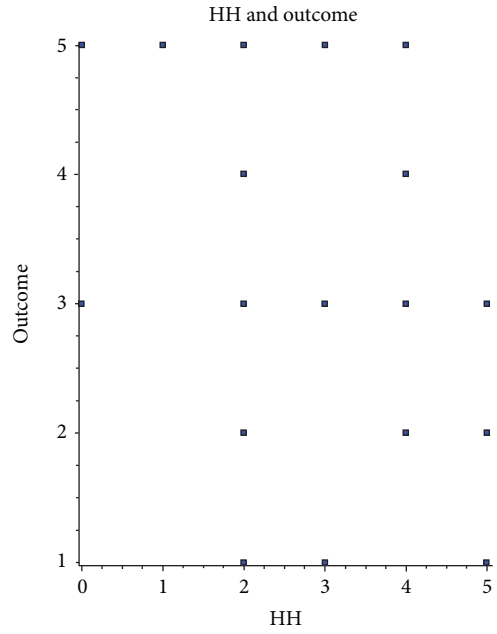

Figure 3: Correlation of H&H grade and patient outcome. Spearman rank test shows inverted correlation of Hunt & Hess grade on admission and outcome (GOS) on discharge.

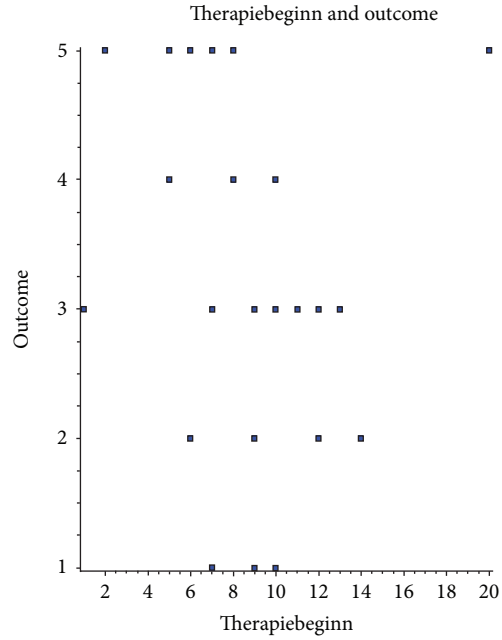

Figure 4: Correlation of onset of selective continuous intra-arterial nimodipine infusion and patient outcome. Spearman rank test shows that inverted correlation of the day nimodipine infusion was started with the outcome (GOS) on discharge.

Results of CT perfusion scanning are shown in Table 5. One can see from the data that initial perfusion scanning missed vasospasm only once and therefore seems to be a very sensitive monitoring parameter.

4. Discussion

Continuous selective intra-arterial infusion of nimodipine has been described before by Musahl et al. [20]. In contrast to our results, none of their patients had "new ischemic lesions caused by vasospasm" on discharge. This aspect is alarming, as ischemia is one of the main reasons for neurologic deficit in these patients. In our cohort, we had started continuous intra-arterial nimodipine on day 9.19 ± 3.31 after SAH. On average, Musahl started more than one day earlier: day 7.5 ± 2.06. Comparing these data, an important issue seems to be the onset of treatment.

In our cohort from thirty patients, two had incidental MCA bifurcation aneurysm and were treated with clipping. One patient had clinical symptoms of confusion and speech disturbance after awakening from surgery. CT perfusion showed reduced perfusion frontotemporal but no area of infarction. Symptoms disappeared within a few hours and, as a result, no angiography was performed. Five days later, motor and sensory speech deficits reoccurred. CT perfusion and native cranial CT (CCT) showed infarction in the median territory frontotemporal. On angiography, vasospasm of a distally from the clip localized MCA branch plus the anterior cerebral artery, segment 1 (A1) left-sided, showed vasospasm. After two days, symptoms improved and the catheter was removed. Under logopedic therapy, the patient was able to articulate and understand with only minor deficits. The

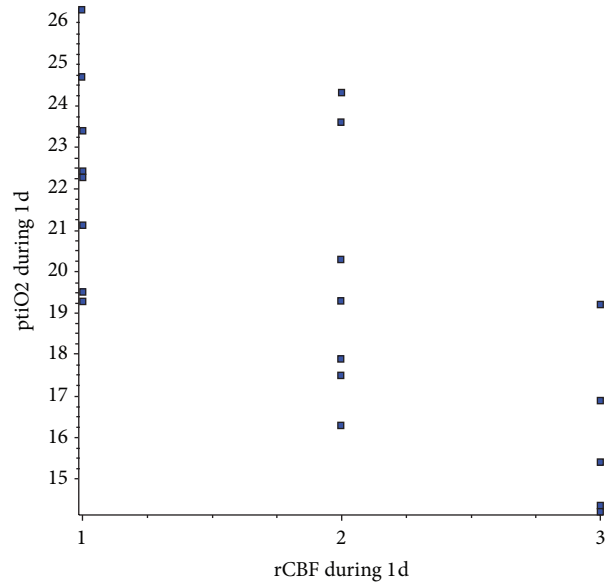

Figure 5: Linear correlation test shows extremely high significance of ptiO2 and rCBF values during (day 1) selective continuous intra-arterial nimodipine infusion.

other Hunt & Hess 0 case was admitted to our hospital because of transitory ischemic attack (TIA) with dysarthria and hemiparesis. On CT angiography, two aneurysms of the right median bifurcation were identified. Transcranial Doppler showed both-sided M1- and left-sided ICA stenosis and a free ICA on the right with a history of thromboendarterectomy (TEA). Both aneurysms were clipped. After

Table 5: Results of CT perfusion scanning before, during, and after treatment with continuous intra-arterial nimodipine infusion.

Case no.	Before		During		After
	Tissue at risk	Infarction	Tissue at risk	Infarction	Infarction
1	Yes	Minor	Yes	Major	Major
2	Yes	No	Yes	Major	Major
3	Yes	No	Yes	Minor	Minor
4	Yes	No	No	No	No
5	Yes	No	Yes	No	No
6	Yes	No	Yes	Minor	Major
7	Yes	Minor	Yes	Minor	Multiple minor
8	Yes	Major	Yes	Major	Major
9	Yes	No	Yes	No	Minor
10	Yes	No	Yes	Minor	Major
11	Yes	No	Yes	No	Minor
12	Yes	No	Yes	Major	Major
13	Yes	No	Yes	Minor	Major
14	Yes	Minor	Yes	No	Multiple minor
15	Yes	No	No	No	No
16	Yes	No	Yes	No	Minor
17	Yes	No	Yes	Minor	Multiple minor
18	Yes	Minor	Yes	No	Minor
19	Yes	No	Yes	No	Minor
20	Yes	No	Yes	Minor	Multiple minor
21	Yes	Minor	Yes	No	Multiple minor
22	Yes	No	Yes	No	Minor
23	Yes	No	Yes	No	Minor
24	Yes	No	Yes	Minor	Multiple minor
25	No	No	Yes	No	No
26	Yes	No	Yes	No	Minor
27	Yes	No	Yes	No	Minor
28	Yes	No	Yes	Minor	Minor
29	Yes	Minor	Yes	Major	Major
30	Yes	No	Yes	Minor	Minor (cerebellar)

anesthesia, epileptic seizures occurred. The perfusion scan showed hyperperfusion of the right hemisphere, especially parietooccipital. The patient did not wake up. CCT and CT perfusion seven days after clipping illustrated a swollen right hemisphere and hypodense brain tissue in the right-sided median and posterior territories, suspect for infarctions. After 3 days of continuous intra-arterial nimodipine infusion, the vasospasm had disappeared, but infarction areas were fixed and, with it, the patients symptoms on waking. On discharge, a left-sided hemiparesis and psychomotor deceleration were noticed.

All of our patients showed persistent vasospasm after 30 minutes of intra-arterial infusion of 10 mL nimodipine solution in the angiography unit. Vasospasm improved in 26 patients after continuous intra-arterial nimodipine infusion. Recurrence of vasospasm was seen in 4 patients who received the same treatment once more. A third cycle was only needed once. All patients who needed more than one treatment cycle of continuous intra-arterial nimodipine infusion were graded Fisher 4 on initial CT scan.

It is remarkable that ptiO2 values showed such prompt and extensive response. Value changes in other cases were not as high as reported by Musahl et al. [20]. Hoelper et al. [21] also have described the increase of ptiO2, but Stiefel et al. [22] have found decreased tissue oxygenation during endovascular vasospasm therapy.

Musahl et al. [20] describe the great effect on flow velocities in transcranial Doppler after onset of intra-arterial nimodipine treatment. In our study, we could not detect reliable changes in flow velocities. In some cases we missed clinical and angiographic improvement of vasospasm and in others we did not detect beginning or manifest vasospasm. A review by Lysakowski et al. [23] describes transcranial Doppler as not decisive and so should not be used as the only neuromonitoring parameter.

Our patients showed great response of rCBF-values on intra-arterial nimodipine administration. The same effect could be shown by Vajkoczy et al. [24], using intra-arterial papaverine for antivasospastic therapy.

In correlation with Moftakhar et al. [25] and Majoie et al. [26] results we found good correlation of vasospasm and findings in CT perfusion scanning. It marked tissue at risk with prolonged time to peak and mean transit time and showed a mismatch of cerebral blood flow and cerebral blood volume with a sensitivity of 97% in our case series. Native CAT scan missed many of these cases especially in early stage of vasospasm. Some of our patients never showed ischemic changes on native CT scan even if CT perfusion detected tissue at risk areas for over a week with correlating angiographic vasospasm.

Our protocol for continuous selective intra-arterial nimodipine infusion is easily feasible. Infrastructural prerequisites include angiography plus intensive or intermediate care unit. The radiologist should be experienced in the interpretation of intracranial digital subtraction angiography and be able to intervene. A neurosurgeon should at least be on call if major problems occur, which need to be treated surgically. Most hospitals treating patients with SAH dispose of these departments anyway. The equipment needed is a 4 or 5 French introducer sheath with a microcatheter + nimodipine solution. Multimodal neuromonitoring is recommended.

Vessel wall dissection, catheter dislocation, and embolic infarction due to thrombotic adhesion at catheter or vessel wall are risks which should be kept in mind but have not been reported so far. There were three suspect findings for thrombotic vessel wall adhesions on CT angiography, but none of these patients suffered embolic infarction. To prevent embolic complications, anticoagulation is an important issue. In our study, 10,000 IU/24 h heparin was infused via the same catheter as nimodipine. Mayer et al. [27] and Musahl et al. [20] used comparable protocols and did not notice serious side effects or complications.

From thirty patients, one died of sepsis three days after catheter removal. Even if the catheter tip was sterile on microbiological tests, we cannot rule out correlation between intra-arterial catheter and sepsis. But having in mind that most of these patients were critically ill a sepsis rate of 3.3% is within the normal range, even lower, than in other ICU series [28].

None of the dead patients were autopsied. Therefore, causes of death are clinical interpretations but cannot be assured. One could say that this issue is a "black box." We could have missed death causing problems connected to the catheter. Risk analysis for that is not purposeful.

We could not detect correlation between patient age and onset of vasospasm, duration of intra-arterial nimodipine application, or outcome. Results were the same for correlation of sex and other parameters. Hunt & Hess did not predict duration of therapy, but the Spearman rank correlation test showed significant difference in outcome; see Figure 3. The onset of continuous intra-arterial nimodipine treatment significantly correlates with the outcome (GOS); see Figure 4.

Results in our study are worse than those reported by Musahl et al. [20]. Comparing the patient population in both studies, mean age is 47 years with Musahl et al. [20] and 49.8 years in our study. The WFNS compared to the Hunt & Hess score used in our study does not show a great difference in the severity of cases included in both studies. Two-thirds of Musahl et al. [20] patients were coiled on their aneurysm whereas only 7% of our patients were coiled as the only aneurysm treatment. One more aspect is the onset of intra-arterial nimodipine treatment. Musahl et al. [20] started one day earlier after bleeding and within 2 hours of onset of symptoms, which presupposes an excellent infrastructure. Patient age, aneurysm coiling, and time onset of treatment seem to be important facts for better patient outcome. The first cannot be influenced. The next two should be analyzed in further studies.

We only included patients that did not respond to triple H therapy plus short-time intra-arterial infusion of nimodipine in the angiography unit, which makes the patients included in our study have more severe vasospasm from the start.

5. Conclusion

As selective continuous intra-arterial nimodipine infusion seems to be a safe and easy therapy, one should think of implementing it as soon as possible to prevent permanent ischemia. Multimodal neuromonitoring seems to be helpful in judging efficacy and safety of this new established treatment. Further investigations could reveal certain criteria, in which patients are likely to profit from continuous intra-arterial nimodipine application and in whom a different therapy should be started. Up till now, patient cohorts are too small to give recommendations. This should change in the near future.

Conflict of Interests

The authors declare that there is no conflict of interests regarding the publication of this paper. The authors declare no competing financial interests.

References

[1] J. P. Broderick, T. Brott, T. Tomsick, R. Miller, and G. Huster, "Intracerebral hemorrhage more than twice as common as subarachnoid hemorrhage," *Journal of Neurosurgery*, vol. 78, no. 2, pp. 188–191, 1993.

[2] F. H. H. Linn, G. J. E. Rinkel, A. Algra, and J. van Gijn, "Incidence of subarachnoid hemorrhage: role of region, year, and rate of computed tomography: a meta-analysis," *Stroke*, vol. 27, no. 4, pp. 625–629, 1996.

[3] C. Sarti, J. Tuomilehto, V. Salomaa et al., "Epidemiology of subarachnoid hemorrhage in Finland from 1983 to 1985," *Stroke*, vol. 22, no. 7, pp. 848–853, 1991.

[4] M. S. Greenberg, "SAH and aneurysms; introduction to SAH," in *Handbook of Neurosurgery*, chapter 30, p. 1034, Thieme, New York, NY, USA, 7th edition, 2010.

[5] N. J. Solenski, E. C. Haley Jr., N. F. Kassell et al., "Medical complications of aneurysmal subarachnoid hemorrhage: a report of the multicenter, cooperative aneurysm study," *Critical Care Medicine*, vol. 23, no. 6, pp. 1007–1017, 1995.

[6] N. F. Kassell, T. Sasaki, A. R. T. Colohan, and G. Nazar, "Cerebral vasospasm following aneurysmal subarachnoid hemorrhage," *Stroke*, vol. 16, no. 4, pp. 562–572, 1985.

[7] J. L. Brisman, J. M. Eskridge, and D. W. Newell, "Neurointerventional treatment of vasospasm," *Neurological Research*, vol. 28, no. 7, pp. 769–776, 2006.

[8] K. Yoshida, H. Watanabe, and S. Nakamura, "Intraarterial injection of amrinone for vasospasm induced by subarachnoid hemorrhage," *American Journal of Neuroradiology*, vol. 18, no. 3, pp. 492–496, 1997.

[9] R. M. Pluta, J. K. B. Afshar, B. G. Thompson, R. J. Boock, J. Harvey-White, and E. H. Oldfield, "Increased cerebral blood flow but no reversal or prevention of vasospasm in response to L-arginine infusion after subarachnoid hemorrhage," *Journal of Neurosurgery*, vol. 92, no. 1, pp. 121–126, 2000.

[10] S. Suzuki, O. Ito, T. Sayama, S. Yamaguchi, K. Goto, and T. Sasaki, "Intraarterial injection of colforsin daropate hydrochloride for the treatment of vasospasm after aneurysmal subarachnoid hemorrhage: preliminary report of two cases," *Neuroradiology*, vol. 48, no. 1, pp. 50–53, 2006.

[11] J. M. Milburn, C. J. Moran, D. T. Cross III, M. N. Diringer, T. K. Pilgram, and R. G. Dacey Jr., "Increase in diameters of vasospastic intracranial arteries by intraarterial papaverine administration," *Journal of Neurosurgery*, vol. 88, no. 1, pp. 38–42, 1998.

[12] L. Feng, B.-F. Fitzsimmons, W. L. Young et al., "Intraarterially administered verapamil as adjunct therapy for cerebral vasospasm: safety and 2-year experience," *American Journal of Neuroradiology*, vol. 23, no. 8, pp. 1284–1290, 2002.

[13] N. Badjatia, M. A. Topcuoglu, J. C. Pryor et al., "Preliminary experience with intra-arterial nicardipine as a treatment for cerebral vasospasm," *American Journal of Neuroradiology*, vol. 25, no. 5, pp. 819–826, 2004.

[14] A. Biondi, G. K. Ricciardi, L. Puybasset et al., "Intra-arterial nimodipine for the treatment of symptomatic cerebral vasospasm after aneurysmal subarachnoid hemorrhage: preliminary results," *American Journal of Neuroradiology*, vol. 25, no. 6, pp. 1067–1076, 2004.

[15] S. Wolf, H. Martin, J. F. Landscheidt, S. O. Rodiek, L. Schürer, and C. B. Lumenta, "Continuous selective intraarterial infusion of nimodipine for therapy of refractory cerebral vasospasm," *Neurocritical Care*, vol. 12, no. 3, pp. 346–351, 2010.

[16] J. K. Liu and W. T. Couldwell, "Intra-arterial papaverine infusions for the treatment of cerebral vasospasm induced by aneurysmal subarachnoid hemorrhage," *Neurocritical Care*, vol. 2, no. 2, pp. 124–132, 2005.

[17] W. McAuliffe, M. Townsend, J. M. Eskridge, D. W. Newell, M. S. Grady, and H. R. Winn, "Intracranial pressure changes induced during papaverine infusion for treatment of vasospasm," *Journal of Neurosurgery*, vol. 83, no. 3, pp. 430–434, 1995.

[18] D. T. Cross III, C. J. Moran, E. E. Angtuaco, J. M. Milburn, M. N. Diringer, and R. G. Dacey Jr., "Intracranial pressure monitoring during intraarterial papaverine infusion for cerebral vasospasm," *American Journal of Neuroradiology*, vol. 19, no. 7, pp. 1319–1323, 1998.

[19] H. Tsurushima, T. Kamezaki, Y. Nagatomo, A. Hyodo, and T. Nose, "Complications associated with intraarterial administration of papaverine for vasospasm following subarachnoid hemorrhage—two case reports," *Neurologia Medico-Chirurgica*, vol. 40, no. 2, pp. 112–115, 2000.

[20] C. Musahl, H. Henkes, Z. Vajda, J. Coburger, and N. Hopf, "Continuous local intra-arterial nimodipine administration in severe symptomatic vasospasm after subarachnoid hemorrhage," *Neurosurgery*, vol. 68, no. 6, pp. 1541–1547, 2011.

[21] B. M. Hoelper, E. Hofmann, R. Sporleder et al., "Transluminal balloon angioplasty improves brain tissue oxygenation and metabolism in severe vasospasm after aneurysmal subarachnoid hemorrhage: case report," *Neurosurgery*, vol. 52, no. 4, pp. 970–976, 2003.

[22] M. F. Stiefel, A. M. Spiotta, J. D. Udoetuk et al., "Intra-arterial papaverine used to treat cerebral vasospasm reduces brain oxygen," *Neurocritical Care*, vol. 4, no. 2, pp. 113–118, 2006.

[23] C. Lysakowski, B. Walder, M. C. Costanza, and M. R. Tramèr, "Transcranial Doppler versus angiography in patients with vasospasm due to a ruptured cerebral aneurysm: a systematic review," *Stroke*, vol. 32, no. 10, pp. 2292–2298, 2001.

[24] P. Vajkoczy, P. Horn, C. Bauhuf et al., "Effect of intra-arterial papaverine on regional cerebral blood flow in hemodynamically relevant cerebral vasospasm," *Stroke*, vol. 32, no. 2, pp. 498–505, 2001.

[25] R. Moftakhar, H. A. Rowley, A. Turk et al., "Utility of computed tomography perfusion in detection of cerebral vasospasm in patients with subarachnoid hemorrhage," *Neurosurgical Focus*, vol. 21, no. 3, article E6, pp. 1–5, 2006.

[26] C. B. L. M. Majoie, L. J. van Boven, D. van de Beek, H. W. Venema, and W. J. van Rooij, "Perfusion CT to evaluate the effect of transluminal angioplasty on cerebral perfusion in the treatment of vasospasm after subarachnoid hemorrhage," *Neurocritical Care*, vol. 6, no. 1, pp. 40–44, 2007.

[27] T. E. Mayer, M. Dichgans, A. Straube et al., "Continuous intra-arterial nimodipine for the treatment of cerebral vasospasm," *CardioVascular & Interventional Radiology*, vol. 31, no. 6, pp. 1200–1204, 2008.

[28] Y. Sakr, C. Elia, L. Mascia et al., "Epidemiology and outcome of sepsis syndromes in Italian ICUs: a multicentre, observational cohort study in the region of piedmont," *Minerva Anestesiol*, vol. 79, no. 9, pp. 993–1002, 2013.

Hindawi Publishing Corporation
BioMed Research International
Volume 2013, Article ID 715170, 9 pages
http://dx.doi.org/10.1155/2013/715170

Clinical Study

Comparison of Neurologic and Radiographic Outcomes with Solitaire versus Merci/Penumbra Systems for Acute Stroke Intervention

Shannon Hann,[1] Nohra Chalouhi,[1] Robert Starke,[1] Ashish Gandhe,[2] Michael Koltz,[1] Thana Theofanis,[1] Pascal Jabbour,[1] L. Fernando Gonzalez,[1] Robert Rosenwasser,[1] and Stavropoula Tjoumakaris[1]

[1] *Department of Neurosurgery, Thomas Jefferson University and Jefferson Hospital for Neuroscience, Philadelphia, PA 19107, USA*
[2] *Department of Radiology, Thomas Jefferson University and Jefferson Hospital for Neuroscience, Philadelphia, PA 19107, USA*

Correspondence should be addressed to Shannon Hann; shannon.hann@jeffersonhospital.org

Received 18 September 2013; Accepted 18 November 2013

Academic Editor: Steven J. Monteith

Background and Purpose. The Solitaire Flow Restoration was approved by the FDA in 2012 for mechanical thrombolysis of proximal occlusion of intracranial arteries. To compare the Solitaire FR device and the Merci/Penumbra (previously FDA approved) systems in terms of safety, clinical outcomes, and efficacy including radiographic brain parenchymal salvage. *Methods*. Thirty-one consecutive patients treated with the Solitaire and 20 patients with comparable baseline characteristics treated with Merci or Penumbra systems were included in the study. Primary outcome measures included recanalization rate and modified Rankin Scale score at followup. Secondary outcomes included length of procedure, incidence of symptomatic intracranial hemorrhage, 90-day mortality, and radiographic analysis of percentage area salvage. *Results*. Compared with the Merci/Penumbra group, the Solitaire group showed a statistically significant improvement in favorable outcomes (mRS ≤ 2) (69% versus 35%, $P = 0.03$) and symptomatic ICH rate (0 versus 15%, $P = 0.05$) with a trend towards higher recanalization rates (93.5% versus 75%, $P = 0.096$) and shorter length of procedure (58.5 min versus 70.8 min, $P = 0.08$). Radiographic comparison also showed a significantly larger area of salvage in the Solitaire group (81.9% versus 71.9%, $P = 0.05$). *Conclusion*. Our study suggests that the Solitaire system allows faster, safer, and more efficient thrombectomy than Merci or Penumbra systems.

1. Introduction

The goal of acute ischemic stroke treatment is arterial recanalization and restoration of brain parenchymal perfusion. Since the Food and Drug Administration (FDA) approval of tissue plasminogen activator (tPA) for treatment of acute ischemic stroke in 1996, intravenous tPA (ivtPA) administration within a 3–4.5 hours window postsroke has been the mainstream of stroke intervention [1].

However, ivtPA therapy has shortcomings including a limited administration window and less than ideal reperfusion outcome especially in large vessel occlusions. In fact, the recanalization rate with ivtPA is as low as 10% in internal carotid artery (ICA) occlusions and less than 30% for proximal middle cerebral artery (MCA) occlusions [2]. As such, intra-arterial thrombolysis within 6 hours and mechanical thrombectomy within 8 hours from symptom onset have been increasingly used to achieve faster and more efficient recanalizations of large arterial occlusions [1].

In the past decade, several randomized controlled trials for intra-arterial thrombolytic therapy and mechanical thrombolysis have been conducted and shown promising results. These trials led to the FDA approval of the first thrombectomy device, the Merci Retriever (Merci, Concentric Medical, Mountain View, CA) in 2004, and the second device, the Penumbra (Penumbra, Alameda, CA), in 2008. Although both devices are associated with relatively high rates of successful recanalization, large clots in major intracranial

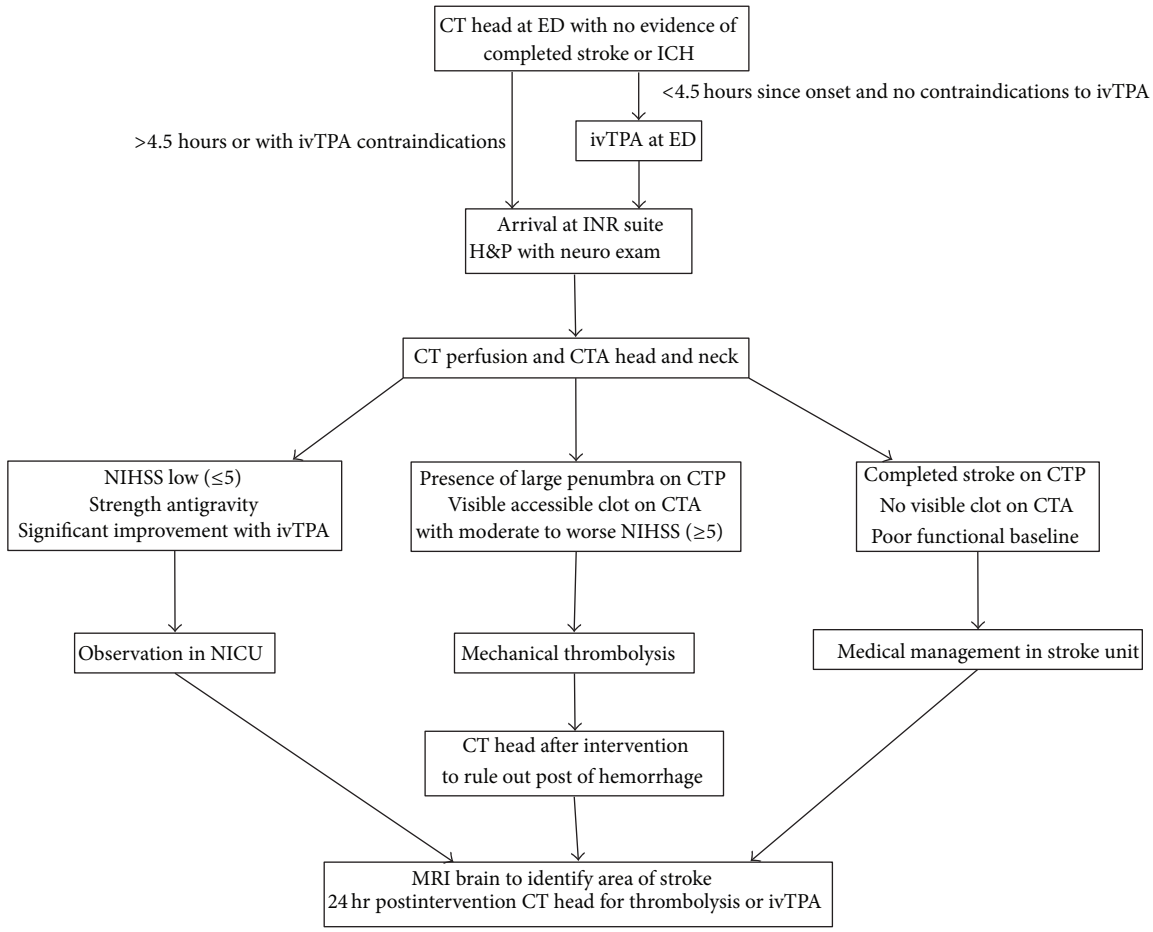

Figure 1: Thrombolysis protocol for acute ischemic stroke.

arteries remain quite resistant and require a prolonged time for recanalization [3]. The Solitaire Flow Restoration (FR) (ev3/Covidien, Irvine, CA) is a self-expanding, fully retrievable stent that obtained FDA approval in March 2012 based on the results of the Solitaire with the Intention for Thrombectomy (SWIFT) trial. This study found higher recanalization rates (61% versus 24%) and better neurologic outcomes (58% versus 33%) in the Solitaire FR device compared with the Merci device [4].

We present the first study comparing the Solitaire FR device and the Merci and/or Penumbra systems in terms of efficacy, safety, clinical outcomes, and area of territory at risk saved with revascularization by analyzing pre and postintervention imaging studies. We also reviewed published large scale mechanical thrombectomy trials for Merci, Penumbra, Merci 2, Solitaire, and TREVO devices to compare our Solitaire FR results with these various current devices.

2. Patients and Methods

2.1. Eligibility. This is a single-center study of 31 patients treated with mechanical thrombectomy with the Solitaire FR device at the Jefferson Hospital for Neuroscience (JHN) in between March 2012 and November 2012. After neurological examination, suspected acute stroke patients are either admitted from Thomas Jefferson University Hospital emergency department, transferred from affiliated community hospitals, or directly accepted by the attending physician on stroke telemedicine call. Upon arrival to the JHN, patients are directly brought to the interventional neuroradiology (INR) suite for full history and physical exam by neurosurgical residents, fellows, and attending physicians. Subsequently, patients meeting clinical criteria for intervention with no CT evidence of completed stroke or hemorrhage proceed to immediate CT perfusion of head and CT angiogram of head and neck to determine the extent of territory at risk and to identify a major intracranial arterial occlusion. Based on the clinical signs, National Institute of Health Stroke Scale (NIHSS), and imaging findings the decision is made whether to perform mechanical thrombolysis or not. Figure 1 details our patient selection protocol for thrombolysis. Major criteria for intervention include poor NIHSS $\geq$ 5, large territorial mismatch between cerebral blood volume and blood flow/mean transit time on CT perfusion scan, visible main arterial thrombus on CT angiogram, and worsening neurological performance since time of referral [5]. Our institution uses CT perfusion guided recanalization selection

because it has reported lower intracranial hemorrhage rate and mortality rates compared with time guided selection [6]. Contraindications to interventions are improving neurological status, low NIHSS, and multiple medical comorbidities with poor functional baseline.

2.2. Procedures. Procedures are performed under general anesthesia and neuromonitoring with both somatosensory and motor evoke potentials. Access is obtained on the side contralateral to the intraluminal thrombus. The femoral artery is the first choice followed by the radial, brachial, and carotid arteries. The specific system used to support the Solitaire FR device may be variable depending on the patients peripheral vascular anatomy, presence of concurrent carotid pathology, clot location, and/or operator discretion. The majority of cases presented in this series achieved successful results with a 7F sheath and selective catheterization using a 0.038 Guide wire (Terumo, Somerset, NJ) and 6F Envoy guide catheter (Codman Neurovascular, Raynham, MA). Superselective catheterization of the target vessel was achieved with a 0.014 inch Synchro-2 microwire (Stryker; Fremont, CA) and Prowler Select Plus microcatheter (Cordis Neurovascular, Miami Lakes, FL).

Placement of the microcatheter distal to the thrombus is confirmed by microinjection of 60% contrast under digital subtraction angiography (DSA). The Solitaire FR device is then brought into the field and advanced through the microcatheter with biplane fluoroscopy to confirm its central position over the thrombus. The microcatheter is then pulled back to unsheathe the Solitaire FR device while maintaining a constant position of the Solitaire delivery wire. The Solitaire FR device is left completely unsheathed for 3–5 minutes. Once the appropriate time has elapsed, the proximal 1/4 of the Solitaire stent is retrieved within the microcatheter and then pulled out thru the guide catheter under continuous negative aspiration with a 50 mL syringe. Some operators prefer the 8F Merci Balloon Guide Catheter (Concentric Medical) so that it may be inflated before aspiration with the 50 mL syringe to aid in thrombus retrieval. The substitution of this guide catheter necessitates placement of an 8F sheath for access. Control angiograms are performed after Solitaire retrieval to confirm revascularization.

2.3. Outcome Measure. On admission, NIHSS and ivtPA administration status were checked; NIHSS was reassessed 24 hours after intervention and at time of discharge. Baseline modified Rankin Score (mRS) was obtained from family on admission and reassessed at ≥90 days during a follow-up office visit. CT head was performed within 24 h after intervention to diagnose hemorrhagic complications. MRI brain was also performed 24 h after intervention to document the area of completed stroke.

Primary outcome measures included recanalization rate and modified Rank in Scale score at followup. Secondary outcomes included length of procedure, incidence of symptomatic intracranial hemorrhage, 90-day mortality rate, and radiographic analysis of percentage area salvage. Successful recanalization was defined as a Thrombolysis In Myocardial Ischemia (TIMI) reperfusion grade of 2 or 3 on immediate postprocedural angiograms. The area of brain parenchymal salvage was documented by volumetric analysis. Specifically, the volume of completed stroke on MRI DWI sequence was subtracted from the volume of the territory at risk on initial CT perfusion. The volume of territory at risk was determined on initial CT head perfusion by measuring the mismatched area between mean transit time and blood volume in the axial plane and multiplying the total calculated area by the slice thickness of the corresponding image. The volume of completed stroke was measured on DWI signal abnormality from 24 hr postintervention MRI axial plane multiplied by the respective slice thickness with corresponding signal changes. The difference in the territory at risk on CT head perfusion study and DWI sequence in MRI brain is the area salvage. The percentage salvage is calculated using area salvage divided by the initial territory at risk. All calculations were carried out by a neuroradiologist with no prior knowledge of postoperative outcomes. Figure 3 shows the typical imaging studies from a Solitaire patient. Safety outcome was assessed by (1) symptomatic intracranial hemorrhage after intervention, (2) device-induced damage to vessels and further propagation of thrombus, and (3) mortality rate at 90 days. Postprocedural groin hematoma was not included in safety outcome as this is a complication expected in any angiographic procedure; however, we did collect this data as procedure related complications.

The results from the Solitaire group were compared with those of the Merci/Penumbra group. Comparison group consisted of 20 patients treated with Merci and/or Penumbra system as first choice device from February 2010 to January 2011 at our institution. The characteristics of patients in the Merci, Penumbra group were comparable with the Solitaire group in terms of age, sex, medical comorbidities, and NIHSS in order to eliminate confounding variables. The focus of the comparison was not only the clinical outcomes but also the radiographic outcome of percentage area salvage; thus, patients with nondiagnostic CT perfusion study or with contraindications to MRI study such as those with a cardiac pacer were not included in the comparison group. After adjusting the confounding variables and availability of CT perfusion and MRI study, only twenty patients qualified to be included in the comparison group among the 44 total patients treated with Merci or penumbra system previously. Merci/Penumbra patients are grouped together because there were not enough patients treated in either group alone that would comprise a large enough comparison group.

2.4. Statistical Analysis. Data are presented as mean and range for continuous variables and as frequency for categorical variables. Analysis was carried out using unpaired t-test, Chi-square, and Fisher's exact tests as appropriate. Univariate analysis was used to test covariates predictive of the following dependent outcomes: unfavorable outcome (mRS 3–6) and TIMI-2 or 3. P values of ≤ 0.05 were considered statistically significant. Statistical analysis was carried out with Stata 10.0 (College Station, TX).

Table 1: Solitaire patient characteristics and treatment result.

Patient	Age	Gender	NIHSS on arrival	NIHSS at discharge	ivTPA	Location of thrombus	Time to reperfusion (hrs)	Procedure time (min)	Rescue treatment*	No. of pass	TIMI	F/U mRS
1	87	F	18	13	N	R M2	17	42	N	1	3	4
2	64	M	12	2	N	L M1	11	90	N	2	3	1
3	73	M	12	5	Y	L M1	7	36	N	1	3	2
4	32	M	18	0	Y	R M2	5	33	N	1	3	0
5	50	M	21	2	N	R ICA	5	65	N	1	2	1
6	52	M	7	1	N	Basilar	6	73	N	1	3	0
7	76	M	12	4	N	R M1	10	44	N	2	3	2
8	77	M	13	0	Y	R M1	6	65	N	2	2	0
9	62	M	9	5	N	L M2	5	70	N	1	2	2
10	77	F	13	5	Y	L ICA	10	80	Y (Penum/Plasty)	1	3	2
11	48	M	12	0	N	R M2	6	20	N	1	3	0
12	82	M	9	4	Y	L M1	5	26	N	1	3	4
13	69	M	9	9	N	L vert	6	65	N	1	1	4
14	63	F	21	13	N	L M1	5	41	N	2	3	1
15	87	M	19	27	Y	R ICA	5	54	Y (Merci, PLASTY)	4	0	6
16	63	M	18	12	N	R M1	11	52	N	1	3	4
17	71	M	13	1	Y	R ICA	7.5	57	Y (iaTPA)	1	2	0
18	74	M	10	Expired	N	R M1	16	105	N	2	3	6
19	61	M	15	12	N	R M1	14	80	N	2	2	4
20	61	M	3	1	Y	L M2	4	98	Y (Penum, iaTPA)	2	2	0
21	70	M	24	18	N	L M1	6	70	N	1	3	4
22	73	M	9	16	N	L M2	9	80	Y (Penumbra)	4	3	6
23	26	F	3	0	Y	R ICA	9	30	N	1	3	0
24	77	F	8	4	Y	R M1	7	26	N	1	3	1
25	65	M	15	11	Y	R M2	6.5	32	N	1	2	2
26	45	F	23	5	N	L M1	8	55	N	1	3	1
27	57	M	20	20	Y	R M2	6.5	80	Y (TREVO, iaTPA, Penum)	2	2	NA
28	54	M	12	0	N	L M1	8.5	65	N	5	3	0
29	56	F	17	5	Y	L M1	6	80	N	3	2	2
30	65	M	26	17	N	L ICA	7.5	75	Y(Merci)	3	3	NA
31	71	F	5	5	N	L M1	13.5	25	N	1	3	1

*Rescue treatment: procedures used in case the recanalization failed with attempt of one thrombectomy system. These include intra-arterial thrombolysis, angioplasty, and other thrombectomy systems than the initially attempted one.

3. Results

3.1. Baseline Characteristics. Thirty-one consecutive patients with acute ischemic stroke treated with Solitaire FR device as a first-choice modality of mechanical thrombectomy were included. The mean patient age was 64.1 (range: 32–87) years and 23 (74%) were males. The NIHSS ranged from 3 to 26 (average 14, SD ± 6.02) on arrival. Arterial occlusion sites were as follows: M1 (51%), M2 (29%), ICA or T-occlusion (13%), and posterior circulation (6%).

Thirteen patients (42%) were treated with IV tPA prior to arrival; however, due to persistence of symptoms and identification of retrievable clot associated with a large area of territory at risk on CTA and CTP, Solitaire thrombectomy was performed.

3.2. Recanalization Rate. Table 1 summarizes the outcome of each patient along with the recanalization grade. Twenty-four patients (77%) were treated with the Solitaire FR as a sole thrombectomy device and seven patients underwent additional mode of treatment (i.e., Merci, Penumbra, Trevo, and/or intra-arterial TPA) to achieve maximum restoration of flow (TIMI 2 or 3). The mean time from stroke to recanalization was 8.03 ± 3.37 (SD) hours (range: 4–17 hours).

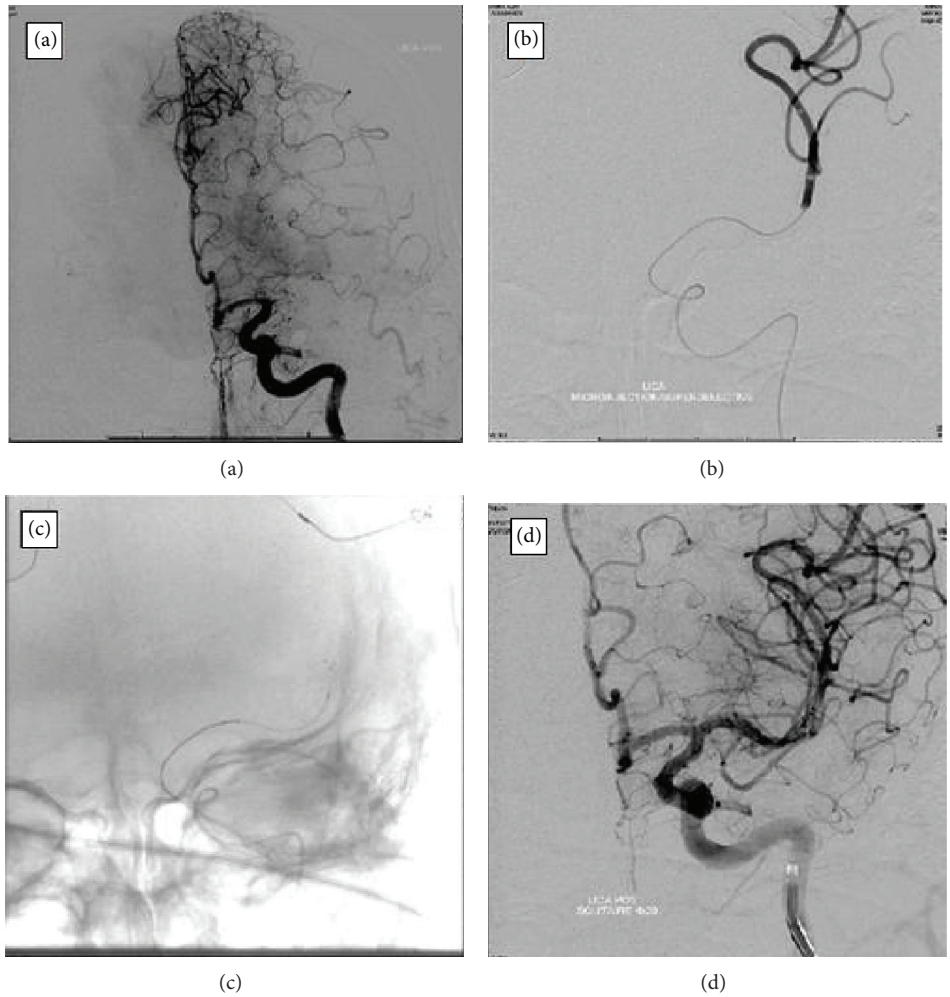

Figure 2: Case 14. (a) DSA of left ICA arterial phase. AP view shows an occlusion of the left M1. (b) Guiding catheter in left MCA, the distal tip of the microcatheter, and the microwire have crossed the occluded portion of the L M1 and moved through the thrombi into M2. This injection shows the distal end of the thrombus. (c) This AP view shows the terminal radiopaque marker of Solitaire FR device which indicates the start of deployment. (d) DSA of L ICA after the stent retrieval shows that the distal L MCA branches have been completely opened.

The mean procedure time defined as time between arterial puncture to flow restoration observed on digital subtraction angiography (DSA) was 58.5 ± 22.9 (SD) minutes overall and only 40.3 ± 19.7 (SD) minutes for the successful procedures that did not require other mechanical thrombectomy rescue treatments. We obtained an overall recanalization rate (TIMI scores of 2 and 3) of 93.5%; treatment with the Solitaire FR device alone achieved a 79.3% recanalization rate. Only two patients failed to recanalize. One (patient 13) had a PCA thrombus subsequent to left vertebral artery dissection, the tortuous anatomy precluded passage of Solitaire FR device as well as proper deployment of stents across the dissection. The other (patient 15) had a high clot burden with a right ICA T-occlusion associated with distal M1 and M2 clots; despite 3 passes with the Solitaire FR device followed by thrombectomy with the Merci device and intra-arterial TPA injection, reperfusion could not be achieved at level of both the superior and inferior M2 branches. The number of device passes ranged from 1 to 5 (average 1.8, SD ± 1.4). There were no device fractures or arterial dissections. The NIHSS scores at 24 hours after intervention ranged from 0 to 26 (average 9.8, SD ± 6.9), while NIHSS at discharge ranged from 0 to 27 (average 7.2, SD ± 7.1).

3.3. Recanalization Grade and Improvements in NIHSS. At discharge, eighteen patients (58%) had a good outcome (NIHSS improvement of ≥5), six (19%) had a fair outcome (NIHSS improvement of 1–4), and seven (23%) had a poor outcome (no improvement or worsening NIHSS). Table 2 summarizes patient recovery with respect to TIMI grade. Of note, 15 of 18 patients (83%) with good NIHSS outcome at discharge had TIMI 3, while 7 out of 13 patients (54%) with fair or poor outcome did not achieve complete recanalization. When this data was analyzed with Fisher's exact test, it was found that TIMI 3 perfusion was a statistically significant predictor of good outcome at discharge ($P = 0.012$).

Table 2: Recanalization grade as compared with NIHSS outcome at time of discharge.

	Good	Fair	Poor
TIMI 3	**15**	2	4
TIMI 2	3	*4*	*1*
TIMI 0 or 1	0	*0*	*2*

Bold emphasizes 15 of 18 patients (83%) with good NIHSS outcome at discharge had TIMI 3, while 7 out of 13 patients (54%) with fair or poor outcome did not achieve complete recanalization (TIMI 2 or 1).
Table graphically shows that TIMI 3 perfusion was a statistically significant predictor of good outcome at discharge ($P = 0.012$).

3.4. Clinical Outcomes and Safety. At three to six months, 69% of the patients had mRS ≤ 2 (see Table 1). Two patients were lost to followup and were not included in the analysis. There was no treatment-related mortality. The overall mortality rate after 3–6 months of followup was 10.3% (total of three patients including one inpatient mortality due to malignant cerebral edema and family withdrew care). No symptomatic hemorrhagic complications were observed after intervention. Seven patients had asymptomatic petechial hemorrhage in the stroke territory on 24 hour postintervention CT head. Luxury perfusion (contrast medium enhancement in CT head) was observed in 13 cases (41.9%). Figure 2 illustrates the typical Solitaire thrombectomy procedure in patient 14. Postprocedural minor groin hematoma occurred in 6 (Solitaire) versus 4 (Merci/Penumbra). Each group had three CAT scan documented retroperitoneal hematoma that did not require vascular surgical intervention.

3.5. Comparison with the Merci-Penumbra Group. A summary of patient characteristics stratified for both groups are presented in Table 3. These confounding factors were similar in both groups of patients. The radiographic recanalization rate and area salvage results of the Solitaire group are tabulated in Table 4 and those of the Merci/Penumbra group in Table 5.

3.5.1. Recanalization Rate Comparison. In the Merci/Penumbra group, ten patients (50%) achieved a TIMI grade of 3, five patients (25%) achieved a TIMI grade of 2, and 5 failed to recanalize (3 TIMI1 and 2 TIMI0). Similarly to the Solitaire group, when the recanalization was not attained, rescue procedure was taken with another device or ia-TPA. Four patients required additional rescue treatment in this group. Average procedure time was 70.8 minutes.

There was a trend towards higher recanalization rates (TIMI 2-3) (93.5% versus 75%, $P = 0.096$) and shorter length of procedure (58.5 min versus 70.8 min, $P = 0.08$) in the Solitaire group versus the Merci/Penumbra group. However, no statistical difference was reached with respect to recanalization grade and time of procedure.

3.5.2. Clinical Outcome Comparison. In the Merci/Penumbra group, the average 90-day mRS was 4 (SD ± 2). Seven of 20 (35.0%) patients had mRS ≤ 2. Three patients had symptomatic intracranial hemorrhage and the 90-day mortality rate was 45% (9 out of 20).

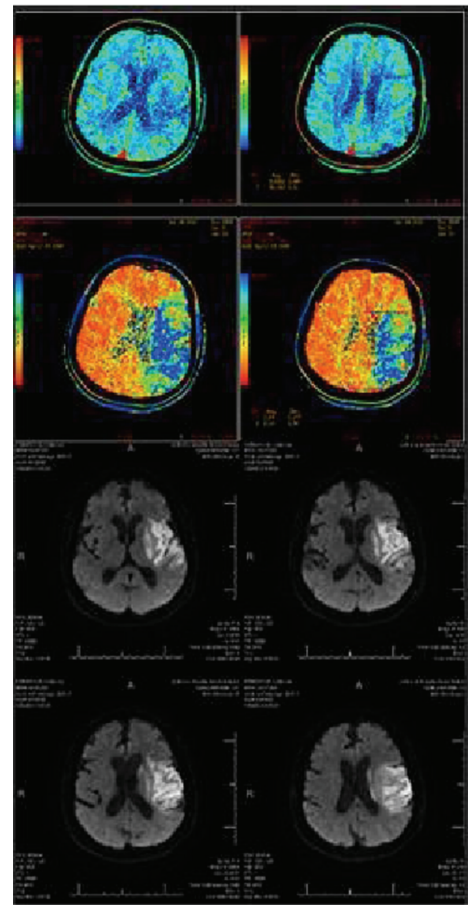

Figure 3: Top shows CT head perfusion study with mismatch in mean transit time and blood volume. Bottom shows smaller final completed stroke area in DWI sequence of MRI. Both used to calculate percentage area salvage.

The 90-day mRS was significantly better in the Solitaire group with 69% versus 35% achieving mRS ≤ 2 ($P = 0.03$) and the hemorrhagic complication rate was significantly higher in the Merci/Penumbra group (0% versus 15%, $P = 0.05$).

3.5.3. Area Salvage Comparison. The mean percentage salvage area was significantly larger in the Solitaire group (81.9% ± 17.6) versus the Merci/penumbra group (71.9% ± 19.7) ($P = 0.05$).

4. Discussion

4.1. Key Results and Interpretation. We assessed the safety, efficacy, and clinical outcome of the Solitaire FR system in our institution and compared these results with a group of patients treated with the Merci/Penumbra system. Most recently, two randomized clinical trials (SWIFT and TREVO2

Table 3: Baseline demographic and clinical characteristics of the patients.

	Solitaire ($n = 31$)	Merci/Penumbra ($n = 20$)	
Age (years; range)	64.1 (32–87)	67.5 (31–85)	$P = 0.02$
Sex (% male)	74%	65%	$P = 0.07$
NIHSS score (Mean; Range)	13.7 (3–26)	14.3 (8–22)	$P = 0.17$
Body-mass index (mean)	28	29	$P = 0.03$
ivTPA administration	42%	45%	$P = 0.02$
Medical history			
HTN	75%	70%	
DM	17%	25%	
Smoking	42%	40%	
Atrial Fibrillation	35%	45%	
Use of antiplatelet or anticoagulation	48%	55%	
Most proximal occlusion location			
Internal carotid artery	13%	25%	
M1 middle cerebral artery	51%	50%	
M2 middle cerebral artery	29%	20%	
Posterior circulation	6%	5%	
Occlusion side (left)	61%	55%	
Time to arterial puncture (min; range)	432 min (242–962 min)	351 min (240–600 min)	

Table 4: Results of Solitaire tabulated for area of salvage, recanalization rate, intervention time and clinical results.

Patient	Age	Gender	NIHSS on arrival	NIHSS at 24 h	ivTPA	Location of thrombus	% Salvage	Time to reperfusion (hrs)	Procedure time (min)	TIMI	Symptomatic ICH	mRS
1	87	F	18	13	N	R M2	61	17	42	3	N	4
2	64	M	12	7	N	L M1	90.7	11	90	3	N	1
3	73	M	12	8	Y	L M1	1	7	36	3	N	2
4	32	M	18	5	Y	R M2	83.5	5	33	3	N	0
5	50	M	21	7	N	R ICA	61.4	5	65	2	N	1
6	52	M	7	3	N	Basilar	NA	6	73	3	N	0
7	76	M	12	6	N	R M1	95.2	10	44	3	N	2
8	77	M	13	3	Y	R M1	1	6	65	2	N	0
9	62	M	9	7	N	L M2	1	5	70	2	N	2
10	77	F	13	6	Y	L ICA	96.9	10	80	3	N	2
11	48	M	12	1	N	R M2	59	6	20	3	N	0
12	82	M	9	4	Y	L M1	82.1	5	26	3	N	4
13	69	M	9	9	N	L vert	NA	6	65	1	N	4
14	63	F	21	16	N	L M1	73.9	5	41	3	N	1
15	87	M	19	27	Y	R M1	57.6	5	54	0	N	6
16	63	M	18	10	N	R M1	NA	11	52	3	N	4
17	71	M	13	7	Y	R ICA	95.7	7.5	57	2	N	0
18	74	M	10	10	N	R M1	1	16	105	3	N	6
19	61	M	15	13	N	R M1	86.6	14	80	2	N	4
20	61	M	3	2	Y	L M2	90.9	4	98	2	N	0
21	70	M	24	18	N	L M1	91.5	6	70	3	N	4
22	73	M	9	14	N	L M2	NA	9	80	3	N	6
23	26	F	3	0	Y	R ICA	88.8	9	30	3	N	0
24	77	F	8	5	Y	R M1	81.1	7	26	3	N	1
25	65	M	15	11	Y	R M2	90.6	6.5	32	2	N	2
26	45	F	23	17	N	L M1	82.8	8	55	3	N	1
27	57	M	20	20	Y	R M2	39.3	6.5	80	2	N	NA
28	54	M	12	5	N	L M1	97.8	8.5	65	3	N	0
29	56	F	17	18	Y	L M1	28.9	6	80	2	N	2
30	65	M	26	26	N	L ICA	NA	7.5	75	3	N	NA
31	71	F	5	7	N	L M1	92.9	13.5	25	3	N	1
Average							81.9					

Table 5: Data for 20 comparison group who received Merci/Penumbra treatment.

Patient	Age	Sex	IVtpA	NIH A	% Salvage	Location of clot	Time to intervention	Intervention time	TIMI	Symptomatic ICH	mRS at F/U
1	73	M	1	15	80.7	L M1	7	75	3	Y	2
2	85	F	0	14	73.4	L ICA	10	77	0	N	4
3	53	M	1	11	76.4	R M1	9	69	2	N	4
4	86	F	0	14	59.0	R ICA	8	88	1	N	6
5	47	M	0	14	52.4	R M2	NA	48	0	N	6
6	58	M	0	22	81.0	R M1	6	72	1	N	6
7	49	M	0	21	86.5	L M1	NA	28	3	N	3
8	86	F	1	16	83.2	L M1	4	33	3	N	2
9	63	M	1	12	97.2	R ICA	5	80	3	N	1
10	67	M	0	14	78.7	R M1	5	38	2	N	6
11	59	F	1	15	96.0	R M1	5	65	3	N	2
12	78	M	0	16	27.7	L M1	5	73	2	N	6
13	68	F	0	20	48.8	L ICA	NA	111	3	N	6
14	68	M	1	22	36.8	L M1	4	113	2	Y	6
15	59	F	1	16	58.6	R M1	4	57	1	N	6
16	69	M	1	20	67.5	R ICA	7	100	3	Y	3
17	75	M	0	12	92.6	R M1	4	59	3	N	2
18	59	F	1	12	87.9	R M1	4	85	2	N	6
19	62	M	1	10	92.5	R ICA	7.5	110	3	N	1
20	67	M	1	8	61.7	L M2	5	38	3	N	2
Average					**71.9**		5.85	**70.95**			

trails) have compared newer clot retrieval devices in treatment of acute ischemic stroke. In the SWIFT study, patients were significantly more likely to have flow restoration (TIMI scale 2 or 3) and a favorable outcome with the Solitaire FR device compared with the Merci device [4]. In the TREVO2 trial, patients treated with the Trevo device were 4.2 times more likely to achieve revascularization, with a significantly higher rate of favorable outcomes compared with the Merci device [7]. In our study, we not only reproduced higher rates of flow restoration and favorable outcomes with the Solitaire device but also demonstrated that Solitaire patients attained radiographically a significantly higher percentage salvage rate than Merci/Penumbra patients.

Comparing the outcomes of the present study with the results of five large mechanical thrombolysis trials (see Table 6): Merci, Multi-Merci, Penumbra Pivotal, SWIFT, and TREVO2 trials, our study obtained a higher recanalization rate than the Merci, Multi-Merci, and Penumbra pivotal stroke trials [3, 4, 8]. Our recanalization results were similar to those of the SWIFT and TREVO2 trials. The clinical outcome as represented by mRS ≤ 2 and three-month mortality rates in our study were significantly improved compared with all of these studies.

We believe that radiographic analysis enables more direct comparison of treatment efficacy in restoring viable brain tissue without introducing confounding variables such as patients' age, baseline heath status, and recovery process during rehabilitation. Clinical outcome assessment by means of mRS tends to involve these confounding factors that modify recovery from stroke in addition to the results of thrombectomy. Thus, in a sense, area salvage analysis is a simpler measure for the efficacy of thrombectomy device. Of course, in clinical medicine, our ultimate goal is to provide better clinical outcome for patients and this necessitates correlation between area salvage and clinical recovery from stroke.

Other key findings include a longer procedure time and a higher incidence of symptomatic intracranial hemorrhage after intervention for Merci/Penumbra group. Taken together, these findings suggest that the Solitaire FR device allows safer, faster, and more efficient treatment of acute ischemic stroke patients than older devices used in our institute.

4.2. Limitations. Our study is limited by the small number of patients treated with old generation systems: Merci and Penumbra (only twenty patients). Because of this, we decided to combine patients treated with Merci and Penumbra systems together as a comparison group. Though this demonstrated that the newest system (Solitaire FR) is superior to the older systems, it does not effectively convey whether the Solitaire is better than the Merci or the Penumbra individually. This grouping does not mean that authors believe that the Merci and the Penumbra systems yield similar recanalization results, clinical, or radiographic outcomes, rather it is just a grouping constructed based on the time course of thrombolysis device used in our institution. Another limitation is baseline characteristics of the Solitaire group and the Merci/Penumbra groups are not

Table 6: The outcomes of the present study compared to the results from large mechanical thrombectomy trials.

Present study		Merci [9]	Multi-Merci [8]	Penumbra pivotal stroke [3]	SWIFT trial [10] (solitaire arm)	TREVO2 trial [7] (TREVO2 arm)
Sample, *n*	31	141	164	125	58	88
Recanalization, *n* (%)	29 (93.5%)*	68 (48.2%)	112 (68.2%)	102 (81.6%)	48 (88.9%)	76 (86%)
symptomatic ICH, *n* (%)	0 (0)	11 (7.8%)	16 (9.7%)	14 (11.2%)	1 (1.7%)	4 (4%)
3 month mortality, *n* (%)	3 (10.3%)	61 (43.2%)	56 (34.1%)	31 (32.8%)	10 (17.2%)	29 (33%)
3 month mRS ≤ 2, *n* (%)	20 (69%)	39 (27.6%)	59 (35.9%)	52 (41.6%)	32 (58.2%)	38/85 (40%)

*This is the final recanalization rate which includes rescue treatment with other devices as well as iaTPA. With Solitaire FR device alone, the recanalization rate was 79.5%.

matched due to the retrospective nature of the study and the limited number of patients. Furthermore, despite that authors do acknowledge the TREVO trial and its efficacy being reported to be comparable if not superior to the Solitaire, our institution does not currently have enough patients treated with TREVO system so they were not included in this study. Another inherent limitation of our study is its retrospective design. The main methodological limitation to our study relates to its small sample size causing the study to be underpowered to detect small differences in outcome. Our results reflect the experience of a single institution with specific protocols for mechanical thrombectomy and may not be entirely applicable to other centers.

5. Conclusion

We presented the first single-center study comparing the Solitaire FR device and the Merci/Penumbra systems. We found significantly higher recanalization rates and improved outcomes with a statistically significant increase in the percentage area salvaged among patients treated with the Solitaire device. Our study adds to the growing body of evidence supporting the safety and efficacy of mechanical thrombectomy with the Solitaire FR system in large proximal arterial occlusions.

Disclosure

The paper has not been submitted elsewhere nor published elsewhere in whole or in part.

Conflict of Interests

The authors declare that they have no conflict of interests.

References

[1] H. P. Adams Jr., G. Del Zoppo, M. J. Alberts et al., "Guidelines for the early management of adults with ischemic stroke: a guideline from the american heart Association/American stroke association stroke council, clinical cardiology council, cardiovascular radiology and intervention council, and the atherosclerotic peripheral vascular disease and quality of care outcomes in research interdisciplinary working groups: the American academy of neurology affirms the value of this guideline as an educational tool for neurologists," *Stroke*, vol. 38, no. 5, pp. 1655–1711, 2007.

[2] R. M. Starke, R. J. Komotar, and E. S. Connolly, "Mechanical clot retrieval in the treatment of acute ischemic stroke," *Neurosurgery*, vol. 72, no. 2, pp. 19–21, 2013.

[3] Penumbra Pivotal Stroke Trial Investigators, "The penumbra pivotal stroke trial: safety and effectiveness of a new generation of mechanical devices for clot removal in intracranial large vessel occlusive disease," *Stroke*, vol. 40, no. 8, pp. 2761–2768, 2009.

[4] J. L. Saver, R. Jahan, E. I. Levy et al., "Solitaire flow restoration device versus the merci retriever in patients with acute ischaemic stroke (SWIFT): a randomised, parallel-group, non-inferiority trial," *The Lancet*, vol. 380, no. 9849, pp. 1241–1249, 2012.

[5] N. Chalouhi, H. Shannon, R. Starke et al., "Endovascular stroke intervention in young patients with large vessel occlusions," *Neurosurgical Focus*, vol. 35, 2011.

[6] N. Chalouhi, G. Ghobrial, and S. Tjoumakaris, "CT perfusion-guided versus time-guided mechanical recanalization in acute ischemic stroke patients," *Clinical Neurology and Neurosurgery*, 2013.

[7] R. G. Nogueira, H. L. Lutsep, R. Gupta et al., "Trevo versus merci retrievers for thrombectomy revascularisation of large vessel occlusions in acute ischaemic stroke (TREVO 2): a randomised trial," *The Lancet*, vol. 380, no. 9849, pp. 1231–1240, 2012.

[8] J. D. Fields, H. L. Lutsep, and W. S. Smith, "Higher degrees of recanalization after mechanical thrombectomy for acute stroke are associated with improved outcome and decreased mortality: pooled analysis of the MERCI and multi MERCI trials," *American Journal of Neuroradiology*, vol. 32, no. 11, pp. 2170–2174, 2011.

[9] Z.-S. Shi, Y. Loh, G. Walker, and G. R. Duckwiler, "Clinical outcomes in middle cerebral artery trunk occlusions versus secondary division occlusions after mechanical thrombectomy: pooled analysis of the mechanical embolus removal in cerebral ischemia (MERCI) and multi MERCI trials," *Stroke*, vol. 41, no. 5, pp. 953–960, 2010.

[10] J. L. Saver, R. Jahan, E. I. Levy et al., "Solitaire flow restoration device versus the merci retriever in patients with acute ischaemic stroke (SWIFT): a randomised, parallel-group, non-inferiority trial," *The Lancet*, vol. 380, no. 9849, pp. 1241–1249, 2012.

Hindawi Publishing Corporation
BioMed Research International
Volume 2013, Article ID 151643, 8 pages
http://dx.doi.org/10.1155/2013/151643

Review Article

Endovascular Treatment of Cerebral Mycotic Aneurysm: A Review of the Literature and Single Center Experience

Mario Zanaty,[1] Nohra Chalouhi,[1] Robert M. Starke,[2] Stavropoula Tjoumakaris,[1] L. Fernando Gonzalez,[1] David Hasan,[3] Robert Rosenwasser,[1] and Pascal Jabbour[1,4]

[1] *Department of Neurosurgery, Thomas Jefferson University, Jefferson Hospital for Neuroscience, Philadelphia, PA, USA*
[2] *Department of Neurological Surgery, University of Virginia School of Medicine, Charlottesville, VA, USA*
[3] *Department of Neurosurgery, University of Iowa, Iowa City, IA, USA*
[4] *Division of Neurovascular Surgery and Endovascular Neurosurgery, Department of Neurological Surgery, Thomas Jefferson University Hospital, 901 Walnut Street 3rd Floor, Philadelphia, PA 19107, USA*

Correspondence should be addressed to Pascal Jabbour; pascal.jabbour@jefferson.edu

Received 13 September 2013; Accepted 18 November 2013

Academic Editor: Steven J. Monteith

The management of mycotic aneurysm has always been subject to controversy. The aim of this paper is to review the literature on the intracranial infected aneurysm from pathogenesis till management while focusing mainly on the endovascular interventions. This novel solution seems to provide additional benefits and long-term favorable outcomes.

1. Introduction

Intracranial infectious aneurysms (IIAs) or mycotic aneurysms are a rare entity and represent 0.7 to 5.4% of all cerebral aneurysms [1]. The name mycotic originated from the fact of their resemblance to fungal vegetation [2]. Although they can be caused by fungal pathogen, they are most commonly due to bacterial infection [3]. Historically the management of mycotic aneurysms relied on surgery and antibiotics with limited use of endovascular therapy fearing the risk of overwhelming infection by introducing a foreign body to an infected region [4]. This theoretical fear exists in spite of the absence of reports in the literature on persistent infection or abscesses formation following endovascular surgery [5]. A recent review of the literature that examined 287 cases of cerebral mycotic aneurysms (CMAs) [5] found no postprocedural infection in the 46 cases treated by endovascular coiling. In another study, coiling was successful even in the presence of active bacteremia [6]. However, the safety and efficacy of these techniques are published in case-series and case-reports. Therefore, endovascular treatment remains an individualized therapy with no standard guidelines [7]. Given the inconsistency in IIA's evolution and response to treatment and given the lack of randomized controlled trials (RCTs), there has not been any widely accepted standard management [5]. The purpose of this paper is to briefly review cerebral mycotic aneurysms while focusing on the endovascular approach for their management.

2. Methodology

We performed a literature review using MEDLINE. The following meshwork words were used individually or in combination: mycotic, cerebral, infectious, intracranial, aneurysm, endovascular, treatment, management, and Onyx. We managed to find 3 articles on the use of Onyx in the treatment of IIAs. Other articles were included in our study using a more extensive search to briefly review the pathogenesis of the disease and to evaluate other alternative managements. The search was limited to the studies published in English.

3. Epidemiology

IIAs represent 5% of all intracranial aneurysms [8]. Currently there are no rigorous population-based epidemiological studies, but an analysis of a pooled cohort by Ducruet et al.

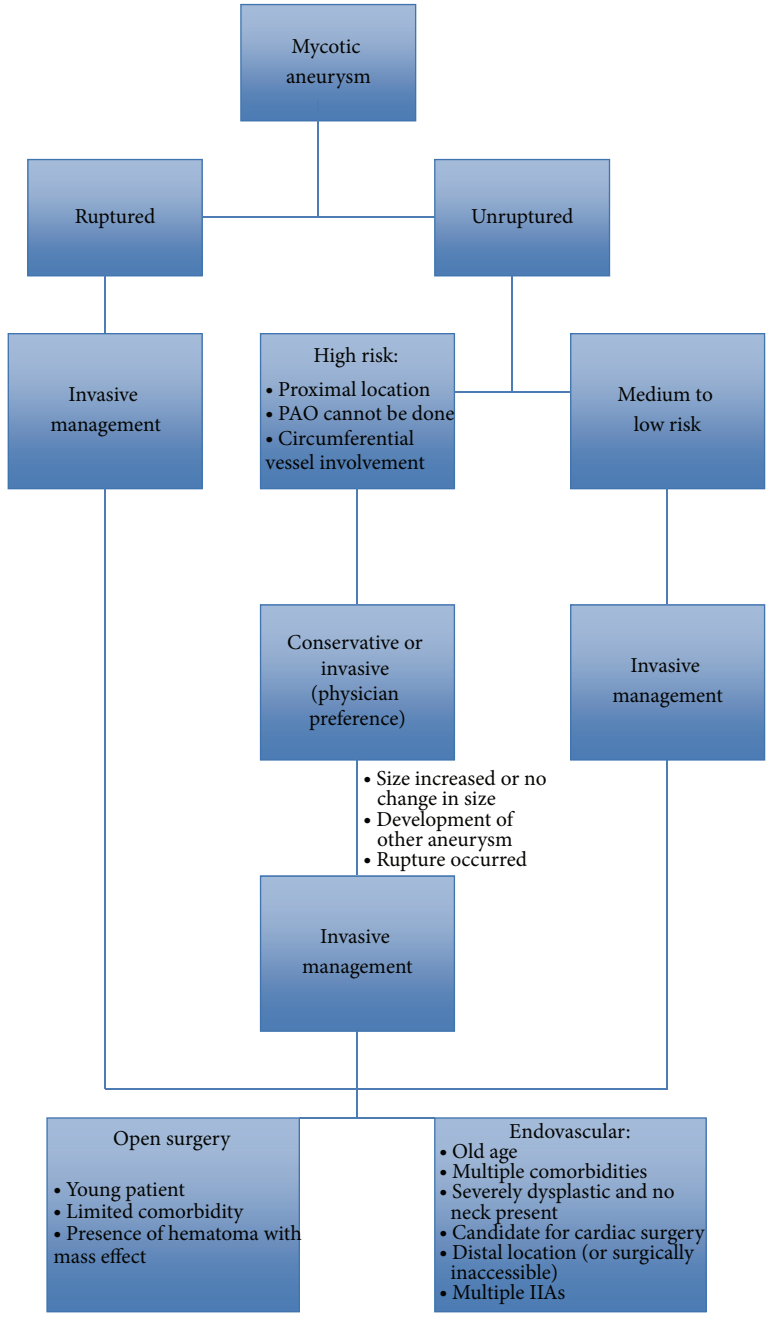

Figure 1: Management algorithm.

revealed that 65% of patients with IIA have an underlying endocarditis [5]. The prevalence has decreased from 86% after the advent of antibiotic era [9]. The most common sources of infectious bacteremia remain to be intravenous (IV) drug abuse and poor dental hygiene. Direct invasion of the vascular wall from a nearby infectious focus, such as cavernous sinus thrombophlebitis and bacterial meningitis, is also common cause of IAA. The median age tend to vary depending on the reviews between 35.1 [5] and 53 years [10]. Some studies reported a higher male predominance while the pooled cohort done by Ducruet et al. showed similar proportions of both genders (52% males and 48% females) [5].

4. Pathology and Pathogenesis

The process is the result of a developing infectious process involving the arterial wall [11]. The acute inflammation leads to neutrophils infiltration followed by degradation of the media and adventitia, fragmentation of the internal elastic lamina and proliferation of the intima. The weakened vessel wall in combination with the pulsatile pressure in the vasculature leads to an aneurysm formation and consequential growth [5]. Most of the authors prefer the term pseudoaneurysm [12], although both are widely used. Many processes may contribute to the development of IIAs: septic emboli lodging at distal branches, spreading infection involving

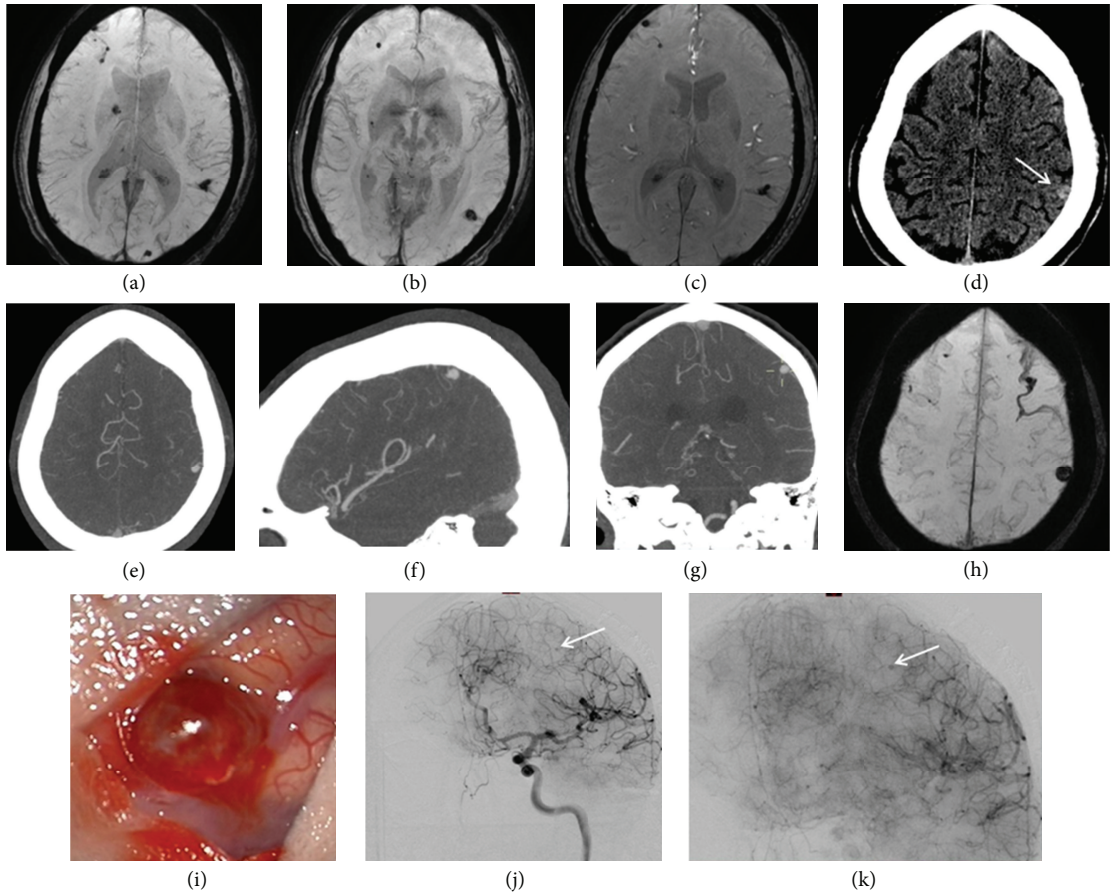

Figure 2: A patient with a history of intravenous drug abuse was admitted to an outside hospital for treatment of endocarditis. MRI at this time demonstrated multiple cerebral septic emboli and mycotic aneurysms (a–c). Two weeks after initiation of antibiotics, the patient had a significant headache and CT scan demonstrated new hemorrhage in the superior parietal lobe (d). The patient was transferred to our hospital for further care, and CTA and MRI at this time demonstrated 2 persistent mycotic aneurysms with hemorrhage surrounding the 7 mm aneurysm arising from the distal cortical branch from the middle cerebral artery (e–h). As the patient required a cardiac valve replacement and would receive full anticoagulation and had a hemorrhage 2 weeks after initiation of antibiotics, the intervention with the ruptured aneurysm was considered the best course of therapy. Due to the distal nature of the aneurysm, microsurgical removal was deemed the best therapy ((i), intraoperative image of cortically based aneurysm). Intraoperative angiogram demonstrated complete resection of the cortically based aneurysm with only the single aneurysm remaining (j, k). Follow CTA demonstrated resolution of the final remaining aneurysm.

the vasa vasorum, and periarterial lymphatic and vascular manipulation precipitating infection [2], all of which can lead to focal polymorphic neutrophil infiltration with enzymes and proinflammatory cytokine secretions. Consequently, the inflammatory reaction contributes to vessel friability, weakening, and pseudoaneurysm formation. Grossly, the aneurysm appears friable, having a thin-wall and wide or absent neck. This predisposes the aneurysm to rupture and consequent bleeding. If it ruptures, the mortality rate can be extreme, as high as 80% [13, 14]. Even though a fusiform morphology points toward a mycotic pseudoaneurysm, a saccular morphology does not exclude it, as it has been shown that approximately 41% of mycotic aneurysm in the literature are saccular [5].

Even though virus and fungi can cause IIAs, bacterial infection remains by far the most predominant cause. The most commonly reported bacterial pathogens are *S. aureus* and *Streptococcus* species. IIAs have been described following viral infection such as HIV-1 and VZV [15, 16] and fungal infection such as *Candida* and *Aspergillus* [4]. IIAs can be formed at distal branching points when the infectious agent spreads by hematogenous route, as seen in endocarditis, or it can be formed near the infected foci when the infectious agent spreads by direct invasion of the arterial wall from the extravascular site [5, 9]. The latter is more commonly seen in immunocompromised patients [9, 17]. The most common location of IIA seems to be the anterior circulation, mainly the MCA and its distal branches, contributing to as much as 50–78% of all IIAs [4, 5, 9].

5. Clinical Manifestations and Diagnosis

IIA's natural history is somewhat unpredictable but linked to significant mortality ranging from 30% to 80% if rupture occurs [18]. Some studies reported rupture as the most common presentation of IIAs, and most of the studies

Table 1: Response of aneurysm to medical treatment.

	Disappearance	Decrease in size	No change in size	Increase in size	Additional aneurysm development
Bartakke et al. [20]	29%	18.5%	15%	22%	15%
Corr et al. [24]	33%	17%	33%	17%	

reported that headache followed by fever is the most common symptom [18]. However, a recent review found septic infarct to be more common than intraparenchymal hemorrhage (IPH) and focal neurologic deficit to be a more common initial presentation than fever [5]. The bleeding can be subarachnoid, intraparenchymal, or intraventricular [5]. Other signs and symptoms of IIAs are due to the underlying etiology [19], such as septic emboli, fever, and chills, or to the mass effect of the aneurysm. Silent IIAs are not uncommon and can represent up to 10% of autopsy cases [20]. It is noteworthy that in contrast to saccular aneurysm, size does not seem to predict the risk of rupture [21]. When the CMA is extracranial, the presentation tends to be different. When this is the case, the most common presentation is a pulsatile painful lateral cervical mass, which may compress the cranial nerves resulting in dysphagia and dysphonia [22]. If it is left untreated, it may rupture causing a hemorrhagic shock or may deliver septic emboli to the anterior circulation of the brain [22].

The diagnosis of mycotic aneurysms relies on the presence of a predisposing infectious process with an aneurysm documented by vascular imaging. Some pieces of literature even recommend screening patient with bacterial endocarditis for intracranial aneurysms given the strong correlation between the two [5]. Digital subtraction angiography (DSA) continues to be the gold standard for the diagnosis of IIA [20], although CT angiography and magnetic resonance imaging can be used [5]. Some of the findings on DSA that points toward IIA are the fusiform shape, the multiplicity, the distal location, and the change in size on follow-up angiography [5]. Positive culture from the wall itself can confirm the diagnosis [5]. Other indicators are positive blood culture (only found in 35.6%), leukocytosis, elevated erythrocyte sedimentation rate (ESR), and elevated C-reactive protein (CRP) [5].

6. Treatment

6.1. Approach to Management. Given the lack of RCTs, there are currently no standards to guide clinical decision-making. Treatment involves antimicrobial agents, surgery, endovascular approach, and/or a combination of them [9]. As a rule, IIAs management depends essentially on whether it has ruptured or not [9], the aneurysm characteristics, and the overall health status of the patient.

For unruptured IIAs in patients with high surgical risk, conservative treatment with antibiotic is the mainstay therapy. Antibiotics are guided by blood and cerebrospinal fluid (CSF) cultures. If the results were negative, empiric treatment based on suspected pathogens is continued. A period of four to six weeks of antimicrobial therapy is generally recommended [23]. An aneurysm has a high surgical risk if there is a circumferential vessel involvement, if the location is proximal, or if parent artery sacrifice cannot be done due to considerable neurological deficits. These characteristics render the surgery or the endovascular therapy difficult and unsafe. Follow-up angiography is necessary to assess the risk of rupture, which is always present even with appropriate medical therapy [5]. Conservative management yields different outcomes in terms of change in size or disappearance of the aneurysm. The outcome with conservative management is worse than that of invasive treatment when the latter is indicated [20, 24]. Table 1 summarizes some of the outcomes after conservative management. Resistance to conservative treatment is suspected when the aneurysm size increases or remains the same and/or when other aneurysms develop while the patient is on the appropriate antibiotics. In this case, invasive management is warranted [1, 9]. However, some authors advise for endovascular or surgical management whenever the aneurysm is accessible [21], regardless of the rupture status.

In the case of unruptured aneurysm without high surgical risk, endovascular or surgical treatment is advised irrespectively of the size because of the high risk of rupture and the weak association between size and rupture [21].

Ruptured aneurysms on the other hand should be immediately secured by surgical or endovascular means. The success of endovascular or surgical treatment depends mostly on the aneurysm morphology, the comorbidities of the patient, and the presence of an associated intracerebral hemorrhage [25]. The choice between endovascular and open surgery is complex and should be individualized.

6.2. Surgical Management. A good candidate for surgery would be a young symptomatic patient with surgically accessible IIA and/or when a significant hematoma with mass effect is present [9]. Open surgery however would be challenging when the location of the aneurysm is in the distal anterior circulation. From a technical point of view, clipping a mycotic aneurysm is more difficult than a regular saccular aneurysm due to the friable nature of the aneurysm and the absence or the deformity of the neck. In addition, localizing a distal branch aneurysm might be challenging. However, image guidance technology may help in that issue. Open surgery faces a major limitation when the patient is candidate for cardiothoracic surgery, which requires heparinization and anticoagulation. This puts the patient at higher risk of intracranial bleeding after craniotomy. Even more, studies have shown that cardiothoracic surgery following craniotomy increases the risk of perioperative heart failure [26–28]. The major complications of surgery are perioperative rupture and clip erosion of the parent artery [7, 29]. An alternative option in an unruptured aneurysm to delay surgery and give adequate time for the aneurysm to become fibrotic, minimizing therefore the risk of perioperative rupture and

Table 2: Characteristics of different agents used in embolization.

Agent	Properties	Advantages	Inconvenience
NBCA	(i) Nonabsorbable, adhesive (ii) Rapid polymerization	(i) High durability (ii) Minimal inflammatory effect	High risk of gluing the microcatheter (instant polymerization)
Detachable coil	(i) New generation soft coil (ii) Hydrogel coated coils (increase in volume once in contact with blood, therefore decreasing initial coil-packing density)	(i) Durable (ii) Decreased risk of rupture (versus old-generation coil)	Risk of rupture (transient increase in pressure while deployment)
Onyx	Nonabsorbable, adhesive	(i) Slow polymerization (ii) Multiple injection from single catheter	(i) Requires familiarity (ii) Requires special catheter

enabling direct clipping [5]. Even then, the risk of surgery remains high [5]. For all the previous reasons and given that many patients with IIA are quite ill and have multiple comorbidities, surgery is falling out of favor [29]. In these settings, the endovascular option seems to replace surgery as standard of care in treatment of IIAs [29], yet the optimal treatment paradigm remains controversial.

6.3. Endovascular Management. Endovascular techniques are rapidly gaining ground in the management of all types of cerebral aneurysms [30–41]. For mycotic lesions, the advantages of endovascular therapy over surgery are a decreased risk of anesthesia particularly in patients with impaired valve function, rapid institution of anticoagulation therapy, and shortening of the delay between aneurysm treatment and cardiac surgery. The delay can be reduced from 2-3 weeks to as little as 1 day [5, 9, 25, 27]. A major indication for endovascular therapy would be a patient with high surgical risk, a patient candidate for cardiac surgery [5], and a surgically inaccessible or multiple IIAs [42].

Current strategies in endovascular therapy include an indirect approach by parent artery occlusion (PAO) using coils or liquid embolic agents (LEAs) and direct approach by embolization of the aneurysm using coils, stent-assisted coiling (SAC), flow diverters, and LEAs [7, 43, 44]. PAO is attempted when the aneurysm is distally located, dysplastic, involving the whole circumference of the parent vessel, and having a complex morphology, provided that the area of the brain supplied by that artery is noneloquent. Intracranial balloon test occlusion or amobarbital injection testing can help determining whether the area is eloquent or not when the provider is unsure [7]. IIAs that are proximal in location such as those arising from cavernous ICA tend to be more treated by a direct approach, while both approaches are equally used for aneurysms that are distal in location such as those arising from MCA and posterior cerebral artery (PCA). When the aneurysm is difficult to reach, LEAs can be used for distal PAO (N-butyl 2-cyanoacrylate, NBCA, ethylen-vinyl alcohol copolymer, Onyx). The advantages and disadvantages of the different agents used are summarized in Table 2.

Endovascular coiling has been attempted by Andreou et al. [10] and Chapot et al. [42] with successful occlusion, without any rupture or death (Table 3) [1, 42, 45]. Sugg et al. [25] presented a case-report in which an IIA was treated by Neuroform stent. The major drawback was the use of antiplatelet agents [27], which can be critical if the aneurysm ruptured. Jadhav et al. [29] used Onyx 18 to treat 2 cases of mycotic aneurysm, one due to its resistance to antibiotic treatment and the other due to its high risk of rupture in the setting of chronic anticoagulation in a patient with antiphospholipid syndrome [29]. Onyx has the advantage over NBCA of being nonadhesive, with a long precipitation time. This allows for more precise control resulting in more satisfactory embolization [7, 29].

Katakura et al. treated pediatric IIAs using NBCA and coils for PAO with no complications from the occlusion of distal MCA branches [46]. Eddleman et al. approached pediatric patients with IIAs that presented with rupture [7]. One patient was treated with PAO using Onyx and another patient was treated by direct coiling followed by Onyx embolization due to persistent filling of the aneurysm on follow-up DSA [7]. The treatment was effective and safe (Tables 3 and 4). For management algorithm, please refer to Figure 1.

At our institution, Thomas Jefferson University Hospital, 4 mycotic aneurysms, 3 of which were associated with arteriovenous malformation and 1 with moyamoya disease, were successfully treated. Complete aneurysm obliteration was achieved in all patients by using Onyx 18 to occlude the aneurysm or to trap the parent vessel, with a procedural related mortality and morbidity rate of 0%. Unfortunately, 2 of our patients died from cardiac complications caused by their endocarditis. The technique that seemed to provide additional safety was the injection just proximal to the aneurysm, thus limiting the distal migration while the filling is taking place. There was neither instances of reflux nor accidental migration of embolic material. There were no recanalization or rebleeding on followup. We conclude that parent vessel trapping with Onyx 18 offers a simple, safe, and effective means of achieving obliteration of distal challenging aneurysms. Avoiding the need for aneurysm catheterization reduces intra-arterial manipulation and thus practically eliminates the risk of aneurysm perforation. Figure 2 illustrates a case of IIA that was treated by Onyx 18.

7. Conclusion

IIAs have a rupture risk of less than 2% [47]. Nevertheless the mortality rate after rupture could reach as high as

Table 3: Aneurysm coiling with or without stent.

GDC* ± stent	Modality of treatment	Response
Yen et al. [45]	(i) Helistent 3.5 × 9 mm + GDC for left cavernous carotid (ii) Helistent 4 × 9 mm + GDC for right cavernous carotid	Complete occlusion No complication
Nakahara et al. [1]	(i) 9.2 mm PCA, ultrasoft GDC (ii) 5.7 mm distal left ACA, ultrasoft GDC, treated by PAO	Complete occlusion No complication
Chapot et al. [42] (18 cases)	(i) Nonselective cyanoacrylate (ii) Coil embolization	Complete occlusion No rupture or death

*GDC: Guglielmi detachable coils.

Table 4: Results from treatment with Onyx.

Onyx Rx	Location	Treatment/complication
Eddleman et al. [7, 49]: Case 1	M3 4 × 4 mm	Onyx 18, no complication, no filling
Eddleman et al. [7, 49]: Case 2	MCA anterior division 4 × 6 mm	Coiling but persistent filling → Onyx 18 Complications: radiologic distal occlusion due to reflux, but clinically insignificant.
Zhao et al. [43]	(i) 11 × 14 mm (ii) P3 of PCA	Onyx 18 under local anesthesia No complications
la Barge et al. [52]	(i) Right parietooccipital artery (fusiform) (ii) Left parietotemporal artery	Onyx 18 No complications Complete occlusion
Our institution	(i) Left MCA at M2 (ii) Left distal ACA (iii) 2 other patients	Complete occlusion 0% combined mortality morbidity

80% [21, 48]. In the last decade the flourishing advances in endovascular techniques expanded the scope of its application and have transformed it from a rescue procedure to a first-line treatment as recommended by many authors [28, 42, 48–51]. The majority of the patients with IIAs are quite ill with multiple comorbidities. Therefore, an endovascular approach would be a more suitable treatment option [29]. Unruptured IIAs can be treated with antibiotics and follow-up imaging in 1-2 weeks after therapy. If the aneurysm decreased in size or resolved, then the patient most likely will not need an invasive therapy. Continuation of the antimicrobial in that case would be appropriate while noting that a decrease in size does not correlate with a decrease in the risk of rupture [4]. If the aneurysm is increasing in size or remaining the same, invasive procedures become mandatory. The choice between open surgery and endovascular management depends on a multitude of factors already described above, but the most important are the following: the morphology and location of the aneurysm, whether it is possible or not to sacrifice the parent artery, whether the patient needs or has received valve replacement surgery, and lastly the patient overall health status. Even though there is no head to head RCTs comparing endovascular and open surgery, most infectious aneurysms are being treated by endovascular method [7]. The IIAs of patients considered "strongly immunocompromised" such as those with AIDS, those on chemotherapy, or those on immunosuppressive drugs, have higher rates of growth and rupture [6, 51]. The prognosis of these patients depends on the prompt recognition and early aggressive treatment. Both endovascular and surgical techniques are safe and effective options that have been shown to increase survival when compared to conservative management alone [4].

Authors' Contribution

All authors have approved the final form of the paper and concur with the submission. The responsible authorities at our institution have approved the work. Pascal Jabbour is a consultant at Covidien and CNV.

References

[1] I. Nakahara, M. M. Taha, T. Higashi et al., "Different modalities of treatment of intracranial mycotic aneurysms: report of 4 cases," *Surgical Neurology*, vol. 66, no. 4, pp. 405–409, 2006.

[2] S. H. Lee, Y. K. Cho, J. M. Park, C. Chung, H. S. Kim, and J. J. Woo, "Treatment of an acute mycotic aneurysm of the common carotid artery with a covered stent-graft," *Yonsei Medical Journal*, vol. 53, no. 1, pp. 224–227, 2012.

[3] S. Dhomne, C. Rao, M. Shrivastava, W. Sidhartha, and U. Limaye, "Endovascular management of ruptured cerebral mycotic aneurysms," *British Journal of Neurosurgery*, vol. 22, no. 1, pp. 46–52, 2008.

[4] L. M. Allen, A. M. Fowler, C. Walker et al., "Retrospective review of cerebral mycotic aneurysms in 26 patients: focus on treatment in strongly immunocompromised patients with a brief literature review," *American Journal of Neuroradiology*, vol. 34, no. 4, pp. 823–827, 2013.

[5] A. F. Ducruet, Z. L. Hickman, B. E. Zacharia et al., "Intracranial infectious aneurysms: a comprehensive review," *Neurosurgical Review*, vol. 33, no. 1, pp. 37–45, 2010.

[6] W. Z. Ray, M. N. Diringer, C. J. Moran, and G. J. Zipfel, "Early endovascular coiling of posterior communicating artery saccular aneurysm in the setting of staphylococcus bacteremia: case report and review of the literature," *Neurosurgery*, vol. 66, no. 4, p. E847, 2010.

[7] C. S. Eddleman, D. Surdell, A. DiPatri Jr., T. Tomita, and A. Shaibani, "Infectious intracranial aneurysms in the pediatric population: endovascular treatment with Onyx," *Child's Nervous System*, vol. 24, no. 8, pp. 909–915, 2008.

[8] R. Agid, M. P. S. Souza, G. Reintamm, D. Armstrong, P. Dirks, and K. G. TerBrugge, "The role of endovascular treatment for pediatric aneurysms," *Child's Nervous System*, vol. 21, no. 12, pp. 1030–1036, 2005.

[9] P. J. Peters, T. Harrison, and J. L. Lennox, "A dangerous dilemma: management of infectious intracranial aneurysms complicating endocarditis," *Lancet Infectious Diseases*, vol. 6, no. 11, pp. 742–748, 2006.

[10] A. Andreou, I. Ioannidis, and A. Mitsos, "Endovascular treatment of peripheral intracranial aneurysms," *American Journal of Neuroradiology*, vol. 28, no. 2, pp. 355–361, 2007.

[11] J. O. Yoon, "Not just an aneurysm, but an infected one: a case report and literature," *Journal of Vascular Nursing*, vol. 24, no. 1, pp. 2–8, 2006.

[12] G. F. Molinari, L. Smith, M. N. Goldstein, and R. Satran, "Pathogenesis of cerebral mycotic aneurysms," *Neurology*, vol. 23, no. 4, pp. 325–332, 1973.

[13] S. Powell and A. Rijhsinghani, "Ruptured bacterial intracranial aneurysm in pregnancy: a case report," *Journal of Reproductive Medicine*, vol. 42, no. 7, pp. 455–458, 1997.

[14] A. Biondi, "Intracranial aneurysms associated with other lesions, disorders or anatomic variations," *Neuroimaging Clinics of North America*, vol. 16, no. 3, pp. 467–482, 2006.

[15] A. Mahadevan, R. Tagore, N. B. Siddappa et al., "Giant serpentine aneurysm of vertebrobasilar artery mimicking dolichoectasia—an unusual complication of pediatric AIDS. Report of a case with review of the literature," *Clinical Neuropathology*, vol. 27, no. 1, pp. 37–52, 2008.

[16] G. Modi, K. Ranchod, M. Modi, and A. Mochan, "Human immunodeficiency virus associated intracranial aneurysms: report of three adult patients with an overview of the literature," *Journal of Neurology, Neurosurgery and Psychiatry*, vol. 79, no. 1, pp. 44–46, 2008.

[17] T. V. Mincheff and A. W. Cooler, "Ruptured mycotic aneurysm presenting initially with bacterial meningitis," *American Surgeon*, vol. 74, no. 1, pp. 73–75, 2008.

[18] A. R. Tunkel and D. Kaye, "Neurologic complications of infective endocarditis," *Neurologic Clinics*, vol. 11, no. 2, pp. 419–440, 1993.

[19] M. P. Trivedi, C. Carroll, and S. Rutherford, "Infective endocarditis complicated by rupture of intracranial mycotic aneurysm during pregnancy," *International Journal of Obstetric Anesthesia*, vol. 17, no. 2, pp. 182–187, 2008.

[20] S. Bartakke, U. Kabde, M. N. Muranjan, and S. B. Bavdekar, "Mycotic aneurysm: an uncommon cause for intra-cranial hemorrhage," *Indian Journal of Pediatrics*, vol. 69, no. 10, pp. 905–907, 2002.

[21] S. Kannoth and S. V. Thomas, "Intracranial microbial aneurysm (Infectious Aneurysm): current options for diagnosis and management," *Neurocritical Care*, vol. 11, no. 1, pp. 120–129, 2009.

[22] T. C. Tsai, N. Barot, R. Dalman, and F. Mihm, "Combined endovascular and open operative approach for mycotic carotid aneurysm," *Journal of Vascular Surgery*, vol. 51, no. 6, pp. 1514–1516, 2010.

[23] L. K. Phuong, M. Link, E. Wijdicks et al., "Management of intracranial infectious aneurysms: a series of 16 cases," *Neurosurgery*, vol. 51, no. 5, pp. 1145–1152, 2002.

[24] P. Corr, M. Wright, and L. C. Handler, "Endocarditis-related cerebral aneurysms: radiologic changes with treatment," *American Journal of Neuroradiology*, vol. 16, no. 4, pp. 745–748, 1995.

[25] R. M. Sugg, R. Weir, D. G. Vollmer, and E. D. Cacayorin, "Cerebral mycotic aneurysms treated with a neuroform stent: technical case report," *Neurosurgery*, vol. 58, no. 2, pp. E381–E381, 2006.

[26] K. Oohara, T. Yamazaki, H. Kanou, and A. Kobayashi, "Infective endocarditis complicated by mycotic cerebral aneurysm: two case reports of women in the peripartum period," *European Journal of Cardio-Thoracic Surgery*, vol. 14, no. 5, pp. 533–535, 1998.

[27] T. Asai, A. Usui, S. Miyachi, and Y. Ueda, "Endovascular treatment for intracranial mycotic aneurysms prior to cardiac surgery," *European Journal of Cardio-Thoracic Surgery*, vol. 21, no. 5, pp. 948–950, 2002.

[28] H. B. Erdogan, V. Erentug, N. Bozbuga, D. Goksedef, E. Akinci, and C. Yakut, "Endovascular treatment of intracerebral mycotic aneurysm before surgical treatment of infective endocarditis," *Texas Heart Institute Journal*, vol. 31, no. 2, pp. 165–167, 2004.

[29] A. P. Jadhav, J. C. Pryor, and R. G. Nogueira, "Onyx embolization for the endovascular treatment of infectious and traumatic aneurysms involving the cranial and cerebral vasculature," *Journal of NeuroInterventional Surgery*, vol. 5, pp. 562–565, 2013.

[30] M. T. Koltz, N. Chalouhi, S. Tjoumakaris et al., "Short-term outcome for saccular cerebral aneurysms treated with the Orbit Galaxy Detachable Coil System," *Journal of Clinical Neuroscience*, 2013.

[31] N. Chalouhi, P. Jabbour, S. Singhal et al., "Stent-assisted coiling of intracranial aneurysms: predictors of complications, recanalization, and outcome in 508 cases," *Stroke*, vol. 44, pp. 1348–1353, 2013.

[32] N. Chalouhi, P. Jabbour, R. M. Starke et al., "Endovascular treatment of proximal and distal posterior inferior cerebellar artery aneurysms," *Journal of Neurosurgery*, vol. 118, pp. 991–999, 2013.

[33] N. Chalouhi, P. Jabbour, S. Tjoumakaris et al., "Single-center experience with balloon-assisted coil embolization of intracranial aneurysms: safety, efficacy and indications," *Clinical Neurology and Neurosurgery*, vol. 115, pp. 607–613, 2013.

[34] N. Chalouhi, D. L. Penn, S. Tjoumakaris et al., "Treatment of small ruptured intracranial aneurysms: comparison of surgical and endovascular options," *Journal of the American Heart Association*, vol. 1, Article ID e002865, 2012.

[35] N. Chalouhi, R. M. Starke, M. T. Koltz et al., "Stent-assisted coiling versus balloon remodeling of wide-neck aneurysms: comparison of angiographic outcomes," *American Journal of Neuroradiology*, vol. 34, pp. 1987–1992, 2013.

[36] N. Chalouhi, R. M. Starke, S. I. Tjoumakaris et al., "Carotid and vertebral artery sacrifice with a combination of Onyx and coils: technical note and case series," *Neuroradiology*, vol. 55, pp. 993–998, 2013.

[37] N. Chalouhi, T. Theofanis, P. Jabbour et al., "Endovascular treatment of posterior communicating artery aneurysms with oculomotor nerve palsy: clinical outcomes and predictors of nerve recovery," *American Journal of Neuroradiology*, vol. 34, pp. 828–832, 2013.

[38] N. Chalouhi, S. Tjoumakaris, A. S. Dumont et al., "Treatment of posterior circulation aneurysms with the pipeline embolization device," *Neurosurgery*, vol. 72, pp. 883–889, 2013.

[39] N. Chalouhi, S. Tjoumakaris, L. F. Gonzalez et al., "Coiling of large and giant aneurysms: complications and long-term results of 334 cases," *American Journal of Neuroradiology*, 2013.

[40] N. Chalouhi, S. Tjoumakaris, R. M. Starke et al., "Comparison of flow diversion and coiling in large unruptured intracranial saccular aneurysms," *Stroke*, vol. 44, pp. 2150–2154, 2013.

[41] N. Chalouhi, S. Tjoumakaris, A. S. Dumont et al., "Superior hypophyseal artery aneurysms have the lowest recurrence rate with endovascular therapy," *American Journal of Neuroradiology*, vol. 33, pp. 1502–1506, 2012.

[42] R. Chapot, E. Houdart, J.-P. Saint-Maurice et al., "Endovascular treatment of cerebral mycotic aneurysms," *Radiology*, vol. 222, no. 2, pp. 389–396, 2002.

[43] P. Zhao, J. Li, M. He, and C. You, "Infectious intracranial aneurysm: endovascular treatment with Onyx case report and review of the literature," *Neurology India*, vol. 58, no. 1, pp. 131–134, 2010.

[44] B. A. Gross and A. S. Puri, "Endovascular treatment of infectious intracranial aneurysms," *Neurosurgical Review*, vol. 36, no. 1, pp. 11–19, 2013.

[45] P. S. Yen, B. T. Teo, S. C. Chen, and T. L. Chiu, "Endovascular treatment for bilateral mycotic intracavernous carotid aneurysms: case report and review of the literature," *Journal of Neurosurgery*, vol. 107, no. 4, pp. 868–872, 2007.

[46] K. Katakura, T. Kayama, R. Kondo et al., "A case of multiple cerebral mycotic aneurysms treated with endovascular surgery," *Neurological Surgery*, vol. 23, no. 12, pp. 1127–1132, 1995.

[47] N. Chalouhi, B. L. Hoh, and D. Hasan, "Review of cerebral aneurysm formation, growth, and rupture," *Stroke*, 2013.

[48] J. Y. Chun, W. Smith, V. van Halbach, R. T. Higashida, C. B. Wilson, and M. T. Lawton, "Current multimodality management of infectious intracranial aneurysms," *Neurosurgery*, vol. 48, no. 6, pp. 1203–1214, 2001.

[49] C. Eddleman, D. Nikas, A. Shaibani, P. Khan, A. J. DiPatri Jr., and T. Tomita, "Hydro Coil embolization of a ruptured infectious aneurysm in a pediatric patient: case report and review of the literature," *Child's Nervous System*, vol. 23, no. 6, pp. 707–712, 2007.

[50] Y. Hara, K. Hosoda, T. Wada, H. Kimura, and E. Kohmura, "Endovascular treatment for a unusually large mycotic aneurysm manifesting as intracerebral hemorrhage—case report," *Neurologia Medico-Chirurgica*, vol. 46, no. 11, pp. 544–547, 2006.

[51] R. W. Hurst, A. Judkins, W. Bolger, A. Chu, and L. A. Loevner, "Mycotic aneurysm and cerebral infarction resulting from fungal sinusitis: imaging and pathologic correlation," *American Journal of Neuroradiology*, vol. 22, no. 5, pp. 858–863, 2001.

[52] D. V. la Barge III, P. P. Ng, E. A. Stevens, N. K. Friedline, J. R. Kestle, and R. H. Schmidt, "Extended intracranial application for ethylen vinyl alcohol copolymer (Onyx): mycotic and dissecting aneurysms. Technical note," *Journal of Neurosurgery*, vol. 111, no. 1, pp. 114–118, 2009.

Hindawi Publishing Corporation
BioMed Research International
Volume 2013, Article ID 640638, 4 pages
http://dx.doi.org/10.1155/2013/640638

Clinical Study

Cerebral Blood Flow Dynamics and Head-of-Bed Changes in the Setting of Subarachnoid Hemorrhage

David K. Kung,[1] Nohra Chalouhi,[2] Pascal M. Jabbour,[2] Robert M. Starke,[3] Aaron S. Dumont,[2] H. Richard Winn,[1] Matthew A. Howard III,[1] and David M. Hasan[1]

[1] *Department of Neurosurgery, University of Iowa Hospitals and Clinics, 200 Hawkins Drive, JCP 1616, Iowa City, IA 52242, USA*
[2] *Department of Neurosurgery, Thomas Jefferson University and Jefferson Hospital for Neuroscience, Philadelphia, PA, USA*
[3] *Department of Neurological Surgery, University of Virginia School of Medicine, Charlottesville, VA, USA*

Correspondence should be addressed to David M. Hasan; david-hasan@uiowa.edu

Received 16 September 2013; Accepted 30 October 2013

Academic Editor: Steven J. Monteith

Head-of-bed (HOB) elevation is usually restricted in patients with aneurysmal subarachnoid hemorrhage (SAH). The goal of this study is to correlate HOB changes (0° and 90°) with cerebral blood flow using transcranial Doppler (TCD) and thermal diffusion probe in SAH patients. Thirteen patients with SAH were prospectively enrolled in the study. Eight patients underwent placement of a thermal diffusion probe for regional CBF measurement. CBF values were measured with the patients in flat (0°) and upright sitting positions (90°) at days 3, 7, and 10. The average increase in blood flow velocity when changing HOB from 0° to 90° was 7.8% on day 3, 0.1% on day 7, and 13.1% on day 10. The middle cerebral artery had the least changes in velocity. The average regional CBF measurement was 22.7 ± 0.3 mL/100 g/min in the supine position and 23.6 ± 9.1 mg/100 g/min in the sitting position. The changes were not statistically significant. None of the patients developed clinical cerebral vasospasm. Changing HOB position in the setting of SAH did not significantly affect cerebral or regional blood flow. These data suggest that early mobilization should be considered given the detrimental effects of prolonged bed rest.

1. Introduction

Patients who suffer aneurysmal SAH are at risk of secondary injuries including cerebral edema and delayed cerebral vasospasm. Traditionally, as a part of the overall treatment protocol for SAH, patients are kept in prolonged bed rest. The assumption is that bed rest will help maintain adequate blood flow to the brain. However, the data supporting this assumption are limited [1].

Blood flow to the brain is critical and complex. CBF is influenced by multiple factors including systemic arterial pressure, distance of the head above the heart, venous and CSF drainage, and vascular tone of cerebral vessels [2]. In a normal individual, as the head is raised, the systemic arterial pressure is maintained by blood pressure reflexes. At the same time, the arterial perfusion pressure to the head is reduced by the distance the head is raised above the heart, but the intracranial pressure is also reduced because of the improved venous drainage. Together with an intact autoregulation response of the cerebral vasculature, the net effect is little change in CBF [3–5]. However, in patients with impaired autoregulation or with vasospasm following SAH, a raise in head position may theoretically diminish CBF. Conversely, in the case of significant cerebral edema after SAH, it may be important to raise the head to improve venous drainage and maximize cerebral perfusion pressure.

Prolonged bed rest, particularly in the elderly and the critically ill, carries its own morbidity [6]. Extensive research has documented the deleterious effects of prolonged bed rest in multiple organ systems, including cardiovascular, musculoskeletal, cognitive, hematologic, and respiratory [7–10]. Significant physiological deterioration begins on the first few days of bed rest. These complications add to the already devastating neurologic injury incurred by SAH.

Considering the potential deleterious effects of prolonged bed rest and its dubious benefit in maintaining cerebral blood

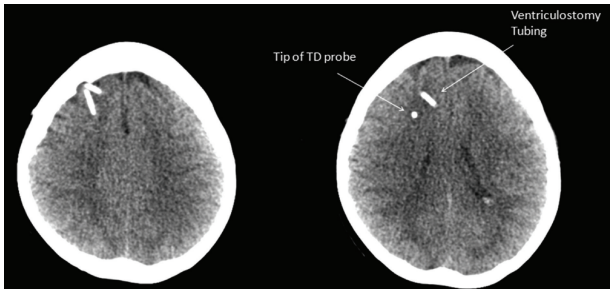

Figure 1: Postoperative head CT scan demonstrating the position of the thermal diffusion blood flow probe.

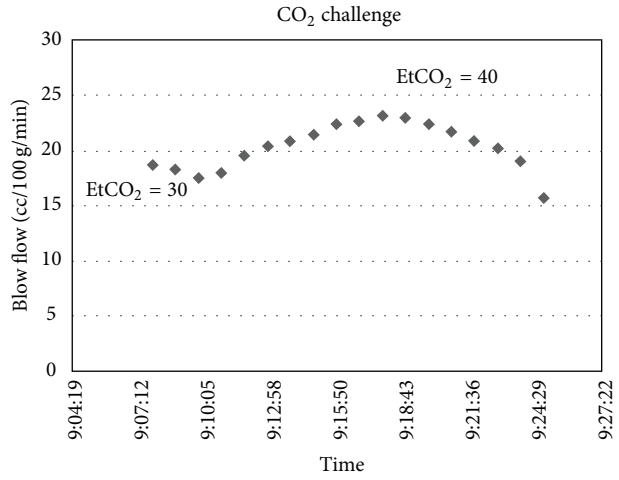

Figure 2: A typical tracing of thermal diffusion CBF measurement in response to change in end-tidal CO_2.

flow, we investigated the effect of head position on cerebral blood flow in SAH patients. We hypothesize that the routine practice of placing SAH patients in prolonged bed rest is unnecessary to maintain stable CBF.

2. Material and Methods

The study protocol was approved by the University of Iowa Institutional Review Boards. In this prospective study, we used two complementary methods to investigate the effects of head position on CBF in SAH patients. SAH patients who underwent placement of ventriculostomy and thermal diffusion CBF monitor were included prospectively. Thermal diffusion probes (Hemedex, Cambridge, MA, USA) were inserted through the same burr hole as the ventriculostomy to a depth of 2 cm but at an angle so that the tip of the probe is away from the ventriculostomy tubing (Figure 1). Immediately after probe placement and before the patients were extubated, the end-tidal CO_2 were adjusted within normal limit to check for associated change in CBF in order to verify proper functioning of the probe (Figure 2). Another group of SAH patients was also enrolled and underwent TCD studies only. Changes in head position and the corresponding changes in CBF parameters were evaluated. Specifically, on days 3, 7, and 10, the patient's CBF measurements (as measured by transcranial Doppler and thermal diffusion probe) were recorded in the supine and the 90-degree upright position 10 minutes later. TCD data were obtained in the medial cerebral arteries (MCA), the anterior cerebral arteries (ACA), and the posterior cerebral arteries (PCA) bilaterally using a handheld probe. Basic patient information such as age, sex, clinical exam, and hospital course was recorded. Delayed cerebral ischemia was defined as symptomatic vasospasm or infarction on CT attributable to vasospasm [11]. The percentage changes in mean blood flow velocity in each distribution from supine to sitting were calculated. Paired Student's t-test was used to determine statistical significance.

3. Results

The demographic details of the patients enrolled are shown in Table 1. Thirteen patients were enrolled, and the average age was 63 (ranging from 21 to 85). Seventy-seven percent (10/13) were females . Eight patients were studied with both thermal diffusion probe and TCD; five patients were studied with TCD only. The average Fisher grade was 3.3 ± 0.75 SD, and the average Hunt-Hess grade on admission was 2.5 ± 1.3 SD (ranging from 1 to 5). None of the patients had an adverse event with the manipulation of the head-of-bed. None of the patients developed delayed cerebral ischemia.

3.1. TCD Results. The MCA, ACA, and PCA were individually insonated bilaterally in both the supine and the upright sitting positions. The average increase in blood flow velocity from supine to sitting was 7.8% on day 3, 0.1% on day 7, and 13.1% on day 10. When each vessel was examined individually, the MCA appears to have the least changes in velocity depending on position (average 0.9% on day 3, −3.2% on day 7, and 1% on day 10). The ACA had 11.1% increase in velocity on day 3, −9.2% on day 7, and 24.2% on day 10. The PCA had 12.9% increase on day 3, 11.3% on day 7, and 14.7% on day 10. The absolute velocities were illustrated in Table 2. None of the velocity changes reaches statistical significance except for MCA changes on day 7 ($P = 0.008$). TCD value changes did not have any associated clinical manifestations, irrespective of Fisher or Hunt-Hess grade.

3.2. Thermal Diffusion CBF Measurement Results

3.2.1. PCO_2 Challenge and Regional CBF. Regional cerebral blood flow changed expectedly with changes in end-tidal PCO_2 induced by adjusting ventilation (Figure 1). The regional cerebral blood flow increased with increased PCO_2 and decreased with decreased PCO_2. The average CBF changed from 13.7 to 23.6 cc/100 g/min with end-tidal PCO_2 changes from 30 to 40 mmHg ($n = 4$).

3.2.2. Postural Changes and Regional CBF. Thermal diffusion CBF measurement was done in 8 patients. The average CBF measurement in the supine position was 22.7 ± 10.3 mL/100 g/min. The average measurement in the 90-degree sitting

Table 1: Patients demographic.

Patient	Age	Sex	Fisher grade	WFNS	Hunt-Hess	Aneurysm location	Thermal diffusion probe
1	53	Female	2	1	1	pcom	y
2	72	Female	4	4	3	acom	y
3	74	Female	4	5	5	PICA	y
4	42	Female	3	1	2	pcom	y
5	63	Female	3	2	2	pcom	y
6	85	Female	4	2	3	acom	y
7	39	Female	4	1	2	acom	y
8	21	Female	2	1	1	pcom	y
9	77	Male	3	4	4	pcom	n
10	76	Male	3	2	3	acom	n
11	69	Male	4	2	4	acom	n
12	81	Female	4	2	2	acom	n
13	71	Female	3	1	1	acom	n

Table 2: Average blood flow velocities and percentage changes in each vascular distribution.

(a)

Average velocity (cm/s)	Day 3		Day 7		Day 10	
	Supine	Upright	Supine	Upright	Supine	Upright
MCA	79	73	111	106	90	92
SD	56	41	49	46	46	52
ACA	69	72	72	62	56	68
SD	42	46	23	23	26	39
PCA	70	75	59	68	67	72

(b)

Percentage changes from supine to upright (%)	Day 3	Day 7	Day 10
MCA	0.9	−3.2	1.0
ACA	11.1	−9.2	24.2
PCA	12.9	11.3	14.6

position was 23.6 ± 9.1 mg/100 g/min. There was no statistically significant difference between the two groups (P = 0.196).

4. Discussion

Prolonged bed rest results in multiple physiological changes that could be detrimental. Supine positioning decreases tidal volume and minute ventilator volume [12, 13] and impairs the ability to clear secretions, resulting in atelectasis and pneumonia. Prolonged immobilization also results in negative nitrogen balance, calcium loss, diminished muscle strength, and orthostatic intolerance [10]. The risk of oxygen desaturation is higher in the supine position [14]. These changes are particularly pronounced in the elderly [15]. The rationale for supine positioning of SAH is to avoid hypoperfusion of the brain, especially considering the risk of delayed cerebral ischemia after SAH. However, several studies have shown that the incidence of clinical vasospasm is lower in the elderly [16, 17]. Therefore, it is unclear whether the risks of bed rest outweigh its presumed benefit, particularly in the older SAH population.

Zhang and Rabinstein [18] investigated the effects of HOB positioning on mean flow velocity in SAH patients using TCD. Measurements were taken for two HOB positions: first at 30°–45° and then at 0°– 15°. The authors found that HOB position did not significantly affect mean flow velocity and concluded that HOB position does not need to be specifically considered when interpreting the results of TCD studies in SAH patients. Blissitt et al. [19] also used TCD to study the effect of HOB elevation (at 20 and 45 degrees) on cerebrovascular dynamics in patients with mild or moderate vasospasm and found no consistent pattern of CBF changes. The measurements in both studies, however, were restricted to only one cerebral artery territory (MCA), the measurements were done in only one time point, and other modalities for cerebral perfusion assessment were not employed. The results of our study are in line with those of previous studies.

4.1. Implications. The current preference of restricting patients with SAH to only flat bed rest should be reconsidered, and HOB should be liberated pending changes in clinical exam. Changes in clinical examination when HOB is elevated are possibly suggestive of loss of autoregulation in these patients and/or early signs of vasospasm although this remains speculative and no such changes were observed herein.

4.2. Limitations. This study is limited by the small number of patients enrolled and that none of the patients developed delayed cerebral ischemia. The thermal diffusion probe provided continuous and absolute bedside measurement of regional CBF. However, the probe only samples a very small area in the white matter. We, therefore, performed TCD studies in multiple vascular territories as well in order to cross-validate the findings from these two complimentary methods.

5. Conclusion

We used two complimentary methods of CBF measurement to study cerebral hemodynamic in association with postural changes in the SAH patients. Changing HOB did not significantly affect either cerebral blood flow velocity or regional cerebral blood flow. These data suggest that early mobilization is not harmful and should be considered given the detrimental effects of prolonged bed rest.

Conflict of Interests

The authors declare that there is no conflict of interests regarding the publication of this paper.

References

[1] A. W. Wojner-Alexandrov, Z. Garami, O. Y. Chernyshev, and A. V. Alexandrov, "Heads down: flat positioning improves blood flow velocity in acute ischemic stroke," *Neurology*, vol. 64, no. 8, pp. 1354–1357, 2005.

[2] T. Kulik, Y. Kusano, S. Aronhime, A. L. Sandler, and H. R. Winn, "Regulation of cerebral vasculature in normal and ischemic brain," *Neuropharmacology*, vol. 55, no. 3, pp. 281–288, 2008.

[3] K. March, P. Mitchell, S. Grady, and R. Winn, "Effect of backrest position on intracranial and cerebral perfusion pressures," *The Journal of Neuroscience Nursing*, vol. 22, no. 6, pp. 375–381, 1990.

[4] T. Lovell, A. C. Marshall, C. E. Elwell, M. Smith, and J. C. Goldstone, "Changes in cerebral blood volume with changes in position in awake and anesthetized subjects," *Anesthesia and Analgesia*, vol. 90, no. 2, pp. 372–376, 2000.

[5] G. Lefthériotis, M. P. Preckel, L. Fizanne, J. Victor, J. M. Dupuis, and J. L. Saumet, "Effect of head-upright tilt on the dynamic of cerebral autoregulation," *Clinical Physiology*, vol. 18, no. 1, pp. 41–47, 1998.

[6] R. A. Asher, "The dangers of going to bed," *The British Medical Journal*, vol. 2, no. 4536, p. 967, 1947.

[7] D. K. Dittmer and R. Teasell, "Complications of immobilization and bed rest—part 1: musculoskeletal and cardiovascular complications," *Canadian Family Physician*, vol. 39, pp. 1428–1432, 1435–1437, 1993.

[8] R. Teasell and D. K. Dittmer, "Complications of immobilization and bed rest—part 2: other complications," *Canadian Family Physician*, vol. 39, pp. 1440–1445, 1993.

[9] M. B. Drakulovic, A. Torres, T. T. Bauer, J. M. Nicolas, S. Nogué, and M. Ferrer, "Supine body position as a risk factor for nosocomial pneumonia in mechanically ventilated patients: a randomised trial," *The Lancet*, vol. 354, no. 9193, pp. 1851–1858, 1999.

[10] J. E. Deitrick, G. D. Whedon, and E. Shorr, "Effects of immobilization upon various metabolic and physiologic functions of normal men," *The American Journal of Medicine*, vol. 4, no. 1, pp. 3–36, 1948.

[11] J. A. Frontera, A. Fernandez, J. M. Schmidt et al., "Defining vasospasm after subarachnoid hemorrhage: what is the most clinically relevant definition?" *Stroke*, vol. 40, no. 6, pp. 1963–1968, 2009.

[12] R. W. Stremel, V. A. Convertino, E. M. Bernauer, and J. E. Greenleaf, "Cardiorespiratory deconditioning with static and dynamic leg exercise during bed rest," *Journal of Applied Physiology*, vol. 41, no. 6, pp. 905–909, 1976.

[13] L. Svanberg, "Influence of posture on the lung volumes, ventilation and circulation in normals, a spirometric-bronchospirometric investigation," *Scandinavian Journal of Clinical & Laboratory Investigation*, vol. 9, supplement 25, pp. 1–195, 1957.

[14] T. Elizabeth, J. Singarayar, J. Ellul, D. Barer, and M. Lye, "Arterial oxygen saturation and posture in acute stroke," *Age and Ageing*, vol. 22, no. 4, pp. 269–272, 1993.

[15] E. D. O'Connor and J. Walsham, "Should we mobilise critically ill patients? A review," *Critical Care and Resuscitation*, vol. 11, no. 4, pp. 290–300, 2009.

[16] M. T. Torbey, T.-K. Hauser, A. Bhardwaj et al., "Effect of age on cerebral blood flow velocity and incidence of vasospasm after aneurysmal subarachnoid hemorrhage," *Stroke*, vol. 32, no. 9, pp. 2005–2011, 2001.

[17] C. Charpentier, G. Audibert, F. Guillemin et al., "Multivariate analysis of predictors of cerebral vasospasm occurrence after aneurysmal subarachnoid hemorrhage," *Stroke*, vol. 30, no. 7, pp. 1402–1408, 1999.

[18] Y. Zhang and A. A. Rabinstein, "Lower head of the bed position does not change blood flow velocity in subarachnoid hemorrhage," *Neurocritical Care*, vol. 14, no. 1, pp. 73–76, 2011.

[19] P. A. Blissitt, P. H. Mitchell, D. W. Newell, S. L. Woods, and B. Belza, "Cerebrovascular dynamics with head-of-bed elevation in patients with mild or moderate vasospasm after aneurysmal subarachnoid hemorrhage," *American Journal of Critical Care*, vol. 15, no. 2, pp. 206–216, 2006.

Hindawi Publishing Corporation
BioMed Research International
Volume 2013, Article ID 304320, 10 pages
http://dx.doi.org/10.1155/2013/304320

Review Article

Role of Stenting for Intracranial Atherosclerosis in the Post-SAMMPRIS Era

Dale Ding,[1] Robert M. Starke,[1] R. Webster Crowley,[1] and Kenneth C. Liu[2]

[1] *Department of Neurosurgery, University of Virginia, Charlottesville, VA 22908, USA*
[2] *Neurological Surgery and Radiology, Division of Cerebrovascular and Skull Base Surgery, Department of Neurosurgery, University of Virginia Health System, P.O. Box 800212, Charlottesville, VA 22908, USA*

Correspondence should be addressed to Kenneth C. Liu; kenneth.c.liu@virginia.edu

Received 3 October 2013; Accepted 30 October 2013

Academic Editor: Steven J. Monteith

Introduction. The initial promise of endovascular stenting for the treatment of intracranial atherosclerotic disease (ICAD) has been tempered by the results of the SAMMPRIS trial which demonstrated better outcomes with medical management compared to stenting for symptomatic ICAD. We review post-SAMMPRIS ICAD stenting outcomes. *Methods*. A comprehensive literature search was performed using PubMed to identify all ICAD stenting series published after the SAMMPRIS in September 2011. The type and design of the stent, number of patients and lesions, inclusion criteria, and clinical and angiographic outcomes were noted. *Results*. From October 2011 to August 2013, 19 ICAD stenting series were identified describing the interventional outcomes for 2,196 patients with 2,314 lesions. Of the 38 different stents used, 87% were balloon-expandable stents (BESs) and 13% were self-expanding stents. The median minimum stenosis was 50%. The median rates of technical success rate, postprocedural ischemic events, and symptomatic in-stent restenosis (ISR) were 98% (range 87–100%), 9.4% (range 0–25%), and 2.7% (range 0–11.1%), respectively. The median follow-up durations were one to 67 months. *Conclusions*. The management of severe ICAD remains controversial. Future trials are needed to define the optimal patient, lesion, and stent characteristics which will portend the best outcomes with intervention.

1. Introduction

Intracranial atherosclerotic disease (ICAD) accounts for approximately 10% of ischemic stroke in Western society and approximately 33–50% of stroke in Asia [1, 2]. Black and Hispanic ethnicities, diabetes mellitus, and metabolic syndrome predispose patients to developing ICAD [3]. The natural history of ICAD is significantly different for asymptomatic compared to symptomatic patients. The Warfarin-Aspirin Symptomatic Intracranial Disease (WASID) trial was a prospective, randomized study which demonstrated aspirin to have equivalent efficacy but superior safety to warfarin for the treatment of symptomatic ICAD [4]. Despite treatment with aspirin, the rate of ischemic stroke was 15% and 20% at one- and two-year followup, respectively. Coexisting asymptomatic ICAD lesions of 50–99% stenosis were detected in 27% of WASID study patients on magnetic resonance angiography [5]. The rate of ischemic stroke in the territory of the stenotic artery for symptomatic compared to asymptomatic patients was 12% versus 3.5% at one year, respectively [4, 5].

In order to improve the poor outcomes associated with symptomatic ICAD, endovascular revascularization of affected intracranial arteries utilizing stents has become popularized over the past decade [6]. Initial results were promising with high rates of technical success, excellent angiographic outcomes, acceptable complication rates, and noted reductions in posttreatment ischemic events compared to the natural history [7–9]. In 2011, the Stenting versus Aggressive Medical Management for Preventing Recurrent Stroke in Intracranial Stenosis (SAMMPRIS) trial was published and demonstrated superiority of medical therapy to endovascular stent intervention [10]. As a result, the validity of stenting for ICAD has become a subject of significant debate [11, 12]. Previous reviews describing ICAD stenting outcomes have primarily described studies published

prior to SAMMPRIS [13–15]. It is unknown whether these interventional outcomes have changed following the publication of SAMMPRIS due to alterations in referral patterns from primary care physicians and neurologists, stricter patient selectivity from neurointerventionalists, and changes in stent preference including newer generation intracranial stents and bare metal and drug-eluting coronary stents. We review the stenting outcomes for ICAD in the post-SAMMPRIS era.

2. Methods

Utilizing PubMed, we performed a comprehensive literature search for all endovascular stenting series for the treatment of ICAD following the publication of SAMMPRIS in September 2011 [10]. The terms "intracranial atherosclerosis," "stent," "stroke" and "endovascular procedures" were used to search for relevant publications. Single case reports and small case series comprising less than 10 patients were excluded. Case series including patients who received angioplasty alone without stent placement were also excluded [16]. The stent name, stent design, stent type, number of patients, number of ICAD lesions, minimum degree of arterial stenosis to be considered for stenting, technical success rate, duration of clinical followup, rate of postprocedural stroke (including TIAs) in the ipsilateral vascular territory and in all territories, and the rate of symptomatic in-stent restenosis (ISR) were noted when available. The stent design was classified as balloon-expandable stent (BES) or self-expanding stent (SES), and the stent type was classified as coronary, intracranial, or biliary.

3. Results

3.1. Stenting Outcomes for Intracranial Atherosclerosis in the Post-SAMMPRIS Era. From October 2011 to August 2013, we identified 19 single-center and multicenter case series. Table 1 summarizes the ICAD stenting series published after SAMMPRIS [17–34]. The median number of patients per series was 60.5 (range 11–637), and the median number of treated lesions was 62 (range 11–670). A total of 2,196 patients with 2,314 ICAD lesions were treated with endovascular stenting. The average number of lesions treated per patient was 1.05. The vast majority of patients were treated for symptomatic ICAD although some studies also treated a small minority of patients with asymptomatic ICAD. The minimum stenosis of the diseased artery which warranted intervention was 50% in 11 series, 70% in six series, and not reported in one series (median 50%).

Technical success, typically defined as greater than 50% revascularization of the diseased artery, was very high in most series, with a median rate of 98% (range 87–100%). Over a median or mean follow-up period which ranged from one to 67 months, the median rate of ipsilateral ischemic events, including all TIAs and strokes, was 5.4% (range 0–13.7%), and the median rate of ischemia in any territory was 9.4% (range 0–25%). In-stent restenosis (ISR), typically defined as at least 50% recurrent stenosis of the stented arterial segment at follow-up angiographic evaluation, was classified as asymptomatic or symptomatic. Symptomatic ISR occurred at a median rate of 2.7% (range 0–11.1%). Of the 19 series, 11 utilized a single stent (57.9%) and eight utilized multiple stents (42.1%). Table 2 lists the stents and their manufacturers. A total of 38 different stents produced by 14 manufacturers were used in the reviewed series. The stent designs included 33 BESs (86.8%) and five SESs (13.2%). The stent types were coronary in 27 (71.1%), intracranial in nine (23.7%), and biliary in two (5.3%). All coronary stents were BESs and six of the coronary BESs were drug-eluting (paclitaxel $N = 3$ and sirolimus, zotarolimus, and dexamethasone each $N = 1$).

3.2. Self-Expanding Intracranial Stents. The Wingspan stent (Boston Scientific, Natick, MA, USA) is a self-expanding nitinol stent which was approved by the Food and Drug Administration (FDA) in 2005 under a humanitarian device exemption (HDE) for patients with symptomatic, severe ICAD of at least 50% who have failed medical management with antiplatelet therapy [7]. The Wingspan stent system is used in conjunction with the Gateway percutaneous transluminal angioplasty (PTA) balloon (Boston Scientific) which is used to dilate the diseased segment of the artery prior to stent deployment. The Gateway PTA balloon and Wingspan stent system were used exclusively in the SAMMPRIS trial, and it was this specific SES which failed to demonstrate superiority over medical management [10]. Nonetheless, 12 of the 19 ICAD stenting studies we reviewed used the Wingspan. Seven studies used the Wingspan stent exclusively comprising 377 patients with 402 lesions [17, 19, 20, 25, 27, 30, 32]. The median minimum stenosis was 70% (range 50–70%) which was the same cutoff used in SAMMPRIS. The median technical success rate was 98% (range 93–100%). The median or mean follow-up periods were 3–13 months, and the median rate of symptomatic ISR was 3.3% (range 0–5.3%). The median rates of ipsilateral and all territory TIA or ischemic stroke were 6.2% (range 3.1–13.3%) and 9.5% (4.8–16.7%), respectively.

One of the potential mechanisms of ISR is stimulation of intimal hyperplasia by the radial force of the stent. The Wingspan stent is an open-cell stent with a high radial opening force. In contrast, the Enterprise stent (Cordis Corporation, Miami Lakes, FL, USA) is a closed-cell, intracranial SES with reduced radial force compared to the Wingspan stent. The Enterprise stent has been used under the hypothesis that a stent with lower radial force will be less likely to result in ISR than one with high radial force. Vajda et al. reported a large series of 189 ICAD patients with 209 lesions treated with the Enterprise stent [29]. The majority of the lesions (57%) were located in the posterior circulation, the minimum degree of arterial stenosis was 50%, and 84% of patients were symptomatic. The technical success rate was 100%, and the combined rate of neurological morbidity and death was 7.7% at 30 days and 0.9% after 30 days. Major periprocedural complications were more common in the treatment of symptomatic (8.5%) compared to asymptomatic (3.1%) lesions. The rate of ISR in this study (24.7%) was not significantly different than the rate of ISR reported in the NIH Wingspan registry (25%) which comprised of data from 16 United States centers [9]. However, the proportion

Table 1: Summary of endovascular stenting series for the treatment of intracranial atherosclerosis published after SAMMPRIS.

Series	Year	Type of stent	Number of patients (lesions)	Minimum arterial stenosis	Technical success rate	Mean/median clinical follow-up duration (months)	Rate of postprocedural ischemia (ipsilateral)	Rate of postprocedural ischemia (all)	Rate of symptomatic in-stent restenosis
Gandini et al. [20]	2013	Wingspan	21 (42)	70%	100%	20	4.8%	4.8%	0
Jin et al. [33]	2013	Multiple[1]	226 (233)	NR	NR	39	11.6%	11.6%	5.2%
Park et al. [18]	2013	Cypher	11 (11)	50%	100%	67	0	0	0
Rohde et al. [21]	2013	Multiple[2]	100 (100)	50%	94.0%	1	NR	25%	NR
Yu et al. [17]	2013	Wingspan	95 (95)	70%	93.7%	41	3.1% in 30 days, 0% from 30 days to 1 year	9.5% in 1 year	NR
Zhang et al. [19]	2013	Wingspan	61 (61)	70%	98.4%	24	10.0%	11.7%	3.3%
Jiang et al. [28]	2012	Multiple[3]	637 (670)	50%	94.6%	NR	5.8% at 30 days, 13.7% overall	5.8% at 30 days, 13.7% overall	11.1%
Kim et al. [22]	2012	Multiple[4]	77 (85)	50%	87.1%	29	7.7%	9.2%	3.1%
Kurre et al. [31]	2012	Multiple[5]	397 (409)	50%	98.0%		NR	11.6%	NR
Li et al. [30]	2012	Wingspan	30 (31)	70%	100%	18	13.3%	16.7%	5.3%
Mohammadian et al. [24]	2012	Multiple[6]	34 (34)	70%	97.0%	15	2.9%	5.8%	0
Tarlov et al. [26]	2012	Multiple[7]	41 (41)	50%	100%	14	NR	20.0%	7.5%
Vajda et al. [29]	2012	Enterprise	189 (209)	50%	99.5%	7	2.3%	7.7%	2.3%
Vajda et al. [23]	2012	Coroflex Please	95 (106)	50%	93.4%	16	1.9%	3.8% in 30 days, 0.9% after 30 days	0
Yu et al. [27]	2012	Wingspan	57 (57)	50%	93.0%	NR	NR	8.8%	NR
Zhang et al. [25]	2012	Wingspan	53 (53)	50%	98.1%	18	6.0%	10.0%	4.0%
Costalat et al. [32]	2011	Wingspan	60 (63)	50%	95.2%	13	6.3%	6.3%	2.0%
Park et al. [34]	2011	FlexMaster	12 (14)	70%	100%	9	0	0	0

NR: not reported.

[1]Multiple stents were used in this study including Wingspan (Boston Scientific), Apollo (MicroPort Medical), and coronary balloon-expandable stents.

[2]Multiple stents were used in this study including AVE (Medtronic), Neurolink (Guidant), Neuroform (Boston Scientific), and Wingspan (Boston Scientific) stents.

[3]Multiple stents were used in this study including Vision (Abbott), Mini-Vision (Abbott), Penta (Abbott), Taxus Express (Boston Scientific), Cypher (Cordis Corp), S70 (Medtronic), Driver (Medtronic), Apollo (MicroPort Medical), BiodivYsio (Biocompatibles), and Wingpan (Boston Scientific) stents.

[4]Multiple stents were used in this study including Endeavor (Medtronic), Vision (Abbott), FlexMaster (Abbott), Arthos pico (AMG International), Neuroform (Boston Scientific), Tsunami (Terumo), and Driver (Medtronic) stents.

[5]Multiple stents were used including Wingspan (Boston Scientific), LEO (BALT Extrusion), Neuroform (Boston Scientific), Enterprise (Cordis Corp), Xpert (Abbott), Pharos (Micrus), BOA (BALT Extrusion), Apollo (MicroPort Medical), Arthos (AMG), AVE S660 and S670 (Medtronic) BX Sonic and Velocity (Cordis Corp), Cerebrence (Medtronic), Coroflex blue (Braun), Driver (Medtronic), Endeavour (Medtronic), FlexMaster (Abbott), INX (Medtronic), Lekton Motion (Biotronik), Multi-Link (Abbott), S7 (Medtronic), Taxus Express and Liberte (Boston Scientific), Tecnic carbostent (Sorin Biomedica), and Tsunami Gold (Terumo) stents.

[6]Multiple stents were used including balloon-mounted, coronary bare metal stent for internal carotid artery stenosis, and self-expanding stents for middle cerebral artery stenosis.

[7]Multiple stents were used including Wingspan (Boston Scientific), AVE (Medtronic), ACS, Voyager (Abbott), Vision (Abbott), Palmaz-Schatz (Cordis Corp), Multilink (Abbott), and other Guidant and Medtronic stents.

Table 2: Stent types and manufacturers used in endovascular stenting series published after SAMMPRIS.

Manufacturer	Location	Stent name	Stent design*	Stent type	Eluting drug
Abbott Vascular	Abbott Park, IL, USA	FlexMaster	BES	Coronary	None
		Mini Vision	BES	Coronary	None
		Multi-Link	BES	Coronary	None
		Penta	BES	Coronary	None
		Vision	BES	Coronary	None
		Voyager	BES	Coronary	None
		Xpert	SES	Biliary	None
AMG International GmbH	Raesfeld-Erle, Germany	Arthos Pico	BES	Coronary	None
BALT Extrusion	Montmorency, France	Boa	BES	Intracranial	None
		LEO	SES	Intracranial	None
Biocompatibles	San Jose, CA, USA	BiodivYsio	BES	Coronary	Dexamethasone
Biotronik	Bulach, Switzerland	Lekton Motion	BES	Coronary	None
Boston Scientific	Natick, MA, USA	Neuroform	SES	Intracranial	None
		Taxus Express	BES	Coronary	Paclitaxel
		Taxus Liberte	BES	Coronary	Paclitaxel
		Wingspan	SES	Intracranial	None
B. Braun Medical	Melsungen, Germany	Coroflex Blue	BES	Coronary	None
		Coroflex Please	BES	Coronary	Paclitaxel
Cordis Corporation	Miami Lakes, FL, USA	BX Sonic	BES	Coronary	None
		BX Velocity	BES	Coronary	None
		Cypher	BES	Coronary	Sirolimus
		Enterprise	SES	Intracranial	None
Guidant Corporation	Indianapolis, IN, USA	Palmaz-Schatz	BES	Coronary	None
		Neurolink	BES	Intracranial	None
Medtronic	Minneapolis, MN, USA	AVE	BES	Biliary	None
		AVE S660	BES	Coronary	None
		AVE S670	BES	Coronary	None
		Cerebrence	BES	Coronary	None
		Driver	BES	Coronary	None
		Endeavor	BES	Coronary	Zotarolimus
		INX	BES	Intracranial	None
		S7	BES	Coronary	None
		S70	BES	Coronary	None
MicroPort Medical	Shanghai, China	Apollo	BES	Intraranial	None
Micrus Endovascular Corporation	Sunnyvale, CA, USA	Pharos	BES	Intracranial	None
Sorin Biomedica	Saluggia, Italy	Tecnic Carbostent	BES	Coronary	None
Terumo Corporation	Tokyo, Japan	Tsunami	BES	Coronary	None
		Tsunami Gold	BES	Coronary	None

*BES: balloon-expandable stent; SES: self-expanding stent.

of the ISR lesions which were symptomatic was lower in the Enterprise study (9.3%) compared to the Wingspan registry study (15.3%). The overall rate of symptomatic ISR associated with the Enterprise stent was 2.3%.

3.3. Balloon-Expandable and Drug-Eluting Stents. BESs were not utilized in the SAMMPRIS trial and have not been rigorously compared to medical management or SESs in a prospective manner. Intracranial BESs are derived from coronary BESs. The majority of BESs used to treat ICAD are, in fact, coronary stents. We only identified one series in which a single, non-drug-eluting BES was used [34]. The remaining reports of BES outcomes involved multiple stent designs and types. Due to lack of demarcation in reporting outcomes between BESs and SESs in many series, the safety and efficacy of BESs alone were not always evident. Rhode et al. treated 46 patients with BESs including 35 patients with the AVE stent (Medtronic, Minneapolis, MN, USA) and 11 patients with the Neurolink stent (Guidant Corporation, Indianapolis, IN, USA). The locations of the lesions were vertebral artery in 41.3%, basilar artery in 37.0%, internal carotid artery (ICA) in 21.7%, and none in the middle cerebral artery (MCA).

The minimum degree of stenosis was 50% with an average of 81%. The combined rate of stroke and death at 30 days was 23.9%, the majority of which was major stroke (13.0%).

Kurre et al. analyzed the stenting outcomes from the INTRASTENT registry which comprised of multicenter data from 18 institutions throughout Europe. BESs were used in 246 patients with 254 lesions. The locations of the lesions were ICA in 40.9%, vertebral artery in 26.4%, basilar artery in 18.1%, and MCA in 14.6%. The cumulative rate of stroke and mortality was 9.4% including nondisabling stroke (4.9%), defined as modified Rankin Scale (mRS) score less than 2, disabling stroke (3.7%), defined as mRS score at least 2, and death (0.8%). Jiang et al. treated 454 ICAD lesions located in the MCA (40.7%), basilar artery (24.7%), ICA (18.9%), and vertebral artery (15.6%) with BESs [28]. The rate of technical success was 92.9%, and the rate of periprocedural strokes was 6.0%. The mean pre- and posttreatment stenosis were 78% and 12%, respectively.

Drug-eluting stents (DES) were initially described in the cardiology literature and began to be deployed for ICAD lesions in the mid-2000s in an effort to chemically combat the high rates of ISR associated with bare metal stents [35–37]. Early studies were associated with high rates of technical failure and periprocedural complications due to the poor flexibility of the DESs in combination with the tortuous anatomy of the intracranial vasculature. However, given advances in stent design and delivery techniques since the advent of DESs for ICAD treatment, the enthusiasm for DESs appears to have returned. Currently, all DESs used for ICAD are balloon-mounted coronary stents. Vajda et al. used the Coroflex Please paclitaxel-eluting stent (B. Braun, Melsungen, Germany) to treat 95 patients with 106 ICAD lesions of at least 50% stenosis [23]. Of the treated lesions, 61% were symptomatic, 25% were associated with multiple vessel disease, and 13% were asymptomatic. All of the lesions were located proximal to the circle of Willis including in the petrous (42%), cavernous (41%), and paraclinoid (4%) ICA, basilar artery (4%), and intradural vertebral artery (10%). The technical success rate was 93.4%, and the combined rate of morbidity and mortality was 3.8% at 30 days and 0.9% beyond 30 days. The rate of ISR was an impressive 3.8%, and all cases of ISR were asymptomatic. In a smaller study of 11 patients treated with the Cypher paclitaxel-eluting stent (Cordis Corp, Johnson & Johnson, Warren, New Jersey, USA), Park et al. reported long-term outcomes over a mean follow-up period of 67 months [18]. The technical success rate was 100%, and there were no periprocedural complications, postprocedural strokes, or cases of ISR.

3.4. Technical Success Rates and Complications. While the rate of technical success was very high in most series, the rate of technical complications varied significantly. This is, in part, due to the variability in which events are classified as technical complications. For example, the development of intraprocedural stent thrombus which resolves with anticoagulant or antiplatelet infusion without postprocedural neurological deficit may not be reported as a complication. Another similar example is the development of intraprocedural vasospasm which resolves with calcium channel blockers without postprocedural symptoms. Tarlov et al. treated 41 patients with single ICAD lesions using either Wingspan stents or coronary BESs [26]. The rate of symptomatic groin hematoma treated with antibiotics or surgery was 14%, intraprocedural embolism requiring tissue plasminogen activator was 5%, and dissection was 23%. A study of 100 patients treated with both BESs and SESs reported 23% rate of technical complications including failure of stent placement (6%), dissection (5%), symptomatic vasospasm (5%), stent thrombosis (4%), and arterial perforation or rupture (4%) [21]. The major cause of periprocedural stroke or death (75%) in a study of 95 ICAD patients treated with the Wingspan stent was hemorrhage-related intraprocedural complications during guidewire manipulation or angioplasty [17].

3.5. Clinical Outcomes. While the angiographic goal of stenting is remodeling of diseased vasculature in order to revascularize inadequately perfused brain tissue, the true measure of its success is with the clinical outcome of the patient. The etiology of stroke following ICAD stenting is likely multifaceted in nature. In addition to procedural complications, poor outcomes following stenting for ICAD are largely attributable to ischemic stroke resulting in neurological morbidity and mortality. The causes of ischemic stroke include ISR, progression of ICAD in treated and untreated vessels, occlusion of perforator branches, and distal thromboembolism. Hemorrhagic strokes may occur, outside the setting of intraprocedural vessel perforation, secondary to reperfusion, hemorrhagic conversion of a prior ischemic stroke, or at distant sites without a clear etiology.

Detailed analysis of the European INTRASTENT registry demonstrated the cause of ischemic and hemorrhagic strokes resulting in clinical disability [31]. Stroke secondary to perforator branch occlusion occurred in 10 patients (2.5%) and was disabling in seven. Thromboembolic infarcts occurred in six patients (1.5%) and was disabling in three patients. Stent thrombosis occurred in four patients (1.0%) but was only disabling in one. Reperfusion hemorrhage occurred in four patients (1.0%) and resulted in disability in two patients and mortality in two patients. Hemorrhagic conversion of a prior ischemic stroke occurred in one patient (0.3%) and was disabling. Hemorrhage of unknown etiology occurred in three patients (0.8%) all of which resulted in mortality. Due to their relatively infrequent occurrences, determining predictors of these events is difficult and may never be achieved given the tenuous future of stenting for ICAD.

3.6. In-Stent Restenosis following Stenting for Intracranial Atherosclerosis. ISR occurs with significant frequency following stenting for ICAD [8]. However, most cases of ISR are asymptomatic. Symptomatic ISR may be managed conservatively with continued antiplatelet therapy and close angiographic surveillance, or it may be treated with further intervention, such as angioplasty or repeat stenting, in select cases of progressive neurological decline. Rigorous angiographic followup is necessary for the detection of ISR. It remains unknown whether technical attempts to reduce ISR

by utilizing SESs with lower radial force or DESs have resulted in significant decreases in its occurrence [18, 23, 29].

Jin et al. reviewed the follow-up angiography of 226 patients with 233 stented lesions and found a significantly higher rate of TIA or stroke in the cohort of patients with ISR compared to the cohort of patients without ISR (21.1% versus 8.5%, $P = 0.005$) [33]. Additionally the patients with ISR developed TIA or stroke significantly earlier than the patients without ISR (9.9 versus 26.6 months, $P = 0.01$). Multivariate analysis identified ISR to be an independent predictor of TIA or stroke following stenting for ICAD ($P = 0.017$). The rate of postprocedural ischemic events was not found to be significantly different between symptomatic and asymptomatic ISR patients ($P = 0.96$). Zhang et al. determined that a ratio of reference artery to stent diameter of less than 0.78 and length of vascular lesion less than 5.39 mm were significantly associated with increased incidence of ISR ($P = 0.013$ for both variables) [25]. Identifying methods to minimize the occurrence of ISR has the potential to substantially improve ICAD stenting outcomes.

4. Discussion

4.1. The SAMMRPIS Trial and Its Criticisms. SAMMPRIS was a multicenter, prospective, randomized clinical trial which enrolled patients with recent (i.e., within 30 days) transient ischemic attack (TIA) or nondisabling stroke which could be attributed to 70–99% stenosis of a major intracranial artery [10]. Patients were randomized to aggressive medical management with or without intervention. Both cohorts received medical therapy which consisted of dual antiplatelet therapy (i.e., aspirin 325 mg daily and clopidogrel 75 mg daily) and treatment of risk factors including hypertension (goal systolic blood pressure less than 140 mm Hg) and hypercholesterolemia (goal low-density lipoprotein cholesterol levels less than 70 mg/dL). Endovascular intervention consisted of initial angioplasty of the diseased arterial segment with the Gateway PTA balloon catheter followed by subsequent deployment of a Wingspan stent. The study's primary end point was stroke or death within 30 days of enrollment or intervention or ischemic stroke in the territory of the diseased artery between day 31 and the end of the follow-up duration.

A total of 451 patients were randomized to medical therapy only ($N = 227$) or intervention ($N = 224$). Of the patients randomized to intervention, 16 (7.1%) did not undergo stent placement, and of the patients randomized to medical therapy, nine (4.0%) underwent intervention for subsequent TIA. The primary end point was observed within 30 days in 33 patients in the intervention cohort (14.7%) compared to 13 patients in the medical cohort (5.7%), demonstrating a significantly better outcome in the medical cohort ($P = 0.002$). A higher proportion of 30-day strokes in the intervention cohort were intracerebral hemorrhages (30.3% versus 0%, $P = 0.04$). At one-year followup, the occurrence rate of the primary end point remained higher in the intervention cohort compared to the medical cohort (20.0% versus 12.2%, $P = 0.009$). In SAMMPRIS, the periprocedural stroke rate following angioplasty and stenting was higher than expected and the stroke rate from medical management was lower than expected.

There have been concerns raised regarding the operator experience of the SAMMPRIS neurointerventionalists [38]. Yu et al. noted a decrease in the rates of technical failure and intraprocedural complications during treatment of ICAD with the Wingspan stent, including guidewire- and angioplasty-related hemorrhages, as operator experience at their institution increased although the difference was not statistically significant [17]. Derdeyn et al. examined the effect of operator and site experience during the SAMMPRIS trial on stenting outcomes [39]. All interventions in the SAMMPRIS trial were performed by 63 neurointerventionalists at 48 sites, and the median number of Wingspan stent procedures submitted for credentialing by each neurointerventionalist was 10 (range 3–20). The median number of procedures performed by each neurointerventionalist was 3 (range 1–13). There were 34 periprocedural complications comprised of 19 ischemic strokes, 11 symptomatic hemorrhagic strokes, two ischemic events with temporary symptoms, and two asymptomatic hemorrhagic strokes. There was no significant association between periprocedural complications and neurointerventionalist or site features. In fact, the periprocedural complication rate for neurointerventionalists credentialed with less than 10 Wingspan procedures was 9.9% compared to 19.0% for those credentialed with at least 10 Wingspan procedures although this difference was not statistically significant ($P = 0.11$).

Another major criticism of SAMMPRIS has been the significant proportion of patients who had not failed medical therapy prior to endovascular intervention [10]. The Wingspan stent was approved by the FDA and generally intended for use in patients who had failed medical management [7, 8]. However, 35.3% of the stenting cohort in SAMMPRIS had not received antithrombotic therapy at the time of the qualifying clinical event. In current clinical practice, patients routinely receive at least one antiplatelet agent, most commonly aspirin 325 mg daily, for secondary stroke prevention following the occurrence of a TIA or ischemic stroke. Therefore, in a practical setting, it is unlikely that a patient who presents with symptomatic ICAD would proceed to endovascular treatment without an initial trial period of antithrombotic therapy [40].

Despite its criticism, the ramifications of SAMMPRIS on the current management of ICAD have been significant in the two years since its publications. Zaidat et al. conducted a poll of 217 attendees at the 2012 ICAD symposium during the 2012 International Stroke Conference to assess the effect of SAMMPRIS on clinical practice and perspectives regarding the management of ICAD [41]. Neurologists, neurointerventionalists, and neurosurgeons comprised 71% of the audience with a predominance of neurologists (57%). The average response rate for each question was 82%. Audience responses of note were as follows: 58% responded that SAMMPRIS had diminished their enthusiasm for stenting of ICAD, 84% agreed with the medical management undertaken in SAMMPRIS, only 28% still recommended treatment of an ICAD patient who failed aggressive medical therapy

with angioplasty and stenting, and 86% believed further clinical trials were needed for ICAD management.

4.2. Effect of Stent Type on ICAD Treatment Outcomes. BESs are typically less malleable than SESs and therefore can be more difficult to navigate through tortuous vascular anatomy. The deployment of an SES is preempted by submaximal dilatation with balloon angioplasty. The target lesion must be traversed twice by a microcatheter for an SES: the first time for balloon predilatation and the second time for stent deployment. In contrast, both of these steps are achieved simultaneously for a BES which only requires traversing the lesion with a microcatheter once. While this difference in stent deployment technique theoretically favors BESs over SESs in regard to periprocedural safety, a significant discrepancy in intraprocedural or periprocedural complications has not been noted between the two stent designs. In a study of 41 patients, Tarlov et al. did not find a difference in postprocedural stroke rate between patients treated with the Wingspan stent ($N = 19$) and those treated with various balloon-mounted coronary stents ($N = 22$, $P = 0.819$) [26].

In a large multicenter, retrospective analysis comprised of 637 patients with 670 ICAD lesions treated with multiple BES compared to the self-expanding Wingspan stent, Jiang et al. found that patients treated with BES had significantly lower degrees of posttreatment stenosis ($P = 0.001$) and were less likely to develop ISR ($P = 0.02$) at three- and six-month followup [28]. On the contrary, BES had a higher rate of technical failure than Wingspan stents (7.1% versus 1.4%, $P < 0.001$). The same study identified Mori type A lesion and presence of higher degrees of postprocedural stenosis to be predictors of ISR development at followup ($P < 0.001$ and $P = 0.006$, resp.). There was no difference between BES and Wingspan stent with regard to the rate of periprocedural stroke ($P = 0.46$). In 100 consecutive patients treated with BES ($N = 46$) or SES ($N = 54$), Rohde et al. found a lower rate of vascular complications with SES compared to BES (11.1% versus 36.9%, $P = 0.002$) but no statistically significant difference in rates of technical success (96.3% for SES versus 89.1% for BES, $P = 0.31$) or combined stroke and mortality rate at 30 days (25.9% for SES versus 23.9% for BES) [21]. Kurre et al. also did not find a difference in postprocedural adverse events, including stroke and death, when comparing BES to SES in 397 patients with 409 lesions retrospectively collected from a multicenter registry [31].

4.3. Defining the Current and Future Roles of Stenting for the Treatment of Intracranial Atherosclerosis. Despite the waning enthusiasm for the treatment of ICAD with stents, a role for stenting ICAD lesions remains. However, the burden lies with the neurointerventional and cerebrovascular communities to define the proper patient population for current interventional therapies and, more importantly, to prove in well-designed, prospective, randomized trials, such as SAMMPRIS, that the safety and efficacy of stenting has not been underestimated. Several factors should also be taken into consideration when planning future studies, including the role of angioplasty without stenting, the outcomes of SESs versus BESs, the role of DESs, and the focused analysis of subgroups based on the location and morphology of the ICAD lesion.

While BESs are generally associated with angiographically superior and more durable results than SESs, including lower rates of ISR, they remain less versatile due to their stiffer nature. Furthermore, current data comparing BESs to SESs is limited by its retrospective nature. Despite both theoretical and reported advantages and disadvantages between BESs and SESs, there has yet to be a well-designed trial which compares one stent design to the other. As advances in endovascular technology continue to be made at a rapid pace, angioplasty without stenting, which was largely abandoned after popularization of the Wingspan stent in the late 2000s, may prove to be a safer alternative to stenting while providing equivalent efficacy [42, 43]. However, this has yet to be proven in a rigorous fashion, and this treatment option should be considered when designing future ICAD trials.

It is understandably difficult to organize large scale prospective studies. In order to maximize the utility of retrospective studies, it is important that the reporting guidelines for all ICAD stenting studies become standardized. The most widely used angiographic classification of ICAD lesions was described by Mori et al. which divided them into three types [44, 45]. Mori type A lesions are short (5 mm or less in length), concentric or moderately eccentric, and nonocclusive; type B lesions are tubular (5–10 mm in length), extremely eccentric or occlusive, and less than three months old; type C lesions are diffuse (greater than 10 mm in length), angulated greater than 90 degrees, extremely tortuous in their proximal segments or completely occluded, and at least three months old. The risk of ipsilateral ischemic stroke was 8%, 12%, and 56% in patients with Mori types A, B, and C lesions, respectively [44]. The MCA is the most commonly affected location for ICAD, accounting for 32.4% of patients in the WASID study and 43.7% of patients in the SAMMRPIS study including 41.1% of patients in the stenting cohort [4, 10]. Due to its distal location relative to the ICA and vertebrobasilar system, stenting an MCA lesion is also relatively more difficult and prone to intraprocedural complication. Arteries with relatively dense and critical perforator branch arteries, such as the lenticulostriate branches of the proximal MCA M1 segment and the pontine perforators of the midbasilar artery are prone to thrombotic occlusion after stenting. Future studies have the potential to identify specific therapies which may be associated with more favorable outcomes for lesions of a specific artery or Mori classification.

Ultimately, further basic and translational science efforts are necessary to better bridge fundamental knowledge gaps in the pathogenesis and progression of ICAD lesion as well as their rupture which leads to end-stage events such as thromboembolism and stroke. Identification of unstable atherosclerotic plaques through novel neuroimaging techniques, such as intravascular ultrasound, is a potentially powerful diagnostic tool which has yet to be clinically validated [46, 47]. Animal models of unstable atherosclerotic plaques may provide insight into the molecular underpinnings of atherosclerosis and mechanisms by which its progression may be halted or even reversed [48].

4.4. Study Limitations. This review is limited by the retrospective nature of the ICAD stenting series it encompasses. The variability in the outcomes and followup reported in each of the series makes comparisons across different patient, lesion, and stent characteristics difficult and unreliable. This study's major limitation is the timing of many of the series. Despite our intention to report ICAD stenting outcomes after the SAMMPRIS trial by including only those studies published after SAMMPRIS, there was likely a six- to 12-month period of publication overlap following SAMMPRIS in which new studies describing ICAD stenting outcomes did not account for the results from SAMMPRIS. This is due to the time difference in various journals' manuscript review and production periods and in authors' time to manuscript revision following review. Additionally, many of the stenting studies published after SAMMPRIS included patients treated prior to 2011 and therefore are not representative of the treatment biases which arose following the dissemination of the SAMMPRIS trial results. Presently, more time is necessary for the effect of SAMMPRIS on ICAD management strategies to be fully recognized and accounted for in the literature.

5. Conclusions

Patients with symptomatic, severe ICAD represent a very high-risk cohort who harbor relatively high prospective risks of recurrent ischemic events. Stenting of ICAD lesions was initially postulated to positively impact the natural history of ICAD by reducing the risk of neurological morbidity secondary to stroke. Surprisingly, the SAMMPRIS trial demonstrated an overestimation of the benefits of angioplasty and stenting with the Wingspan stent system and an underestimation of the efficacy of aggressive medical management. However, stenting for ICAD continues to be performed albeit with significantly more reserve since the release of SAMMPRIS. While results with newer SES systems, BESs, and DESs are promising with regard to relatively low rates of ischemic events and symptomatic ISR, future ICAD trials are needed to rigorously compare across various stent designs and to compare current stenting practices to angioplasty alone and to medical management. Despite maximal medical therapy, patients with significant ICAD may continue to experience TIAs and strokes associated with disease progression. Until novel medical therapies are shown to improve the poor outcomes associated with symptomatic ICAD, endovascular stenting will continue to play a role in the treatment of a carefully selected subset of ICAD patients.

Conflict of Interests

The authors declare that there is no conflict of interests regarding the publication of this paper.

References

[1] L. K. S. Wong, "Global burden of intracranial atherosclerosis," *International Journal of Stroke*, vol. 1, no. 3, pp. 158–159, 2006.

[2] R. L. Sacco, D. E. Kargman, Q. Gu, and M. C. Zamanillo, "Race-ethnicity and determinants of intracranial atherosclerotic cerebral infarction: the Northern Manhattan stroke study," *Stroke*, vol. 26, no. 1, pp. 14–20, 1995.

[3] F. Rincon, R. L. Sacco, G. Kranwinkel et al., "Incidence and risk factors of intracranial atherosclerotic stroke: the northern manhattan stroke study," *Cerebrovascular Diseases*, vol. 28, no. 1, pp. 65–71, 2009.

[4] M. I. Chimowitz, M. J. Lynn, H. Howlett-Smith et al., "Comparison of warfarin and aspirin for symptomatic intracranial arterial stenosis," *The New England Journal of Medicine*, vol. 352, no. 13, pp. 1305–1316, 2005.

[5] F. Nahab, G. Cotsonis, M. Lynn et al., "Prevalence and prognosis of coexistent asymptomatic intracranial stenosis," *Stroke*, vol. 39, no. 3, pp. 1039–1041, 2008.

[6] T. Mori, K. Kazita, K. Chokyu, T. Mima, and K. Mori, "Short-term arteriographic and clinical outcome after cerebral angioplasty and stenting for intracranial vertebrobasilar and carotid atherosclerotic occlusive disease," *American Journal of Neuroradiology*, vol. 21, no. 2, pp. 249–254, 2000.

[7] A. Bose, M. Hartmann, H. Henkes et al., "A novel, self-expanding, nitinol stent in medically refractory intracranial atherosclerotic stenoses: the Wingspan study," *Stroke*, vol. 38, no. 5, pp. 1531–1537, 2007.

[8] D. Fiorella, E. I. Levy, A. S. Turk et al., "US multicenter experience with the Wingspan stent system for the treatment of intracranial atheromatous disease: periprocedural results," *Stroke*, vol. 38, no. 3, pp. 881–887, 2007.

[9] O. O. Zaidat, R. Klucznik, M. J. Alexander et al., "The NIH registry on use of the Wingspan stent for symptomatic 70–99% intracranial arterial stenosis," *Neurology*, vol. 70, no. 17, pp. 1518–1524, 2008.

[10] M. I. Chimowitz, M. J. Lynn, C. P. Derdeyn et al., "Stenting versus aggressive medical therapy for intracranial arterial stenosis," *The New England Journal of Medicine*, vol. 365, no. 11, pp. 993–1003, 2011.

[11] A. I. Qureshi, F. M. Al-Senani, S. Husain et al., "Intracranial angioplasty and stent placement after stenting and aggressive medical management for preventing recurrent stroke in intracranial stenosis (SAMMPRIS) trial: present state and future considerations," *Journal of Neuroimaging*, vol. 22, no. 1, pp. 1–13, 2012.

[12] M. P. Marks, "Is there a future for endovascular treatment of intracranial atherosclerotic disease after Stenting and Aggressive Medical Management for Preventing Recurrent Stroke and Intracranial Stenosis (SAMMPRIS)?" *Stroke*, vol. 43, no. 2, pp. 580–584, 2012.

[13] D. Ding and K. C. Liu, "Applications of stenting for intracranial atherosclerosis," *Neurosurgical focus*, vol. 30, no. 6, 15 pages, 2011.

[14] K. A. Blackham, P. M. Meyers, T. A. Abruzzo et al., "Standard of practice: endovascular treatment of intracranial atherosclerosis," *Journal of NeuroInterventional Surgery*, vol. 4, no. 6, pp. 397–406, 2012.

[15] K. Gröschel, S. Schnaudigel, S. M. Pilgram, K. Wasser, and A. Kastrup, "A systematic review on outcome after stenting for intracranial atherosclerosis," *Stroke*, vol. 40, no. 5, pp. e340–e347, 2009.

[16] P.-H. Lü, J. W. Park, S. Park et al., "Intracranial stenting of subacute symptomatic atherosclerotic occlusion versus stenosis," *Stroke*, vol. 42, no. 12, pp. 3470–3476, 2011.

[17] S. C. Yu, T. W. Leung, K. T. Lee, and L. K. Wong, "Learning curve of Wingspan stenting for intracranial atherosclerosis: single-center experience of 95 consecutive patients," *The Journal of the NeuroInterventional Surgery*, 2013.

[18] S. Park, D. G. Lee, W. J. Chung, D. H. Lee, and D. C. Suh, "Long-term outcomes of drug-eluting stents in symptomatic intracranial stenosis," *Neurointervention*, vol. 8, no. 1, pp. 9–14, 2013.

[19] L. Zhang, Q. Huang, Y. Zhang et al., "A single-center study of Wingspan stents for symptomatic atherosclerotic stenosis of the middle cerebral artery," *Journal of Clinical Neuroscience*, vol. 20, no. 3, pp. 362–366, 2013.

[20] R. Gandini, A. Chiaravalloti, E. Pampana et al., "Intracranial atheromatous disease treatment with the Wingspan stent system: evaluation of clinical, procedural outcome and restenosis rate in a single-center series of 21 consecutive patients with acute and mid-term results," *Clinical Neurology and Neurosurgery*, vol. 115, no. 6, pp. 741–747, 2013.

[21] S. Rohde, J. Seckinger, S. Hahnel, P. A. Ringleb, M. Bendszus, and M. Hartmann, "Stent design lowers angiographic but not clinical adverse events in stenting of symptomatic intracranial stenosis—results of a single center study with 100 consecutive patients," *International Journal of Stroke*, vol. 8, no. 2, pp. 87–94, 2013.

[22] K. S. Kim, D. H. Hwang, Y. H. Ko et al., "Usefulness of stent implantation for treatment of intracranial atherosclerotic stenoses," *Neurointervention*, vol. 7, no. 1, pp. 27–33, 2012.

[23] Z. Vajda, M. Aguilar, T. Göhringer, D. Horváth-Rizea, H. Bäzner, and H. Henkes, "Treatment of intracranial atherosclerotic disease with a balloon-expandable paclitaxel eluting stent : procedural safety, efficacy and mid-term patency," *Clinical Neuroradiology*, vol. 22, no. 3, pp. 227–233, 2011.

[24] R. Mohammadian, A. Pashapour, E. Sharifipour et al., "A comparison of stent implant versus medical treatment for severe symptomatic intracranial stenosis: a controlled clinical trial," *Cerebrovascular Diseases Extra*, vol. 2, no. 1, pp. 108–120, 2012.

[25] L. Zhang, Q. Huang, Y. Zhang et al., "Wingspan stents for the treatment of symptomatic atherosclerotic stenosis in small intracranial vessels: safety and efficacy evaluation," *American Journal of Neuroradiology*, vol. 33, no. 2, pp. 343–347, 2012.

[26] N. Tarlov, R. Jahan, J. L. Saver et al., "Treatment of high risk symptomatic intracranial atherosclerosis with balloon mounted coronary stents and Wingspan stents: single center experience over a 10 year period," *Journal of NeuroInterventional Surgery*, vol. 4, no. 1, pp. 34–39, 2012.

[27] S. C. Yu, T. Leung, E. Hung, K. T. Lee, and L. K. S. Wong, "Angioplasty and stenting for intracranial atherosclerotic stenosis with nitinol stent: factors affecting technical success and patient safety," *Neurosurgery*, vol. 70, no. 1, supplement, pp. 104–113, 2012.

[28] W.-J. Jiang, E. Cheng-Ching, A. Abou-Chebl et al., "Multicenter analysis of stenting in symptomatic intracranial atherosclerosis," *Neurosurgery*, vol. 70, no. 1, pp. 25–30, 2012.

[29] Z. Vajda, E. Schmid, T. Güthe et al., "The modified bose method for the endovascular treatment of intracranial atherosclerotic arterial stenoses using the enterprise stent," *Neurosurgery*, vol. 70, no. 1, pp. 91–101, 2012.

[30] J. Li, Z. W. Zhao, G. D. Gao et al., "Wingspan stent for high-grade symptomatic vertebrobasilar artery atherosclerotic stenosis," *CardioVascular and Interventional Radiology*, vol. 35, no. 2, pp. 268–278, 2012.

[31] W. Kurre, F. Brassel, R. Brüning et al., "Complication rates using balloon-expandable and self-expanding stents for the treatment of intracranial atherosclerotic stenoses : analysis of the INTRASTENT multicentric registry," *Neuroradiology*, vol. 54, no. 1, pp. 43–50, 2012.

[32] V. Costalat, I. L. Maldonado, J.-F. Vendrell et al., "Endovascular treatment of symptomatic intracranial stenosis with the Wingspan stent system and Gateway PTA balloon: a multicenter series of 60 patients with acute and midterm results. Clinical article," *Journal of Neurosurgery*, vol. 115, no. 4, pp. 686–693, 2011.

[33] M. Jin, X. Fu, Y. Wei, B. Du, X. T. Xu, and W. J. Jiang, "Higher risk of recurrent ischemic events in patients with intracranial in-stent restenosis," *Stroke*, vol. 44, pp. 2990–2994, 2013.

[34] T. S. Park, B. J. Choi, T. H. Lee, J. S. Song, D. Y. Lee, and S. M. Sung, "Urgent recanalization with stenting for severe intracranial atherosclerosis after transient ischemic attack or minor stroke," *Journal of Korean Neurosurgical Society*, vol. 50, no. 4, pp. 322–326, 2011.

[35] A. Abou-Chebl, Q. Bashir, and J. S. Yadav, "Drug-eluting stents for the treatment of intracranial atherosclerosis: initial experience and midterm angiographic follow-up," *Stroke*, vol. 36, no. 12, pp. e165–e168, 2005.

[36] R. Gupta, F. Al-Ali, A. J. Thomas et al., "Safety, feasibility, and short-term follow-up of drug-eluting stent placement in the intracranial and extracranial circulation," *Stroke*, vol. 37, no. 10, pp. 2562–2566, 2006.

[37] A. I. Qureshi, J. F. Kirmani, H. M. Hussein et al., "Early and intermediate-term outcomes with drug-eluting stents in high-risk patientswith symptomatic intracranial stenosis," *Neurosurgery*, vol. 59, no. 5, pp. 1044–1051, 2006.

[38] M. J. Alexander, "Intracranial stenting for intracranial atherosclerotic disease: still much to learn," *The Journal of the Society of NeuroInterventional Surgery*, vol. 4, no. 2, pp. 85–86, 2012.

[39] C. P. Derdeyn, D. Fiorella, M. J. Lynn et al., "Impact of operator and site experience on outcomes after angioplasty and stenting in the SAMMPRIS trial," *The Journal of the Society of NeuroInterventional Surgery*, vol. 5, no. 6, pp. 528–533, 2012.

[40] Y. Wang, X. Zhao, L. Liu et al., "Clopidogrel with aspirin in acute minor stroke or transient ischemic attack," *The New England Journal of Medicine*, vol. 369, no. 1, pp. 11–19, 2013.

[41] O. O. Zaidat, A. C. Castonguay, T. N. Nguyen et al., "Impact of SAMMPRIS on the future of intracranial atherosclerotic disease management: polling results from the ICAD symposium at the International Stroke Conference," *The Journal of the Society of NeuroInterventional Surgery*, 2013.

[42] M. P. Marks, J. C. Wojak, F. Al-Ali et al., "Angioplasty for symptomatic intracranial stenosis: Clinical outcome," *Stroke*, vol. 37, no. 4, pp. 1016–1020, 2006.

[43] T. M. Dumont, P. Kan, K. V. Snyder, L. N. Hopkins, A. H. Siddiqui, and E. I. Levy, "Revisiting angioplasty without stenting for symptomatic intracranial atherosclerotic stenosis after the stenting and aggressive medical management for preventing recurrent stroke in intracranial stenosis (SAMMPRIS) study," *Neurosurgery*, vol. 71, no. 6, pp. 1103–1110, 2012.

[44] T. Mori, M. Fukuoka, K. Kazita, and K. Mori, "Follow-up study after intracranial percutaneous transluminal cerebral balloon angioplasty," *American Journal of Neuroradiology*, vol. 19, no. 8, pp. 1525–1533, 1998.

[45] T. Mori, K. Mori, M. Fukuoka, M. Arisawa, and S. Honda, "Percutaneous transluminal cerebral angioplasty: serial angiographic follow-up after successful dilatation," *Neuroradiology*, vol. 39, no. 2, pp. 111–116, 1997.

[46] P. Kan, M. Mokin, A. A. Abla et al., "Utility of intravascular ultrasound in intracranial and extracranial neurointerventions: experience at University at Buffalo Neurosurgery-Millard Fillmore Gates Circle Hospital," *Neurosurgical Focus*, vol. 32, no. 1, p. E6, 2012.

[47] H. Zacharatos, A. E. Hassan, and A. I. Qureshi, "Intravascular ultrasound: principles and cerebrovascular applications," *American Journal of Neuroradiology*, vol. 31, no. 4, pp. 586–597, 2010.

[48] M. R. Alexander, M. Murgai, C. W. Moehle, and G. K. Owens, "Interleukin-1β modulates smooth muscle cell phenotype to a distinct inflammatory state relative to PDGF-DD via NF-κB-dependent mechanisms," *Physiological Genomics*, vol. 44, no. 7, pp. 417–429, 2012.

Hindawi Publishing Corporation
BioMed Research International
Volume 2013, Article ID 524324, 9 pages
http://dx.doi.org/10.1155/2013/524324

Research Article

Estrogen Signaling through Estrogen Receptor Beta and G-Protein-Coupled Estrogen Receptor 1 in Human Cerebral Vascular Endothelial Cells: Implications for Cerebral Aneurysms

Jian Tu and Nurul F. Jufri

Australian School of Advanced Medicine, Macquarie University, 2 Technology Place, North Ryde, Sydney, NSW 2109, Australia

Correspondence should be addressed to Jian Tu; james.tu@mq.edu.au

Received 27 August 2013; Accepted 28 September 2013

Academic Editor: Robert M. Starke

Little is known about estrogen receptors and their signaling mechanisms in human cerebral vascular endothelial cells, which is important for understanding cerebral aneurysm pathogenesis in menopausal and postmenopausal women. Estrogen receptor beta (ERβ) and G-protein-coupled receptor 1 (GPER1) were immunocytochemically identified in human cerebral vascular endothelial cells (HCVECs). ERβ was mainly located at the nuclei of the cells while GPER1 was located at the plasma membrane. Interaction events between 17β-estradiol and ERβ or GPER1 in HCVECs were evaluated by *in situ* proximity ligation assay. The number of interaction events between 17β-estradiol and ERβ was positively correlated with 17β-estradiol concentrations ($r = 0.9614$, $P < 0.01$). The interaction events between 17β-estradiol and GPER1 were dose responsive. Our data support HCVECs to serve as a suitable cellular model for studying cerebral aneurysm pathogenesis in menopausal and postmenopausal women. Subtypes of estrogen receptors and their signaling mechanisms identified in HCVECs could be applicable for developing estrogen-like compounds to specifically bind to a subtype of estrogen receptors with greater specific action on the cerebral arteries, without the estrogen-dependent side effects on the reproductive organs, to prevent cerebral aneurysm formation in menopausal and postmenopausal woman.

1. Introduction

The incidence of cerebral aneurysms is doubled in menopausal and postmenopausal women compared with premenopausal women at the same age [1]. There have been several important studies showing that inflammation underlies cerebral aneurysm formation and rupture [2–4]. A failure of endothelial cells in the cerebral arterial wall to adequately express estrogen receptors abrogates the possibility of direct interaction between estrogen receptors and circulating estrogen, which can trigger inflammation, upregulation of proteolytic pathways, loss of the arterial wall matrix, and degradation of the arterial wall [5, 6]. As no biopsy specimens are possibly obtained during surgery because of high risk of bleeding, there is an increasing interest to develop a cellular model to directly investigate the effect of estrogen deficiency and whether it causes a decline in the function and/or number of estrogen receptors, which may promote inflammation and apoptosis in the endothelial cells of cerebral arterial walls. Since endothelial dysfunction is considered the first step in the pathogenesis of cerebral aneurysms, a human cerebral vascular endothelial cell model was applied in the study.

The arterial protective effects of estrogen act through increased artery compliance, defined as the change in volume for a given change in pressure [7]. Arteries with low compliance less effectively dampen the pulsatile flow of blood by stretching and contracting in response to the systolic and diastolic cardiac phases, respectively. There are three major forms of estrogen, estradiol, estrone, and estriol, in which 17β-estradiol has the highest affinity to estrogen receptors. Physiological plasma levels of 17β-estradiol range from 118 to 914 pmol/L in premenopausal women and fluctuate in healthy women during the menstrual cycle [8]. The level increases during the follicular phase and gradually declines during the luteal phase of the reproductive cycle. In menopausal and postmenopausal women, estrogen level decreased to

less than 73 pmol/L due to reductions in its biosynthesis [9]. 17β-Estradiol binds to estrogen receptor alpha (ERα) and/or estrogen receptor beta (ERβ) in the cell's nucleus [10] and mediates long-term genomic effects (hours to days) in remodeling or lipid alteration. It also can bind to G-protein coupled estrogen receptor (GPER) [11] and mediates nongenomic action that is rapid in onset and short in duration such as changes in vasomotor tones through kinase activation and intracellular signaling pathway [12]. The interaction between estrogen and its receptors generates protective effects and maintains homeostasis of the vascular system. Because of alternative RNA splicing, some estrogen receptor isoforms are known to exist. However, exactly which types of estrogen receptors are expressed in human cerebral arterial endothelial cells, their subcellular location, binding characteristics, and functional selectivity remain unknown. The objectives of this study were to examine whether estrogen receptors would present in human cerebral vascular endothelial cells. If so, which types of receptors? How does estrogen interact with its receptors?

2. Materials and Methods

2.1. Chemicals, Antibodies, and Cell Culture. All chemicals, M199 media with or without phenol red, fetal bovine serum (FBS), penicillin-streptomycin, and 17β-estradiol were purchased from Sigma-Aldrich, Aldrich (St. Louis, MO, USA), unless otherwise specified. Charcoal stripped FBS was purchased from Invitrogen (Carlsbad, CA, USA). Rabbit anti-human monoclonal estrogen receptor beta (ERβ) antibody was purchased from Novus Biologicals (Littleton, CO, USA). Goat anti-human polyclonal 17β-estradiol antibody was purchased from Fitzgerald Industries International (Acton, MA, USA). Rabbit anti-human polyclonal G-protein-coupled estrogen receptor 1 was purchased from MBL International Corporation (Woburn, MA, USA). Alexa-594 conjugated secondary goat anti-rabbit and Alexa-594 conjugated secondary donkey anti-goat antibodies were purchased from Molecular Probe (Eugene, OR, USA). All reagents used for the *in situ* proximity ligation assay (PLA) were purchased from Olink Bioscience (Uppsala, Sweden). Simian virus 40 T antigen immortalized human cerebral vascular endothelial cells (HCVECs) were purchased from Applied Biological Materials (Richmond, BC, Canada) and maintained in M199 medium supplemented with endothelium growth factor, 10% FBS, and 1% penicillin-streptomycin in a humidified atmosphere of 37°C and 5% CO_2. The genotype and phenotype of HCVECs are stable within 150 passages. The cells used in this study were passages 6–12. Nunc Lab-Tek Chamber slides were purchased from ProSciTech (QLD, Australia).

2.2. Immunocytochemistry. Immunocytochemistry was performed as previously described [13]. Briefly, HCVECs were seeded and grown in chamber slides until 50% confluence in M199 phenol red free media supplemented with endothelium growth factor, 10% FBS, and 1% penicillin-streptomycin in a humidified atmosphere of 37°C and 5% CO_2. The cells were washed twice in PBS (pH 7.2) before being fixed using 4% paraformaldehyde for 15 minutes. The cells were rinsed with PBS and permeabilized in 0.1% Triton X-100 and 0.5% BSA in PBS at room temperature for 15 minutes. After washing with PBS, the cells were blocked in 5% BSA in PBS for 1 hour and incubated with anti-ERβ or anti-GPER1 antibody (1 : 250) in 5% BSA at room temperature for 2 hours. After washing with PBS-Tween (PBST), the cells were incubated with Alexa-594 conjugated secondary antibody (1 : 800) in 5% BSA at room temperature in the dark for 1 hour. The cells were washed with PBST before being cover-slipped and examined using a confocal microscope (Leica SP5, Germany), and imaging data were analyzed using Leica LAS AF software. Parallel negative controls were performed without primary or secondary antibody. Isotype controls were performed using rabbit IgG to test the specificity of primary antibodies. Each staining was triplicated and repeated 3 times.

2.3. Proximity Ligation Assay. Proximity ligation assay was applied to examine the interaction events between ERβ or GPER1 and 17β-estradiol. Two antibodies, one anti-ERβ or GPER1 and another anti-17β-estradiol, covalently linked to oligonucleotide mediate amplifiable DNA molecules. If the receptor and its ligand are in close proximity of interaction, the oligonucleotide would direct the formation of a circular DNA molecule before being amplified, a process known as rolling circle amplification. Red fluorescent tagged probes are introduced and can bind to the rolling circle amplification, resulting in DNA replication and signal production as red dots. Each fluorescent red dot would represent one molecular interaction between ERβ or GPER1 and 17β-estradiol. The *in situ* PLA was performed according to the manufacturer's instructions. Briefly, HCVECs were seeded and grown in chamber slides in M199 media without phenol red until 50% confluence. After washing twice with PBS, the cells were incubated with fresh M199 without phenol red for 3 hours and then treated with 17β-estradiol at a concentration of 0, 120, 240, 480, 720, or 960 pmol/L for 24 hours. The cells were washed with PBS, fixed using 4% paraformaldehyde, permeabilized in 0.1% Triton X-100 and 0.5% BSA in PBS, blocked in 10% BSA in PBS, and incubated with a mixture of monoclonal ERβ antibody or GPER1 antibody and polyclonal 17β-estradiol antibody at 1 : 250 dilution at room temperature for 2 hours. Duolink anti-goat PLA PLUS and anti-rabbit PLA MINUS secondary probes were diluted at 1 : 5 in 5% BSA and incubated with the cells at 37°C in a humidified chamber for 1 hour. The ligation and amplification steps for PLA were performed as suggested by Olink using 40 μL volumes. The cells were washed using Olink buffer A and incubated in ligation-ligase solution, containing oligonucleotides that hybridise the PLA probe, at 37°C in a humidity chamber for 30 minutes. The cells were washed using Olink buffer A and incubated in amplification-polymerase solution, containing oligonucleotides probes with red colour fluorophores and polymerase, at 37°C in a humidity chamber for 100 minutes for rolling cycle amplification. The cells were washed using Olink buffer B and stained with DAPI (1 μg/mL) for 1 minute before washing with 0.01% buffer B. The cells were dried in the dark and cover-slipped using Vectashield HardSet Mounting Medium. Fluorescent images were obtained using a confocal microscope (Leica TCS SP5X, Wetzlar, Germany).

Images captured for PLA events were analyzed using Leica LAS AF software (Version 2.4.1; Leica Microsystems GmbH., Wetzlar, Germany). The number of PLA signals was counted from 10 Z-plane images. At least 100 cells per condition were quantified using ImageJ analysis. The positive PLA events were observed as fluorescent particles (size from 2 to 50 pixels in diameter). When PLA events merged to create particles larger than 50 pixels, the area was measured, and number of events was assumed to be particle area divided by 10 since 10 pixels were the median size of most PLA events. A threshold of 100 (gray values) was set for a positive signal prior to signal counting.

2.4. Data Analysis. Data were expressed as mean ± SEM (number of experiments). Statistical difference between groups was determined using the unpaired two-tailed t-test. When there were more than two groups, differences were analyzed using analysis of variance if the variances were equal and the Mann-Whitney nonparametric test if variances were unequal [14]. Linear regressions were calculated using a statistical computer package, Number Cruncher Statistical Systems [14]. A value of $P < 0.05$ was considered statistically significant.

3. Results

3.1. Subcellular Localization of ERβ and GPER1 in Human Cerebral Vascular Endothelial Cells. High density of immunopositive ERβ signals was observed at the nuclei of HCVECs (Figure 1(a)), suggesting the expression of ERβ at the nuclei of human cerebral vascular endothelial cells. There was no positive ERβ signal identified at the cytoplasm of the cells. In order to differentiate the subcellular location of GPER1, the cells were treated with Triton X-100 to increase membrane permeability or without Triton X-100. When the cells were permeabilized, immunopositive GPER1 signals were dispersed throughout the cytoplasm of HCVECs (Figure 1(b)). There were low density GPER1 signals observed at the nuclei of the cells (Figure 1(b)). When the cells were not permeabilized, GPER1 signals were observed on the cell surface (Figure 1(c)), suggesting the plasma membrane location of GPER1 in human cerebral vascular endothelial cells.

3.2. Interaction between ERβ and 17β-Estradiol in Human Cerebral Vascular Endothelial Cells. PLA was applied to examine the interaction events between ERβ and 17β-estradiol in HCVECs. When 17β-estradiol was absent from the cell culture, there was no interaction event observed between ERβ and 17β-estradiol (Figure 2(a)), which represents an estrogen deficient condition in HCVECs. When HCVECs were exposed to physiological concentrations of 17β-estradiol, proximity ligation revealed the interaction events between ERβ and 17β-estradiol at the nuclei of HCVECs (Figures 2(b)–2(f)), suggesting physiological responsiveness of the cells to 17β-estradiol.

3.3. Dose Response of Interaction Events between ERβ and 17β-Estradiol in Human Cerebral Vascular Endothelial Cells. Proximity ligation revealed that the number of interaction events between ERβ and 17β-estradiol at the nuclei of HCVECs increased with increasing physiological concentrations of 17β-estradiol in the cell culture, ranging from 120 to 960 pmol/L (Figures 2 and 3). There was a positive correlation between physiological concentrations of 17β-estradiol and the number of interaction events between ERβ and 17β-estradiol in HCVECs ($r = 0.9614$, $P < 0.01$).

3.4. Interaction between GPER1 and 17β-Estradiol in Permeabilized Human Cerebral Vascular Endothelial Cells. When the plasma membrane of HCVECs was permeabilized by Triton X-100 and exposed to the cell culture condition that 17β-estradiol was absent, there was no interaction event identified between GPER1 and 17β-estradiol (Figure 4(a)), which represents an estrogen deficient condition in permeabilized HCVECs. When permeabilized HCVECs were exposed to physiological concentrations of 17β-estradiol, proximity ligation revealed the interaction events between GPER1 and 17β-estradiol at the cytoplasm and nuclei of permeabilized HCVECs (Figures 4(b)–4(f)), suggesting physiological responsiveness of permeabilized HCVECs to 17β-estradiol. PLA signals in Figures 4(b)–4(f) were an overlayer of 10 Z-plane images, which showed greater number of PLA signals in the nuclei.

3.5. Dose Response of Interaction Events between GPER1 and 17β-Estradiol in Permeabilized Human Cerebral Vascular Endothelial Cells. Compared with the number of interaction events between GPER1 and 17β-estradiol in permeabilized HCVECs cultured at 120 pmol/L of 17β-estradiol, the number of interaction events between GPER1 and 17β-estradiol at the nuclei of permeabilized HCVECs increased by 23%, 14%, 56%, and 34% at 240, 480, 720, and 960 pmol/L of 17β-estradiol, respectively (Figure 5). The highest number of interaction events between GPER1 and 17β-estradiol was observed when permeabilized HCVECs were exposed to 720 pmol/L of 17β-estradiol.

4. Discussion

A human cerebral vascular endothelial cell model has been established for the study of cerebral aneurysm formation. This study has identified ERβ and GPER1 in HCVECs, confirmed their subcellular locations, verified functional interaction between ERβ and 17β-estradiol or GPER1 and 17β-estradiol, and established a positive correlation between physiological dose responsiveness and the interaction events between ERβ and 17β-estradiol or GPER1 and 17β-estradiol in HCVECs. This human cerebral vascular endothelial cell model presents implications of estrogen signalling through ERβ and GPER1 for cerebral aneurysm pathogenesis in menopausal and postmenopausal women. These *in vitro* alterations may provide the foundation for further assessment during *in vivo* assessment.

4.1. Estrogen Signaling through ERβ. Estrogen receptor α has previously been identified in rat cerebral blood vessels [15],

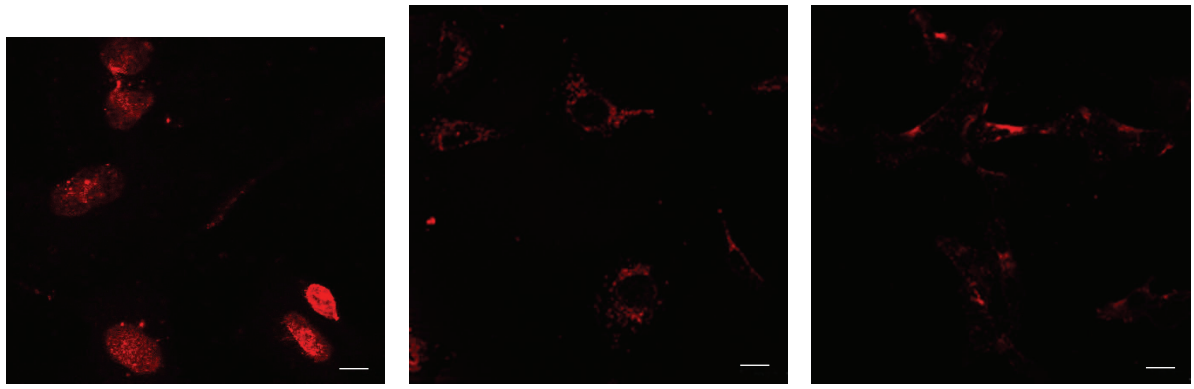

(a) (b) (c)

Figure 1: Localization of ERβ and GPER in human cerebral vascular endothelial cells. (a) ERβ was immunocytochemically stained in red by a rabbit monoclonal antiestrogen receptor beta antibody and Alexa-594 conjugated secondary antibody at the nuclei of the cells. (b) GPER was immunocytochemically identified in red by anti-G-protein-coupled estrogen receptor antibody and Alexa-594 conjugated secondary antibody at the cytoplasm surrounding the nuclei of the cells when the cell membrane was permeabilized by Triton X-100. Low density of GPER was observed at the nuclei of the cells. (c) GPER signals were dispersed around the plasma membrane of the cells when the cells were not permeabilized. Immunocytochemistry, bar = 10 μm.

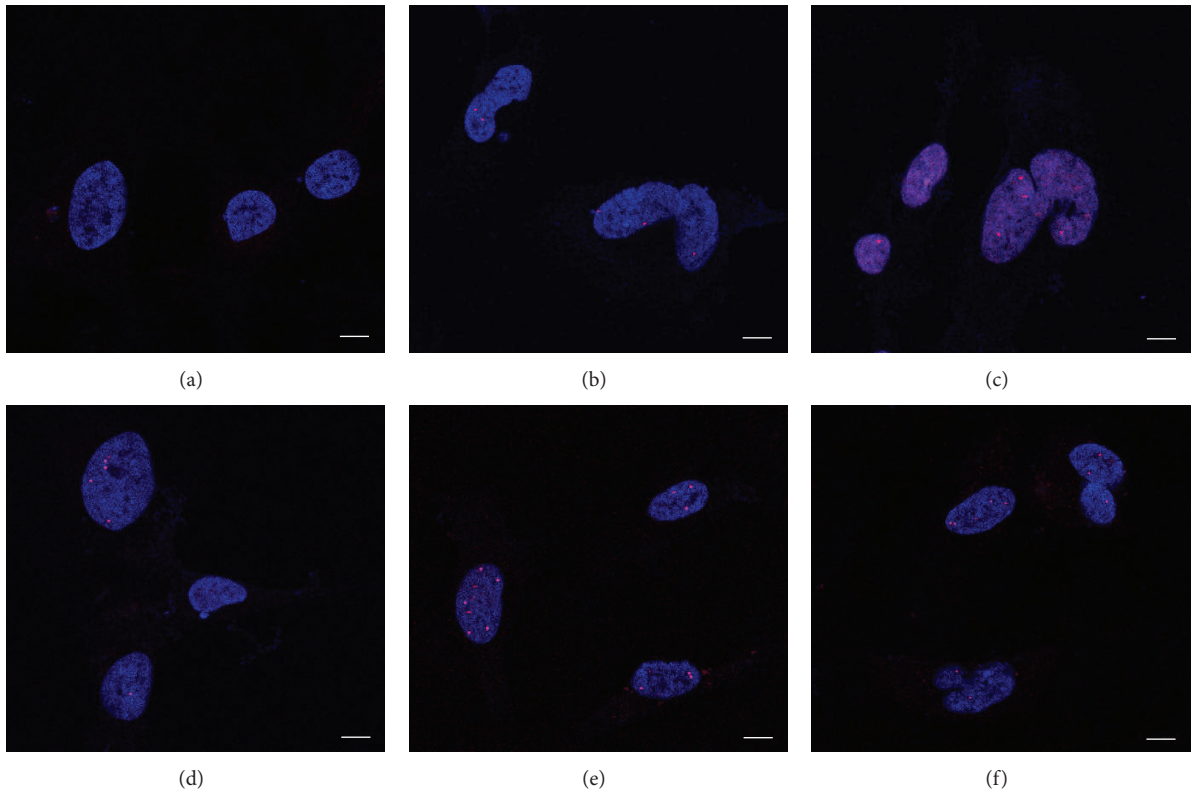

(a) (b) (c)

(d) (e) (f)

Figure 2: The interaction events between ERβ and 17β-estradiol in human cerebral vascular endothelial cells. The interaction events between ERβ and 17β-estradiol were identified by *in situ* proximity ligation assay in the nuclei of the cells. The nuclei of the cells were positively stained by DAPI in blue. The interaction events between ERβ and 17β-estradiol were identified in red dots in the nuclei of the cells when the cells were exposed to the concentration of 17β-estradiol at 0 (a), 120 (b), 240 (c), 480 (d), 720 (e), or 960 pmol/L (f). *In situ* proximity ligation assay, bar = 10 μm.

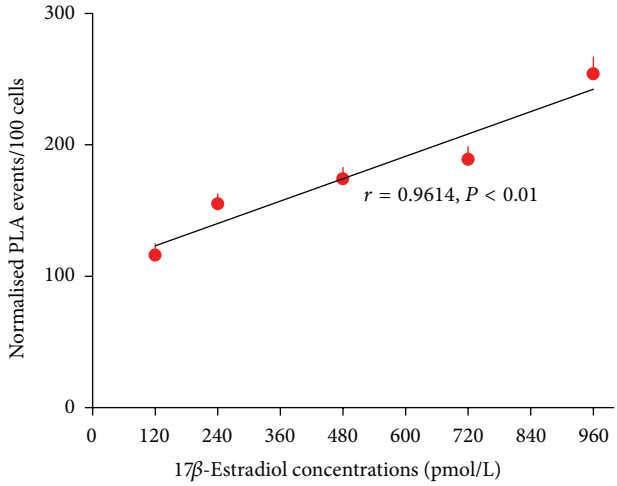

FIGURE 3: The dose-response curve of interaction events between ERβ and 17β-estradiol in human cerebral vascular endothelial cells. When the cells were exposed to the increasing concentrations of 17β-estradiol from 120 to 960 pmol/L, the interaction events between ERβ and 17β-estradiol were increased ($r = 0.9614$, $P < 0.01$). At least 100 cells per concentration were quantified using ImageJ software. The positive PLA events were observed as red fluorescent particles (sizes from 2 to 50 pixels in diameter). When PLA events merged to create particles larger than 50 pixels, the area was measured, and number of events was assumed to be particle area divided by 10 since 10 pixels were the median size of most PLA events. Data were expressed as mean ± SEM of 3 separate experiments.

but there is no report of its expression in human cerebral vascular endothelial cells. This study found that ERβ was located in the nuclei of human cerebral vascular endothelial cells. The interaction events between 17β-estradiol and ERβ were dose dependent and occurred in the nuclei of the cells. These findings provide evidence that estrogen induced effects on the cell's gene expression are mediated via ERβ. In the absence of estrogen molecules, ERβ is inactive and has no influence on gene expression. However, when estrogen molecules enter HCVECs and pass into their nuclei, the estrogen molecules bind to ERβ, thereby causing the shape of ERβ to change. This estrogen-ERβ complex then binds to estrogen response elements, which are located near genes that are controlled by estrogen [16]. After it has become attached to estrogen response elements in DNA, this estrogen-ERβ complex binds to coactivator proteins and the promoter region of estrogen-responsive genes becomes active, resulting in recruitment of coregulatory proteins to the promoter. The active genes produce mRNA molecules, which guide the synthesis of specific proteins [17]. These proteins can then influence the behaviour of HCVECs.

More specifically, the activated nuclear ERβ functions through the following 3 mechanisms (Figure 6) [17]. First, 17β-estradiol causes ERβ dimerization. The ERβ dimer binds to the promoter of the estrogen-responsive gene, phosphorylation of ERβ, and transcriptionally regulates the estrogen-responsive gene. The active genes produce mRNA molecules, which guide the synthesis of specific proteins. These proteins can then influence the behaviour of HCVECs. Second, activated ERβ modulates the function of transcription factors through protein-protein interactions. Third, 17β-estradiol binds to ERβ at the plasma membrane. This estrogen-ERβ complex binds to adaptor 1 protein and signaling molecule such as c-Src, which mediates rapid signaling via PI3K-Akt and MAPK pathway to activate the promoter region of estrogen-responsive genes.

4.2. Estrogen Signaling through GPER1. The estrogen-ERβ signaling pathway is not the only signaling pathway in the estrogen signaling network since GPER1 is identified in the same cell. GPER1 may play an important role in estrogen downstream signaling pathway. GPER1 is a transmembrane protein that generates rapid action compared to nuclear receptor ERβ. GPER1 is situated on the plasma membrane [18] and is also located at endoplasmic reticulum which is continuous with the nuclear membrane [19]. Although the majority of GPER1 is expressed in the plasma membrane, some of it also is functionally expressed at the nuclei of the cells [20]. GPER1 can be translocated to the cell surface or endoplasmic reticulum or nuclei when plasma membrane is permeabilized [21]. When estrogen molecules bind to GPER1, it rapidly activates protein signaling cascade of events via pathways involving G-proteins and stimulating second messenger cAMP production [22], expression of Bcl-2 [23], nerve growth factor [24], cyclin D2 [25], and c-Fos [26]. GPER1 signaling through a pertussis toxin-sensitive G-protein triggers cleavage of membrane-tethered heparin-bound epidermal growth factor (EGF), resulting in transactivation of the EGF receptor [27], intracellular Ca^{2+} mobilization [19, 28], ERK1/2 activation [29], Src activation [11, 30], and PI3K activation (Figure 6) [19]. GPER also regulates transcriptional activity by activating signaling pathways that involve cAMP, ERK, PI3K, and c-Fos (Figure 6) [31]. The distinct mechanism of estrogen-GPER1 signaling is through protein-protein interactions to regulate cellular function.

This study demonstrates that 17β-estradiol can simultaneously activate ERβ and GPER1 at different subcellular locations of HCVECs. Interaction between ERβ and 17β-estradiol triggers a genomic signaling cascade of events, resulting in significant increases in cellular structural protein biosynthesis in HCVECs [32]. There is a positive correlation between dose responsiveness of 17β-estradiol and its signaling through ERβ. Interaction between GPER1 and 17β-estradiol initiates a nongenomic signaling cascade of events, resulting in significant increases in regulatory protein biosynthesis in HCVECs (our unpublished data). The number of interaction events depends on the availability of estrogen molecules. Both ERβ and GPER1 are important in 17β-estradiol mediated effects in HCVECs. Estrogen maintains the normal homeostatic process of HCVECs by stimulating endothelial proliferation and reducing vascular tone via its ERβ and GPER1 [15, 33]. This supports the concept that application of estrogen is beneficial in preserving the normal function of the vascular system [33, 34]. The types of ERs and their signaling mechanisms identified in HCVECs could potentially be applied for developing estrogen-like compounds to specifically bind to a subtype of ERs with

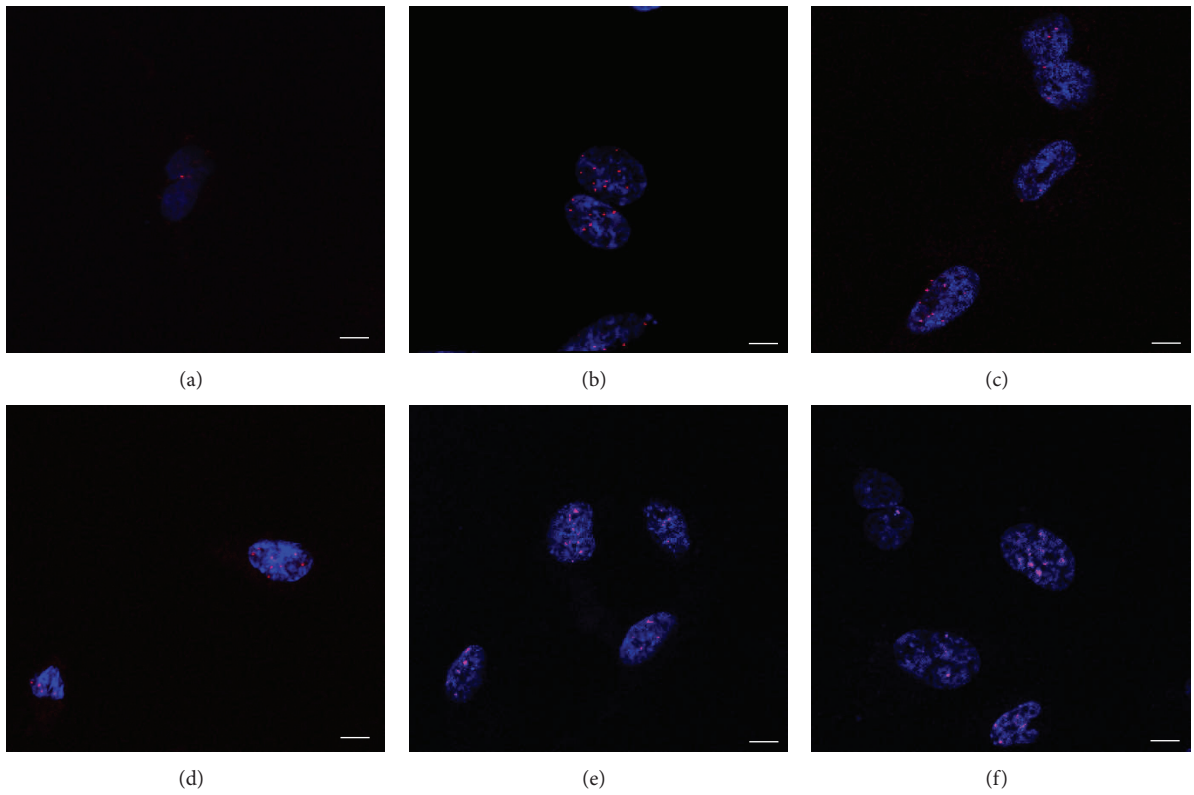

Figure 4: The interaction events between GPER and 17β-estradiol in permeabilized human cerebral vascular endothelial cells. The interaction events between GPER and 17β-estradiol were identified in the nuclei of the cells. The nuclei of the cells were positively stained by DAPI in blue. The interaction events between GPER and 17β-estradiol were identified in red dots when the cells were exposed to the concentration of 17β-estradiol at 0 (a), 120 (b), 240 (c), 480 (d), 720 (e), or 960 pmol/L (f). *In situ* proximity ligation assay, bar = 10 μm.

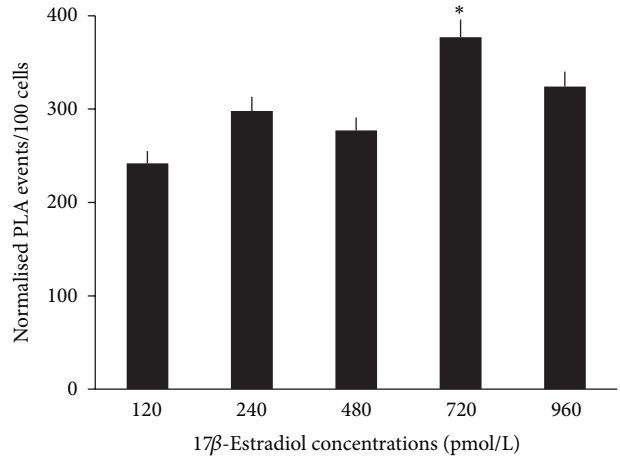

Figure 5: Dose responsiveness of interaction events between GPER and 17β-estradiol in permeabilized human cerebral vascular endothelial cells. When the cells were exposed to different concentrations of 17β-estradiol ranging from 120 to 960 pmol/L, the interaction events between GPER and 17β-estradiol responded to the corresponding dose of 17β-estradiol. $^{*}P < 0.05$ versus the number of interaction signals at other concentrations of 17β-estradiol. At least 100 cells per condition were quantified using ImageJ software. The positive PLA signals were observed as red dots (sizes from 2 to 50 pixels in diameter). When PLA events merged to create particles larger than 50 pixels, the area was measured, and number of events was assumed to be particle area divided by 10 since 10 pixels were the median size of most PLA events. Data were expressed as mean ± SEM of 3 separate experiments.

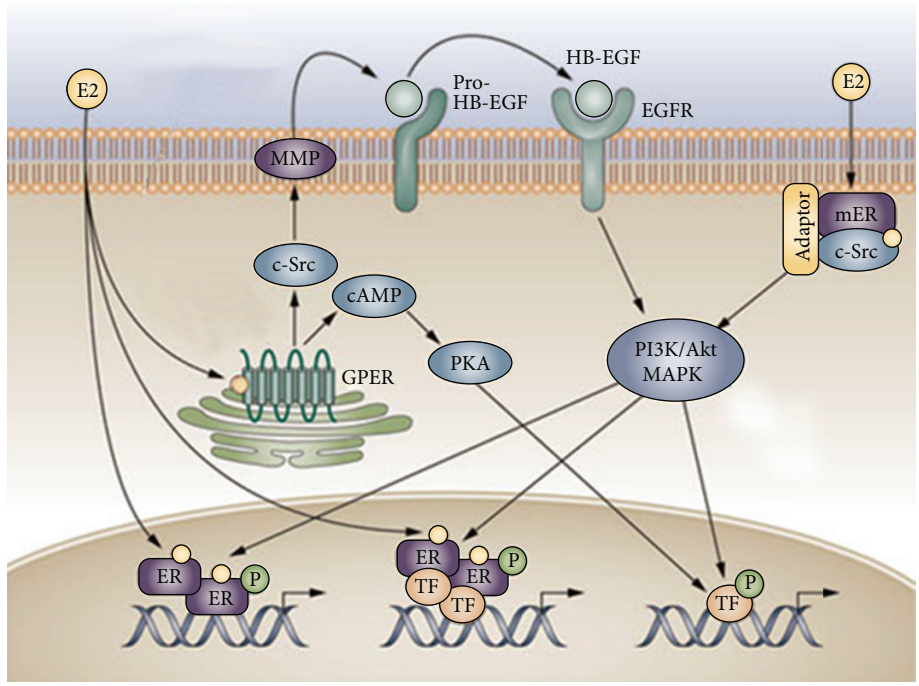

Figure 6: Hypothetical estrogen signaling pathways in human cerebral vascular endothelial cells. 17β-Estradiol (E2) passes through plasma and nuclear membranes activate nuclear ERβ through 3 mechanisms. First mechanism: 17β-estradiol causes ERβ dimerization, binds the ERβ dimer to the promoter of the estrogen-responsive gene, phosphorylation (P) of ERβ, and transcriptionally regulates the estrogen-responsive gene. The active genes produce mRNA molecules, which guide the synthesis of specific proteins. These proteins can then influence the behaviour of HCVECs. Second mechanism: activated ERβ modulates the function of transcription factors (TF) through protein-protein interactions. Third mechanism: 17β-estradiol (E2) binds to ERβ at the plasma membrane (mER). This estrogen-ERβ complex binds to adaptor 1 (Adaptor) protein and the signaling molecule such as c-Src, which mediates rapid signaling via PI3K-Akt and MAPK pathway to activate the promoter region of estrogen-responsive genes. Alternatively, 17β-estradiol (E2) passes through plasma, binds to GPER1 (GPER), and activates c-Src. c-Src activates matrix metalloproteinase (MMP). MMP cleaves pro-heparin-binding-epidermal growth factor (pro-HB-EGF) that transactivates epidermal growth factor receptor (EGFR). EGFR activates phosphatidylinositol 3-kinase-protein kinase B (PI3K-Akt) and mitogen-activated protein kinase (MAPK) pathway. 17β-Estradiol (E2) GPER complex also activates cAMP production to restore EGF-activated MAPK to basal levels through protein kinase A (PKA) dependent inhibition of Raf-1 activity. Akt: protein kinase B; c-Src: protooncogene tyrosine-protein kinase Src; E2: 17β-estradiol; ER: estrogen receptor beta and/or G-protein-coupled estrogen receptor-1; EGFR: epidermal growth factor receptor; GPER: G-protein-coupled ER; MAPK: mitogen-activated protein kinase; mER: plasma membrane ER; MMP: matrix metalloproteinase; P: phosphorylation; PI3K: phosphatidylinositol 3-kinase; PKA: protein kinase A; pro-HB-EGF: pro-heparin-binding-epidermal growth factor; Raf-1: RAF protooncogene serine/threonine-protein kinase; TF: transcription factors. JT modified the image by permission from Macmillan Publishers Ltd. Nature Reviews Endocrinology [17]. Copyright 2011 to Jian Tu for reuse of the original image from Nature Publishing Group (the original image is available in colour at http://www.nature.com/nrendo/index.html).

greater specific action on the cerebral arteries, without the estrogen-dependent side effects on the reproductive organs.

5. Conclusions

This study has identified and functionally characterized estrogen signaling through ERβ and GPER1 in HCVECs. This human cerebral vascular endothelial cell could serve as a cellular model for studying cerebral aneurysm pathogenesis in menopausal and postmenopausal women. Subtypes of ERs and their signaling mechanisms identified in HCVECs could be applicable for developing estrogen-like compounds to specifically bind to a subtype of ERs with greater specific action on the cerebral arteries, without the estrogen-dependent side effects on the reproductive organs, to prevent cerebral aneurysm formation in menopausal and postmenopausal woman.

Abbreviations

c-Src:	Protooncogene tyrosine-protein kinase Src
DAPI:	4,6-Diamidino-2-phenylindole
E2:	17β-Estradiol
EGFR:	Epidermal growth factor receptor
ERβ:	Estrogen receptor beta
FBS:	Fetal bovine serum
HCVECs:	Human cerebral vascular endothelial cells
MAPK:	Mitogen-activated protein kinase
mER:	Plasma membrane ER
MMP:	Matrix metalloproteinase

P:	Phosphorylation
PGER:	G-protein-coupled estrogen receptor 1
PI3K-Akt:	Phosphatidylinositol 3-kinase-protein kinase B
PKA:	Protein kinase A
PLA:	Proximity ligation assay
pro-HB-EGF:	Pro-heparin-binding-epidermal growth factor
Raf-1:	RAF protooncogene serine/threonine-protein kinase
TF:	Transcription factors.

Conflict of Interests

The authors do not have any conflict of interests with the content of the paper.

Acknowledgments

This study was partially supported by an Australian Research Council Discovery Project Grant (DP110102985) to Jian Tu and a scholarship from the Malaysian Ministry of Higher Education to Nurul F. Jufri. The authors thank Professor Mark Baker (Macquarie University) for a gift of rabbit IgG isotype control form.

References

[1] W. T. Longstreth Jr., L. M. Nelson, T. D. Koepsell, and G. van Belle, "Subarachnoid hemorrhage and hormonal factors in women: a population-based case-control study," *Annals of Internal Medicine*, vol. 121, no. 3, pp. 168–173, 1994.

[2] M. S. Ali, R. M. Starke, P. M. Jabbour, S. I. Tjoumakaris, L. F. Gonzalez, R. H. Rosenwasser et al., "TNF-a induces phenotypic modulation in cerebral vascular smooth muscle cells: implications for cerebral aneurysm pathology," *Journal of Cerebral Blood Flow & Metabolism*, vol. 33, pp. 1564–1573, 2013.

[3] N. Chalouhi, M. S. Ali, P. M. Jabbour et al., "Biology of intracranial aneurysms: role of inflammation," *Journal of Cerebral Blood Flow & Metabolism*, vol. 32, no. 9, pp. 1659–1676, 2012.

[4] Y. Kanematsu, M. Kanematsu, C. Kurihara et al., "Critical roles of macrophages in the formation of intracranial aneurysm," *Stroke*, vol. 42, no. 1, pp. 173–178, 2011.

[5] S. E. Francis, J. Tu, Y. Qian, and A. P. Avolio, "A combination of genetic, molecular and haemodynamic risk factors contribute to the formation, enlargement and rupture of brain aneurysms," *Journal of Clinical Neuroscience*, vol. 20, no. 7, pp. 912–918, 2013.

[6] P. E. Norman and J. T. Powell, "Site specificity of aneurysmal disease," *Circulation*, vol. 121, no. 4, pp. 560–568, 2010.

[7] R. E. de Meersman, A. S. Zion, E. G. V. Giardina, J. P. Weir, J. S. Lieberman, and J. A. Downey, "Estrogen replacement, vascular distensibility, and blood pressures in postmenopausal women," *American Journal of Physiology—Heart and Circulatory Physiology*, vol. 274, no. 5, pp. H1539–H1544, 1998.

[8] R. Stricker, R. Eberhart, M.-C. Chevailler, F. A. Quinn, P. Bischof, and R. Stricker, "Establishment of detailed reference values for luteinizing hormone, follicle stimulating hormone, estradiol, and progesterone during different phases of the menstrual cycle on the Abbott ARCHITECT analyzer," *Clinical Chemistry and Laboratory Medicine*, vol. 44, no. 7, pp. 883–887, 2006.

[9] C. J. Gruber, W. Tschugguel, C. Schneeberger, and J. C. Huber, "Mechanisms of disease: production and actions of estrogens," *The New England Journal of Medicine*, vol. 346, no. 5, pp. 340–352, 2002.

[10] N. Heldring, A. Pike, S. Andersson et al., "Estrogen receptors: how do they signal and what are their targets," *Physiological Reviews*, vol. 87, no. 3, pp. 905–931, 2007.

[11] E. R. Prossnitz, J. B. Arterburn, H. O. Smith, T. I. Oprea, L. A. Sklar, and H. J. Hathaway, "Estrogen signaling through the transmembrane G protein-coupled receptor GPR30," *Annual Review of Physiology*, vol. 70, pp. 165–190, 2008.

[12] R. C. Tostes, D. Nigro, Z. B. Fortes, and M. H. C. Carvalho, "Effects of estrogen on the vascular system," *Brazilian Journal of Medical and Biological Research*, vol. 36, no. 9, pp. 1143–1158, 2003.

[13] S. Liu, V. Sammons, J. Fairhall et al., "Molecular responses of brain endothelial cells to radiation," *Journal of Clinical Neuroscience*, vol. 19, no. 8, pp. 1154–1158, 2012.

[14] J. L. Hintze, "Analysis of variance," in *Number Cruncher Statistical Systems (NCSS) 97-User's Guide-I*, pp. 205–278, NCSS, Kaysville, Utah, USA, 1997.

[15] C. Stirone, S. P. Duckles, and D. N. Krause, "Multiple forms of estrogen receptor-α in cerebral blood vessels: regulation by estrogen," *American Journal of Physiology—Endocrinology and Metabolism*, vol. 284, no. 1, pp. E184–E192, 2003.

[16] B. J. Deroo and K. S. Korach, "Estrogen receptors and human disease," *Journal of Clinical Investigation*, vol. 116, no. 3, pp. 561–570, 2006.

[17] E. R. Prossnitz and M. Barton, "The G-protein-coupled estrogen receptor GPER in health and disease," *Nature Reviews Endocrinology*, vol. 7, no. 12, pp. 715–726, 2011.

[18] P. Thomas, Y. Pang, E. J. Filardo, and J. Dong, "Identity of an estrogen membrane receptor coupled to a G protein in human breast cancer cells," *Endocrinology*, vol. 146, no. 2, pp. 624–632, 2005.

[19] C. M. Revankar, D. F. Cimino, L. A. Sklar, J. B. Arterburn, and E. R. Prossnitz, "A transmembrane intracellular estrogen receptor mediates rapid cell signaling," *Science*, vol. 307, no. 5715, pp. 1625–1630, 2005.

[20] F. Gobeil Jr., A. Fortier, T. Zhu et al., "G-protein-coupled receptors signalling at the cell nucleus: an emerging paradigm," *Canadian Journal of Physiology and Pharmacology*, vol. 84, no. 3-4, pp. 287–297, 2006.

[21] E. R. Prossnitz, J. B. Arterburn, and L. A. Sklar, "GPR30: a G protein-coupled receptor for estrogen," *Molecular and Cellular Endocrinology*, vol. 265-266, pp. 138–142, 2007.

[22] E. J. Filardo, J. A. Quinn, A. Raymond Frackelton Jr., and K. I. Bland, "Estrogen action via the G protein-coupled receptor, GPR30: stimulation of adenylyl cyclase and cAMP-mediated attenuation of the epidermal growth factor receptor-to-MAPK signaling axis," *Molecular Endocrinology*, vol. 16, no. 1, pp. 70–84, 2002.

[23] N. Kanda and S. Watanabe, "17β-estradiol inhibits oxidative stress-induced apoptosis in keratinocytes by promoting Bcl-2 expression," *Journal of Investigative Dermatology*, vol. 121, no. 6, pp. 1500–1509, 2003.

[24] N. Kanda and S. Watanabe, "17β-estradiol enhances the production of nerve growth factor in THP-1-derived macrophages or peripheral blood monocyte-derived macrophages," *Journal of Investigative Dermatology*, vol. 121, no. 4, pp. 771–780, 2003.

[25] N. Kanda and S. Watanabe, "17β-estradiol stimulates the growth of human keratinocytes by inducing cyclin D2 expression," *Journal of Investigative Dermatology*, vol. 123, no. 2, pp. 319–328, 2004.

[26] M. Maggiolini, A. Vivacqua, G. Fasanella et al., "The G protein-coupled receptor GPR30 Mediates c-fos up-regulation by 17β-estradiol and phytoestrogens in breast cancer cells," *Journal of Biological Chemistry*, vol. 279, no. 26, pp. 27008–27016, 2004.

[27] E. J. Filardo, J. A. Quinn, K. I. Bland, and A. R. Frackelton Jr., "Estrogen-induced activation of Erk-1 and Erk-2 requires the G protein-coupled receptor homolog, GPR30, and occurs via trans-activation of the epidermal growth factor receptor through release of HB-EGF," *Molecular Endocrinology*, vol. 14, no. 10, pp. 1649–1660, 2000.

[28] E. Brailoiu, S. L. Dun, G. C. Brailoiu et al., "Distribution and characterization of estrogen receptor G protein-coupled receptor 30 in the rat central nervous system," *Journal of Endocrinology*, vol. 193, no. 2, pp. 311–321, 2007.

[29] F. Edwin, G. J. Wiepz, R. Singh et al., "A historical perspective of the EGF receptor and related systems," *Methods in Molecular Biology*, vol. 327, pp. 1–24, 2006.

[30] E. J. Filardo and P. Thomas, "GPR30: a seven-transmembrane-spanning estrogen receptor that triggers EGF release," *Trends in Endocrinology and Metabolism*, vol. 16, no. 8, pp. 362–367, 2005.

[31] M. R. Meyer, E. Haas, E. R. Prossnitz, and M. Barton, "Non-genomic regulation of vascular cell function and growth by estrogen," *Molecular and Cellular Endocrinology*, vol. 308, no. 1-2, pp. 9–16, 2009.

[32] N. F. Jufri, M. Baker, and J. Tu, "Estrogen deficiency reduces cellular structural protein synthesis in a cell model of aneurysm in menopausal and postmenopausal women," in *Proceedings of the Asia Pacific Stroke Conference*, Hong Kong, China, August-September 2013.

[33] M. Chen, B. Ouyang, L. Goldstein-Smith, and L. Feldman, "Oral contraceptive and hormone replacement therapy in women with cerebral aneurysms," *Journal of NeuroInterventional Surgery*, vol. 3, no. 2, pp. 163–166, 2011.

[34] M. A. Jamous, S. Nagahiro, K. T. Kitazato, T. Tamura, K. Kuwayama, and K. Satoh, "Role of estrogen deficiency in the formation and progression of cerebral aneurysms. Part II: experimental study of the effects of hormone replacement therapy in rats," *Journal of Neurosurgery*, vol. 103, no. 6, pp. 1052–1057, 2005.